Sustainable Steel-Timber Hybrid Structures in Fire

Aatish Jeebodh

A thesis submitted in partial fulfilment of the requirements for the degree of

Doctor of Philosophy

The University of Sheffield

School of Mechanical, Aerospace and Civil Engineering

June 2026

Abstract

Steel-timber hybrid structures are emerging as low-carbon alternatives to conventional steel-concrete construction, typically consisting of steel framing supporting cross-laminated timber (CLT) floor systems. However, their structural behaviour in fire remains poorly understood, particularly regarding lateral-torsional buckling (LTB) and composite action. Current fire design practice typically neglects composite action, while the lateral restraint provided by mechanical connectors in steel-timber assemblies remains insufficiently quantified, creating uncertainty in predicting structural stability and fire performance.

To address these gaps, this thesis investigates the structural fire performance of representative steel-CLT downstand configurations using Eurocode-based analytical formulations and advanced finite element simulations. LTB and composite action are examined independently under different boundary conditions to isolate their respective mechanics. The analyses account for variations in heating scenarios, material degradation, connector performance, and restrained thermal expansion.

The results demonstrate that partial lateral restraint enhances stability compared with unrestrained beams, whereas full lateral restraint is not representative of the behaviour of steel-timber hybrid members connected with self-tapping screws in fire. Axial restraint induces compressive forces that accelerate the onset of LTB, highlighting limitations in conventional design assumptions derived from steel-concrete composite systems.

Conversely, composite action increases failure temperatures compared with bare steel beams; however, composite systems may exhibit greater early-stage deflections due to restrained thermal expansion of the steel beam against the cooler CLT slab. As heating progresses, degradation of the bottom CLT layer and the steel-timber interface reduces longitudinal shear transfer, potentially leading to a progressive loss of composite action and a transition towards non-composite behaviour.

Overall, the findings demonstrate that current design approaches do not adequately capture the complex thermo-mechanical response of steel-timber hybrid systems in fire. This study advances understanding of LTB and composite behaviour at elevated temperatures,

providing a foundation for more robust performance-based fire design and future experimental investigation.

Graphical Abstract

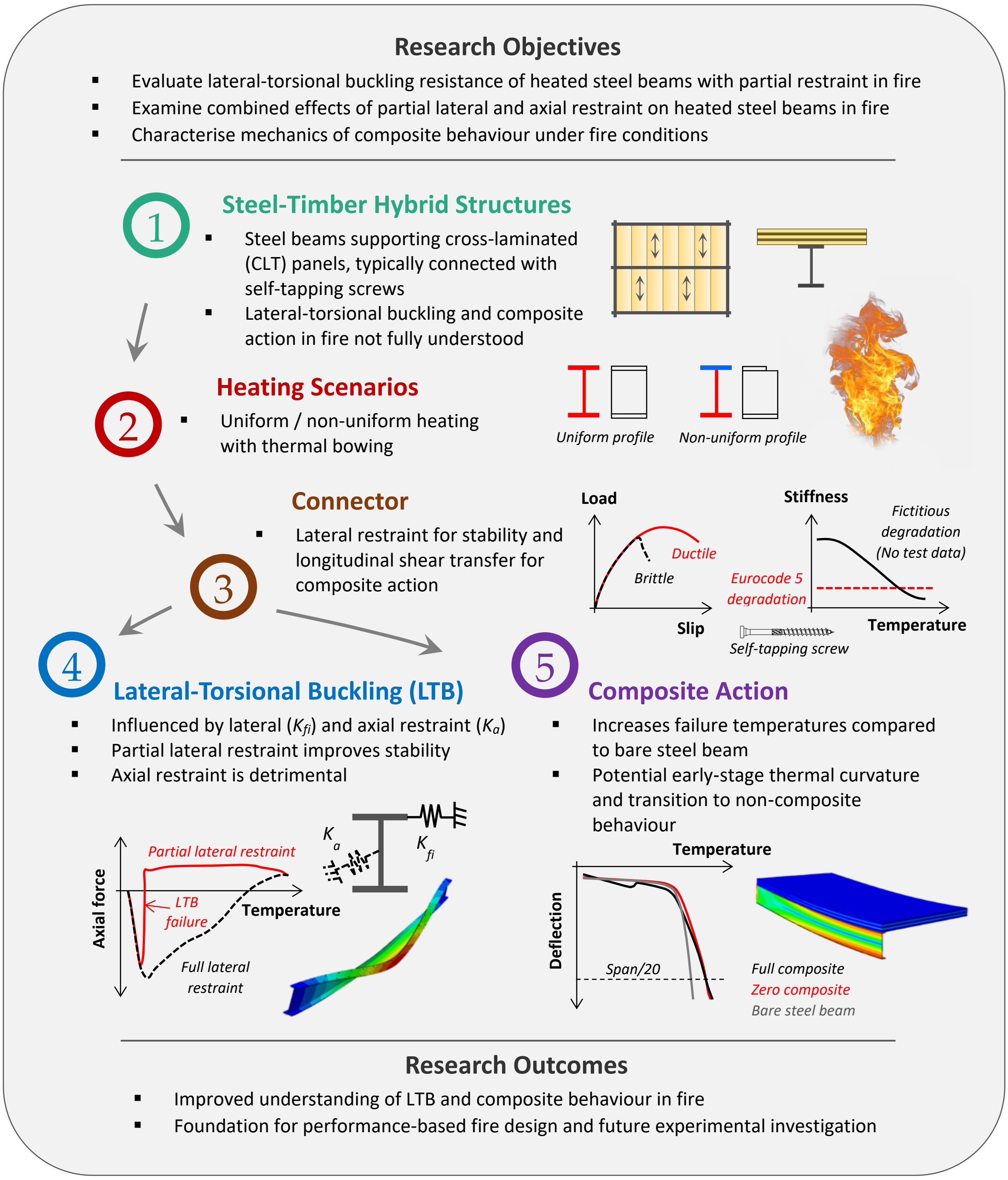

Acknowledgements

I would like to express my sincere gratitude to Professor Buick Davison, Dr Martyn S. McLaggan, Professor Ian Burgess, and Dr Shan-Shan Huang for their invaluable guidance and unwavering support throughout this doctoral research. Their expertise, insightful feedback, constructive criticism, and encouragement have been instrumental in shaping this work.

I would also like to thank Dr Danny Hopkin from OFR Consultants for providing industrial insight, which greatly enhanced the practical relevance and impact of this research.

This study was supported by the UK Engineering and Physical Sciences Research Council [grant number EP/T517835/1] in collaboration with OFR Consultants.

Finally, I wish to thank my family and friends for their invaluable support and encouragement throughout this journey, as well as everyone who has supported me in any way.

Publications

The following journal and conference papers have been published over the course of this thesis.

Published Journal Papers

Jeebodh, A., Davison, B., McLaggan, M. S., Burgess, I., Hopkin, D. and Huang, S.-S. (2024) 'Influence of continuous elastic lateral restraints on beams and beam-columns of steel-timber hybrid structures in fire', Fire Safety Journal, 146, pp. 104172. DOI: https://doi.org/10.1016/j.firesaf.2024.104172.

Jeebodh, A., Davison, B., McLaggan, M. S., Burgess, I., Hopkin, D. and Huang, S.-S. (2026) 'Behaviour of heated steel beams with lateral and axial restraint in steel-timber hybrid structures', Engineering Structures, 349, pp. 121887. DOI: https://doi.org/10.1016/j.engstruct.2025.121887.

Jeebodh, A., Davison, B., Burgess, I., Hopkin, D. and McLaggan, M. S. (2026) 'Composite behaviour of steel-timber hybrid structures in fire', Structures, 92, pp. 112822. DOI: https://doi.org/10.1016/j.istruc.2026.112822.

Conference Paper & Presentation

Jeebodh, A., Davison, B., McLaggan, M. S., Burgess, I., Hopkin, D. and Huang, S.-S. (2024) 'Lateral-torsional buckling of steel beams supporting cross-laminated timber slabs in fire', 13th International Conference on Structures in Fire (SiF 2024), CMM - Portuguese Steelwork Association. DOI: https://doi.org/10.30779/cmm_SIF24.

Declaration

I, the author, confirm that the Thesis is my own work. I am aware of the University's Guidance on Academic Integrity. This work has not previously been presented for an award at this, or any other, university.

Table of Contents

List of Tables

List of Figures

1

Introduction

1.1 Background and Motivation

Climate change represents one of the most pressing challenges of the twenty-first century, necessitating substantial reductions in greenhouse gas emissions across multiple sectors. The construction industry is a major contributor, accounting for approximately 34 to 39% of global energy-related carbon emissions, including both operational energy use and embodied carbon associated with materials and construction processes throughout the building lifecycle (World Green Building Council, 2019; UNEP, 2025). In the United Kingdom, the built environment is responsible for roughly 25% of total national emissions, emphasising the urgent need to adopt low-carbon construction strategies (UK Green Building Council, 2021). These pressures are driving a paradigm shift, reshaping expectations for structural performance and accelerating the transition towards sustainable material selection and innovative design approaches.

Historically, structural design has prioritised safety, economy, and constructability, favouring simplicity and standardisation. In response to climate change, structural systems are increasingly expected to satisfy performance requirements while minimising environmental impact. This drive for decarbonisation has intensified the pursuit of material efficiency through lean structural design and the integration of sustainable construction materials. Notably, CLT has emerged as a technically viable low-carbon alternative to conventional poured-in-situ or precast concrete floor systems used in steel-concrete composite construction. This is particularly significant in low- to mid-rise buildings, where floors are generally the largest contributor to embodied carbon in the superstructure (Watson, 2020; SCI, 2024; Fang, Kenny and Mueller, 2026), although they are no longer the dominant contributor in high-rise and super high-rise buildings (Gan *et al.*, 2017). The relative contribution of the floor system also varies with factors such as the structural grid, loading requirements, and material specifications. In steel-timber hybrid systems, the greatest reductions are typically achieved when a concrete topping slab is omitted (Becker, Anderson and Phillips, 2023).

Meanwhile, structural steel remains the dominant framing material for multi-storey buildings in the UK, accounting for approximately 65% of building frames over the past two decades, compared with around 20% for in situ concrete and smaller proportions for masonry, precast concrete, and timber systems (BCSA, 2024). This sustained dominance suggests that integrating steel frames with CLT floor systems, as illustrated in Figure 1.1, offers a pragmatic pathway to decarbonisation without fundamentally altering established steel construction practices.

Figure 1.1: Hybrid steel frame structure with CLT floors under construction (Source: AISC, 2022)

Cross-laminated timber is an engineered wood product manufactured by bonding layers of solid timber boards in alternating orthogonal directions to create large-scale structural panels. Unlike solid wood, CLT minimises the influence of natural defects and improves dimensional stability through cross-lamination, allowing for larger structural sections and longer spans. Widely used in floor, roof, and wall applications within mass timber construction, CLT offers a favourable strength-to-weight ratio, low embodied carbon, and compatibility with offsite prefabrication (Brandner *et al.*, 2016; Younis and Dodoo, 2022). Its low self-weight reduces foundation demands and facilitates installation, while its prefabricated nature enables rapid, dry construction, making it an attractive flooring solution for steel-framed buildings

(Chiniforush *et al.*, 2018). Steel is well-suited for multi-storey construction due to its high strength, ductility, and well-established design frameworks. Thus, adopting steel framing with CLT floor systems provides a structurally efficient and lower-carbon solution within contemporary steel construction (D'Amico, Pomponi and Hart, 2021; Becker, Anderson and Phillips, 2023).

Steel-CLT hybrid systems combine the tensile capacity and ductility of steel with the biophilic, lightweight, and environmental benefits of timber. When designed to act compositely, these systems enhance load sharing and overall structural efficiency (Hassanieh, Valipour and Bradford, 2017b). However, hybridisation also introduces additional design complexity. Differences in stiffness, moisture sensitivity, acoustic performance, and the time-dependent behaviour of timber (including creep and mechano-sorptive effects) introduce uncertainties that must be addressed to ensure reliable load transfer and sustained composite action (Chiniforush *et al.*, 2019; Chiniforush, Valipour and Akbarnezhad, 2021).

While these considerations are important under ambient conditions, the structural response of steel-timber hybrid systems becomes considerably more complex under fire conditions. At high temperatures, steel and timber exhibit fundamentally different thermal and mechanical responses. Steel experiences rapid reductions in stiffness and strength as temperature increases, while restrained thermal expansion induces axial forces that influence buckling behaviour, member stability, and connection performance (Li and Guo, 2008). Timber, by contrast, undergoes thermal degradation and progressive charring, resulting in section loss and temperature-dependent reduction in mechanical properties.

In a hybrid floor system, the differing thermal and mechanical behaviours of steel and CLT interact, producing complex effects on load redistribution, composite action, and overall structural stability. Heat-induced delamination of CLT panels, char crushing, and variability in fire protection performance further contribute to this complexity. Additionally, degradation of shear connectors at elevated temperatures can reduce lateral restraint to steel members, increasing susceptibility to lateral-torsional buckling (LTB) and diminishing the longitudinal shear transfer necessary for composite action. Collectively, these interacting mechanisms produce a multi-faceted thermo-mechanical response that is not fully captured by current design provisions. While the fire performance of isolated steel members and timber elements has been widely studied, the thermo-mechanical response of hybrid assemblies under fire – particularly the interaction of restraint effects, instability mechanisms, shear transfer at the steel-timber interface, and differential thermal expansion – remains poorly understood (AISC, 2022; SCI, 2024). This uncertainty undermines confidence in applying existing prescriptive or member-based structural fire design provisions to steel-CLT hybrid assemblies and highlights the need for mechanics-based investigations at elevated temperatures.

1.2 Research Problem and Knowledge Gaps

Steel-timber hybrid structures, particularly downstand steel beams supporting CLT slabs, exhibit fire response characteristics that are not fully captured by existing design frameworks. Existing provisions are largely formulated for isolated steel members and steel-concrete composite systems, where material interactions, restraint conditions, and thermal responses differ fundamentally from those in steel-CLT assemblies. As a result, applying established fire design methodologies to such hybrid systems remains uncertain.

The stability of steel beams under fire exposure is affected by both lateral and axial restraint. Conventional fire design approaches for lateral-torsional buckling typically assume either unrestrained or fully laterally restrained boundary conditions, providing limited guidance for intermediate or partially laterally restrained scenarios. Additionally, axial restraint arising from restrained thermal expansion can further amplify lateral-torsional buckling. Nevertheless, the combined influence of these effects on steel beam instability at elevated temperatures remains insufficiently understood.

The fire performance of steel-CLT composite systems is an emerging research area, with only a handful of exploratory studies to date and no established design framework. Factors such as shear connector degradation, temperature-dependent material deterioration, and differential thermal expansion can compromise the longitudinal shear transfer across the steel-timber interface. Consequently, a comprehensive framework describing the mechanics governing composite response in steel-timber assemblies under fire conditions has yet to be developed.

The research problem addressed in this thesis is the need to improve understanding of the structural fire performance of steel-CLT hybrid systems. This problem arises from two closely related knowledge gaps: (i) the stability of steel beams under combined lateral and axial restraint during fire exposure, and (ii) the composite behaviour of steel-CLT assemblies at elevated temperatures. Until these gaps are addressed, current structural fire design provisions cannot be confidently applied to hybrid systems. To address these challenges, this thesis undertakes targeted analytical and numerical investigations of representative hybrid configurations, forming the basis of the three interrelated studies presented herein.

1.3 Aim and Objectives

The aim of this research is to investigate the structural fire performance of steel-timber hybrid systems, focusing on unprotected downstand steel beams supporting CLT slabs, with particular emphasis on lateral-torsional buckling and composite behaviour at elevated temperatures.

To achieve this aim, the research is structured around the following specific objectives:

1) Evaluate the lateral-torsional buckling resistance of steel beams with partial lateral restraint at elevated temperatures using analytical methods, and to assess the adequacy of current fire design assumptions.
2) Examine the influence of partial lateral and axial restraint on the lateral-torsional buckling behaviour of steel beams in hybrid systems under fire conditions through validated finite element simulations.
3) Characterise the mechanics of composite behaviour in steel-CLT beams during fire exposure through validated finite element simulations
4) Synthesise the analytical and numerical findings and assess their implications for the structural fire design of steel-timber hybrid structures.

1.4 Author Contributions and Co-Authorship

This thesis is presented in a paper-based format comprising three published journal papers. Across all three studies, the lead author, Aatish Jeebodh, led the conceptualisation of the research, development of the methodology, software implementation, model validation, formal analysis, data curation, preparation of the original manuscript drafts, and visualisation of results. These activities constitute the author's primary intellectual and technical contributions to the research programme.

The co-authors contributed to the conceptual and methodological direction of the work, provided critical review and editing of the manuscripts, and offered academic supervision throughout the research. They also supported project administration and funding acquisition. Their contributions were primarily supervisory and advisory, ensuring technical rigour, academic quality, and the strategic development of the research programme.

1.5 Structure of Thesis

This thesis addresses the research problem defined in Section 1.2 through three interrelated research papers and is organised into seven chapters.

Chapter 1 presents the research background and motivation, defines the research problem and associated knowledge gaps, outlines the aim and objectives, and summarises the author's contributions and co-authorship.

Chapter 2 provides a comprehensive review of the relevant literature on steel-timber hybrid systems, with particular emphasis on structural behaviour under ambient and fire conditions, and identifies the key research gaps addressed in this study.

Chapters 3 to 5 form the core of the thesis and are presented as individual journal papers. Chapter 3 investigates the lateral-torsional buckling behaviour of steel beams with partial lateral restraint at elevated temperatures using analytical methods. Chapter 4 develops and applies sequential thermo-mechanical finite element numerical models to examine the combined effects of lateral and axial restraint on the instability behaviour of steel beams under heating. Chapter 5 examines the evolution of composite action in steel-CLT hybrid assemblies under fire conditions using finite element simulations, with emphasis on shear interaction and temperature-dependent response.

Chapter 6 synthesises the findings from the three papers and discusses their implications for the fire performance of steel-timber hybrid systems.

Chapter 7 summarises the principal contributions of the research and provides recommendations for future work.

2

Literature Review

This chapter reviews the current state of knowledge relevant to the structural fire performance of steel-CLT hybrid systems. It examines the thermal and mechanical behaviour of steel and timber in fire, the stability of steel beams, and the mechanics of composite action in hybrid assemblies. By synthesising findings across these areas, the chapter establishes the context for the research and identifies the key knowledge gaps that motivate the analytical and numerical studies presented in subsequent chapters. Additional literature relevant to the individual studies is also provided in Chapters 3 to 5, where each chapter includes its own focused review.

2.1 Overview of Steel-Timber Hybrid Structures

Hybrid structural systems combining steel and mass timber have emerged as a structurally efficient and low-carbon alternative to conventional steel-concrete construction. While steel frames can be paired with various engineered timber products, such as glued laminated timber (glulam) and laminated veneer lumber (LVL), cross-laminated timber (CLT) has attracted particular research and industry attention within the UK market (SCI, 2024).

The structural performance of these hybrid systems depends critically on the arrangement of steel beams, connection behaviour, and the degree of composite interaction achieved between steel and CLT. Furthermore, the orthotropic nature of the panels, alongside serviceability considerations such as deflection and vibration, plays a central role in governing their response at ambient temperature (AISC, 2022). Consequently, understanding the mechanisms of load transfer, connection behaviour, and composite action is essential for predicting the structural performance of steel-CLT hybrid structures.

2.1.1 Hybrid Construction Typologies

Steel-timber hybrid beam systems can be configured in different ways, with the chosen typology fundamentally influencing structural behaviour and load transfer mechanisms. These arrangements influence key performance aspects, including structural depth, the degree of composite action, integration of building services, fire strategy, and construction methodology. In contemporary practice, hybrid steel-CLT floors are primarily categorised into two typologies: downstand and slimfloor systems (Swedish Wood, 2022; Pimentel, Simões and Silva, 2024). Figure 2.1 schematically illustrates these configurations, highlighting key structural features and typical performance considerations.

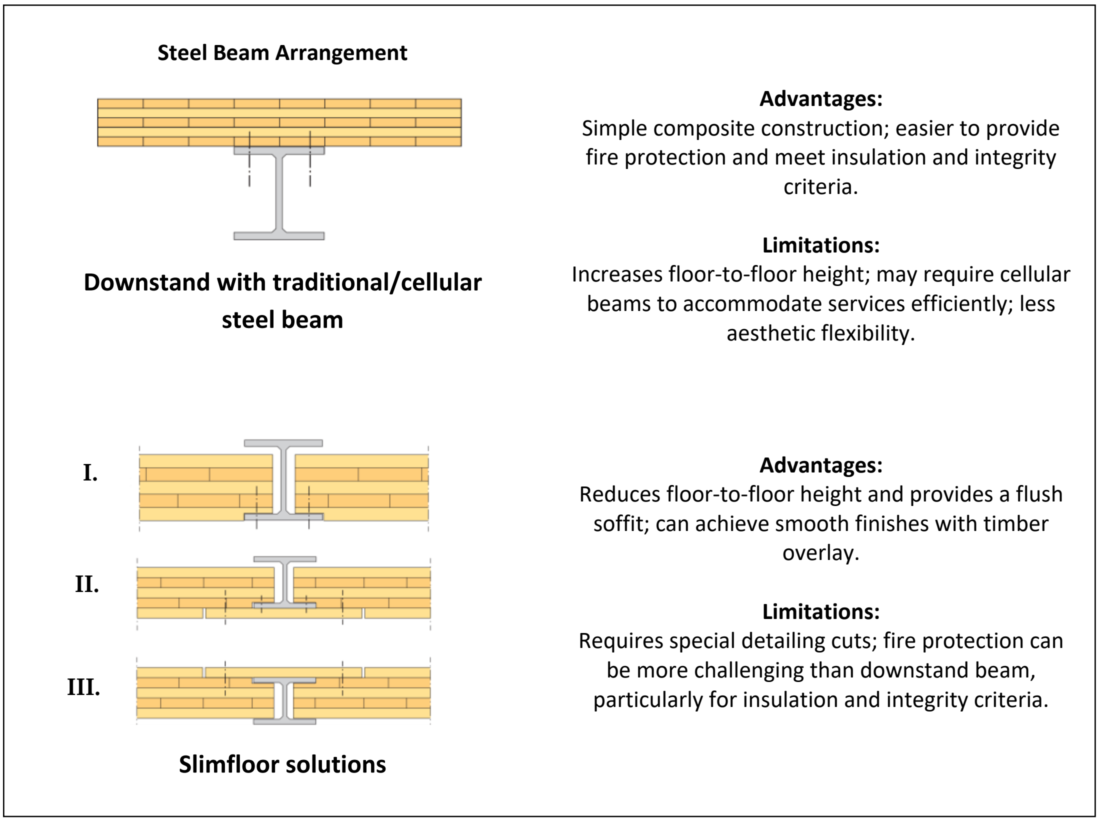

Figure 2.1: Comparison of downstand and slimfloor solutions for steel-timber hybrid structures (Adapted from: Swedish Wood, 2022)

Downstand arrangements, in which a CLT panel is supported on the top flange of a steel beam, are a commonly adopted configuration. This configuration often allows the panel to span multiple beams, reducing slab deflection and providing a relatively balanced loading condition with limited torsional demand on the steel member. At ambient conditions, the top compression flange of the steel beam can be laterally restrained through the CLT panel using conventional connectors; however, this restraint may be partially or fully compromised under fire. The increased overall floor depth associated with downstand beams can also restrict the space available for mechanical, electrical, and plumbing services, necessitating careful coordination during design and construction, with services typically routed either below the beams or through web openings.

Slimfloor systems, by contrast, integrate the steel beam within the depth of the CLT panel, typically employing standard, asymmetric, or welded hollow sections to achieve a shallower floor profile (Malaska *et al.*, 2023; Dumler *et al.*, 2025). These systems generally rely on a single-span panel supported on the bottom flange, which can introduce torsional effects during construction, with open sections requiring particular attention to restraint of the top compression flange against buckling. While the embedded beam geometry reduces floor-to-floor height and facilitates service integration by providing a flat soffit, it introduces additional complexity in connection detailing and in the development of composite action.

Although both typologies can be used in hybrid construction, the present study focuses on downstand configurations. Ultimately, typology selection must reflect wider design needs, especially the durability of timber and the fire performance requirements for load-bearing capacity, integrity, and insulation (SCI, 2024).

2.1.2 Structural Behaviour of CLT Floors

Cross-laminated timber is an engineered wood product formed by stacking an odd number of solid-sawn timber layers orthogonally and bonding them with structural adhesives to create a plate-like element. In the UK, CLT must comply with BS EN 16351 (2021), which specifies material requirements, adhesive types, and manufacturing tolerances. Commercial panels are typically produced up to 16 m in length, 3.5 m in width, and 350 mm in thickness, although transport constraints generally limit practical lengths to around 13.5 m. The moisture content in the boards must be between 8% and 15% when they are glued together (Swedish Wood, 2022).

The orthogonal layup provides dimensional stability and biaxial load-carrying capacity, enabling CLT to resist both in-plane and out-of-plane actions. However, panel dimensions and the discontinuities introduced by panel-to-panel joints have important implications for the global stiffness, continuity, and load redistribution capacity of CLT floor systems. Traditional panel-to-panel joints, such as surface spline, half-lap, and butt joints, typically use self-tapping screws to provide in-plane shear resistance for diaphragm action. However, little guidance is available for their application under out-of-plane loading, particularly regarding the transfer of vertical shear forces and bending moments between adjacent panels (Salgado and Guner, 2021; Ganjali, Pace and Tannert, 2025; Hosseini *et al.*, 2025).

Although CLT is theoretically capable of two-way plate action, design practice generally assumes one-way spanning behaviour. This is due to limited panel widths relative to typical floor spans, the discontinuity introduced by joints, and the difficulty of achieving continuous four-edge support in real building layouts. Panels with a span ratio greater than two, or those supported on only two edges, are effectively restricted to one-way action. As a result, one-way design is widely adopted and is typically conservative with respect to floor behaviour. The distinction between one-way and two-way behaviour in CLT panels is illustrated in Figure 2.2.

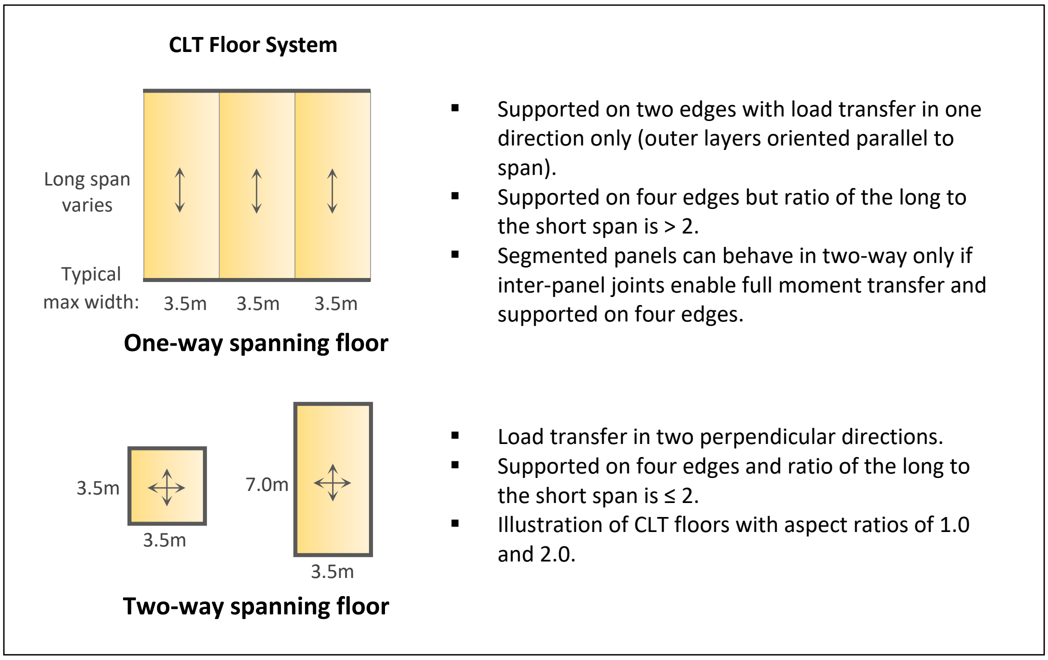

Figure 2.2: Comparison of one-way and two-way bending behaviour of CLT panels as a function of boundary conditions and span aspect ratio

The feasibility of two-way action is further constrained in buildings with large structural grids. For example, a single 3.5 m × 7.0 m panel supported on four sides may theoretically mobilise biaxial bending. However, larger grids require multi-panel assemblies and inter-panel connections, as presented in Swedish Wood (2022). Most commercially available connection systems lack the shear and moment transfer capacity required to achieve true plate-like continuity, limiting the practical realisation of two-way action. Nevertheless, analytical and small-scale experimental work by Doyle, Emberley and Torero (2017) indicates that two-way CLT slabs may achieve stiffness and strength increases exceeding 50%, and that biaxial bending can provide beneficial load redistribution in fire as the outer strong-direction lamella chars and becomes ineffective. This redistribution potential is most pronounced in panels comprising at least five layers, where sufficient orthogonal stiffness exists to sustain two-dimensional load transfer.

The structural design of CLT floors is commonly governed by serviceability limit states rather than ultimate limit states. Due to the relatively low mass and long spans characteristic of CLT construction, deflection and vibration often control panel thickness and span limits. Deflection is primarily influenced by the effective bending stiffness of the panel, which is governed not only by the modulus of elasticity of the longitudinal laminations but also by the shear flexibility of the cross-layers. Vibration performance depends on the mass, stiffness, and damping of the floor system. Lightweight long-spanning floors inherently exhibit lower natural frequencies (Smith, Hicks and Devine, 2009), increasing susceptibility to occupant-induced vibrations. Thiel (2013) reported that vibration often governs for spans exceeding 4 m, whereas Brandner *et al.* (2018) noted that deflection may control shorter spans. In certain circumstances, the fire limit state may also become governing (Doyle, Emberley and Torero, 2017), particularly where sacrificial charring depth requirements influence panel thickness selection.

The structural response of CLT under out-of-plane loading reflects its orthotropic composition. Vertical loading induces bending and shear stresses in both the major and minor axes, while in-plane axial loading such as from wind generates normal stresses aligned with the principal material directions. Figure 2.3 illustrates the distribution of bending, shear, and axial stresses in a typical five-layer CLT panel. In practice, the longitudinal layers parallel to the span provide the dominant contribution to flexural stiffness, while the transverse layers contribute only marginally due to their much lower modulus of elasticity and their primary role in shear transfer.

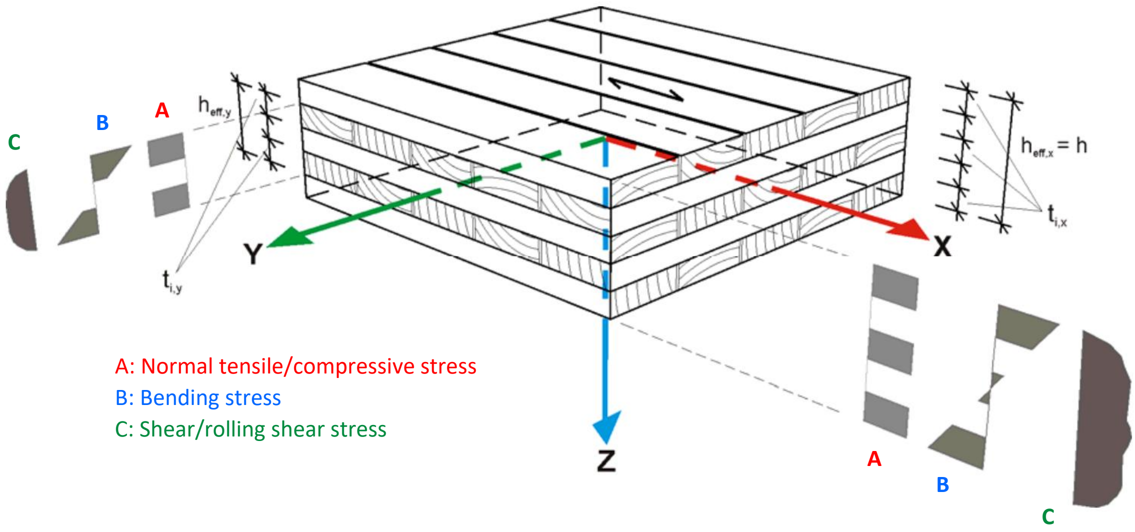

Figure 2.3: Stresses in two main structural directions of a five-layer CLT floor slab (Adapted from: KLH, 2021)

The transverse modulus of elasticity is typically treated as negligible in flexural calculations because it is approximately 3% of the longitudinal modulus, and transverse laminations are generally not edge-bonded (Swedish Wood, 2022). Even when edge bonding is present, shrinkage-induced cracking and the use of non-structural adhesives limit reliable flexural transfer between adjacent boards (Brandner *et al.*, 2016). Treating the transverse modulus as negligible increases the calculated stresses in the longitudinal layers and is therefore conservative.

A characteristic feature of CLT behaviour is rolling shear, a phenomenon in which shear stresses acting perpendicular to the grain direction cause localised shear deformation within transverse laminations. Although rolling shear stresses rarely govern ultimate strength in floor applications, rolling shear deformation can contribute substantially to total deflection, particularly in thick panels or short spans (Brandner *et al.*, 2018).

At ambient temperature, the structural response of CLT floors is governed by their orthotropic composition, panel geometry, boundary conditions, and shear flexibility, which together determine stiffness and load distribution. These factors dictate how the floor carries applied loads and performance is evaluated at the serviceability, ultimate, and fire limit states. When supported by steel beams, CLT panels provide lateral restraint to the compression flange and contribute to load sharing through composite action, directly enhancing the strength, stiffness, and stability of the steel members, forming the basis for steel-CLT hybrid behaviour (AISC, 2022).

2.1.3 Structural Behaviour of Steel-CLT Beams

Steel-CLT hybrid beams, consisting of steel sections with overlying CLT panels, form composite systems in which interaction between the two materials influences their structural behaviour. In isolation, steel beams offer high strength, stiffness, and ductility, with behaviour dominated by flexure, shear, and susceptibility to lateral-torsional buckling. Once CLT panels are attached to the top flange using mechanical fasteners, the beams no longer act as unrestrained steel sections, as the timber components modify their response by providing discrete lateral restraint along the compression flange and enabling composite action to develop.

In practice, CLT panels are connected to steel beams using self-tapping screws or other mechanical fasteners installed at regular spacing. Unlike steel-concrete systems, which typically assume full lateral restraint from the slab, these mechanical fasteners offer a degree of restraint that is neither fully rigid nor negligible. The lateral-torsional buckling behaviour of steel-CLT beams therefore cannot be directly inferred from standard steel or steel-concrete design assumptions and must be assessed using semi-rigid restraint models that explicitly account for connector stiffness and slip characteristics. The behaviour of steel-CLT beams under lateral restraint conditions at elevated temperatures is examined in detail in Chapters 3 and 4. Chapter 3 develops an analytical framework for modelling the semi-rigid lateral restraint provided by self-tapping screws, whereas Chapter 4 extends this work through a numerical investigation of partially restrained beams under fire conditions.

Beyond stability effects, longitudinal shear transfer between the steel beam and CLT panel may lead to partial composite action. Composite behaviour arises when connectors transmit sufficient shear to enable the two materials to act together in bending. As a result, the structural response typically lies between that of a bare steel beam and a fully composite section (Hassanieh, Valipour and Bradford, 2017b). This partial composite behaviour cannot be represented using rigid-connection assumptions.

At the ultimate limit state, composite action is conservatively ignored in current practice due to the absence of standardised design guidance. However, its benefit may be considered when assessing the dynamic response of a floor (SCI, 2024). A clear distinction must be maintained between lateral stability and composite behaviour; a beam may be considered laterally restrained even in the absence of significant longitudinal shear transfer at the interface. The effects of elevated temperature on lateral restraint and composite action are discussed in Section 2.4.

2.1.4 Mechanical Properties Relevant to Hybrid Structural Design

Timber exhibits an orthotropic nature, with markedly different mechanical properties parallel (longitudinal) and perpendicular (radial and tangential) to the grain. The linear elastic behaviour of orthotropic materials can be described by nine independent elastic constants (Senalik and Farber, 2021). However, it is often difficult to distinguish between radial and tangential properties in practice, and therefore it is common to assume that these properties are similar. As a result, the mechanical properties of timber are typically described in terms of parallel and perpendicular directions to the grain for design purposes.

At ambient temperature, the structural response of hybrid systems is governed by the mechanical properties of the constituent materials and their interaction. For CLT, the orthotropic elastic moduli, shear moduli, and rolling-shear characteristics determine flexural and shear behaviour (BS EN 16351, 2021). For steel beams, the elastic modulus and yield strength govern stiffness and ultimate resistance (BS EN 1993-1-1, 2005), while torsional and warping stiffness influence stability performance. The relative stiffness ratio between steel and CLT, together with the slip characteristics of the connectors, governs the development of composite action or effective lateral restraint. These ambient-temperature properties form the basis for understanding hybrid behaviour prior to consideration of thermo-mechanical degradation under fire conditions.

2.2 Material Behaviour of Timber and Steel at Elevated Temperatures

Timber and steel undergo distinct thermal and mechanical degradation mechanisms at elevated temperatures. Understanding their temperature-dependent properties is therefore essential for predicting thermo-mechanical behaviour under fire, which is fundamental to structural fire design. The material properties presented in this section are based on the first-generation Eurocodes. The second-generation Eurocode 5 includes provisions for engineered timber products such as CLT and distinguishes between maintained and non-maintained bond-line integrity in the charring model (Frangi *et al.*, 2025).

2.2.1 CLT as a Material in Fire

When heated, timber undergoes complex physical and chemical changes. The thermal response of CLT is characterised by the formation of distinct degradation zones, as illustrated in Figure 2.4, which develop as heat penetrates the cross-section (Bartlett, Hadden and Bisby, 2019). The virgin zone is unaffected by fire and retains the original ambient temperature properties of the timber. It is hypothesised that as heat moves inward, it creates a condensation zone with high local moisture content, where some water vapour generated from hotter regions migrates into the cooler core and condenses. This is followed by the dehydration zone, where free water begins to evaporate as temperatures approach 100 °C, with some vapour migrating and accumulating in the condensation zone (White and Dietenberger, 2001).

At temperatures above approximately 200 °C, the solid phase of timber undergoes irreversible physical and chemical decomposition known as pyrolysis, resulting in the release of volatile gases and the formation of char (White and Dietenberger, 2001). While pyrolysis generates the volatile gases required for flaming combustion (gas-phase oxidation) and the residual char may undergo smouldering combustion (solid-phase oxidation), the reaction itself is driven primarily by heat and occurs independently of oxygen availability. Above approximately the 300 °C isotherm, the material is completely converted into a char layer (Browne, 1958; BS EN 1995-1-2, 2004). Although char is mechanically ineffective, it provides significant thermal insulation due to its low conductivity, thereby slowing heat penetration into the underlying layers. Cracking of the char layer can locally increase heat transfer into the underlying pyrolysis zone (Šejna *et al.*, 2025).

At the exposed surface, a char oxidation zone develops, where the char reacts with oxygen at elevated temperatures to produce ash and other gases. This zone is associated with smouldering-type combustion processes, which progressively consume the char layer. In CLT, the development of these thermal degradation zones is further complicated by the adhesive performance at the bond lines, which can lead to delamination and exposes virgin wood to the fire (Brandon and Dagenais, 2018). This can result in loss of the protective char layer, fire regrowth, and more complex fire behaviour than in solid timber. Further details are provided in Section 2.3.1.

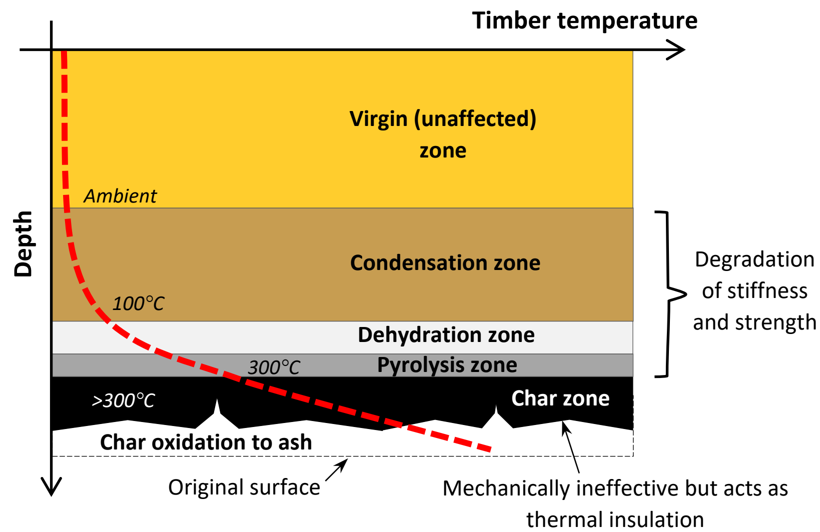

Figure 2.4: Schematic representation of thermal degradation zones in burning timber

2.2.2 Thermal Properties of CLT

The thermal response of CLT in fire is governed by its thermal conductivity, specific heat capacity, and density, all of which are temperature-dependent. BS EN 1995-1-2 (2004) provides thermal properties for wood specifically calibrated for standard heating conditions. Although CLT is not explicitly addressed in Eurocode 5, it is commonly simulated using the thermal properties prescribed for solid timber, provided that panel or bond line integrity is maintained. For numerical modelling, these properties are typically implemented as effective values, which implicitly account for the complex interactions of moisture migration and the physicochemical degradation of the timber matrix (König, 2005; König, 2006). As these effective properties were developed for standard fire conditions, they may not accurately represent non-standard fire exposure or cases where adhesive thermal delamination occurs (Kleinhenz, Just and Frangi, 2021). One approach to non-standard fire exposures would be to artificially modify the thermal properties to incorporate heat generation of the timber combustion to better capture the observed behaviour (Chen *et al.*, 2026).

Figure 2.5 illustrates the temperature-dependent thermal conductivity, specific heat capacity, and density of timber according to Eurocode 5. Thermal conductivity increases with temperature, while the specific heat exhibits a peak around 100 °C due to moisture evaporation. The density is represented through a reduction factor to account for mass loss associated with thermal degradation. Although Eurocode 5 neglects the thermal expansion of timber, this effect is investigated in the present study by adopting coefficients of thermal expansion (CTE) of 4×10^{-6} /°C parallel to the grain and 25×10^{-6} /°C perpendicular to the grain between 20 °C and 200 °C, decreasing linearly to zero at 300 °C (Goli *et al.*, 2019; Adibaskoro *et al.*, 2021). This is illustrated in Figure 2.5(d).

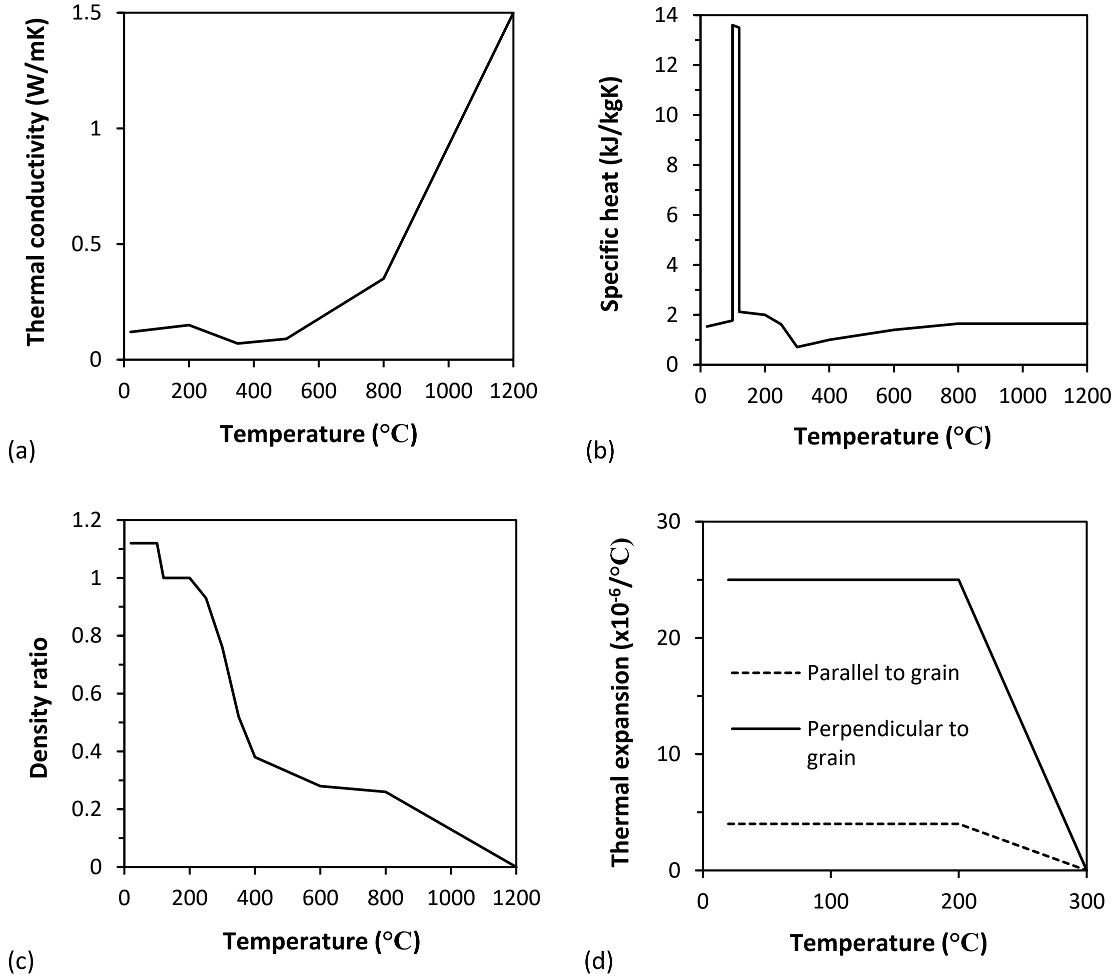

Figure 2.5: (a) Thermal conductivity, (b) specific heat capacity, (c) density ratio with 12% moisture content, and (d) coefficient of thermal expansion (CTE) of timber

2.2.3 Mechanical Properties of CLT

Numerical modelling of CLT relies on an accurate representation of the mechanical properties of timber. Key properties include Young's modulus of elasticity, shear modulus, Poisson's ratio, and strength, which are influenced by factors such as wood species, density, moisture content, temperature, loading direction relative to the grain, load duration, and natural defects (LaMalva and Hopkin, 2021). Timber exhibits brittle behaviour in tension and more ductile behaviour in compression, with higher stiffness and strength parallel to the grain than perpendicular to it. As temperature increases, both strength and stiffness degrade progressively. BS EN 1995-1-2 (2004) provides temperature-dependent reduction factors for these properties, as illustrated in Figure 2.6, which are commonly used in structural fire design. However, these have been calibrated for standard fire exposure and a comprehensive constitutive model for the non-linear behaviour of timber is lacking (Ma *et al.*, 2025).

Although Eurocode 5 defines distinct stiffness reductions for tension and compression, simplified material models often assume a symmetric elastic law. Consequently, a single mean stiffness reduction factor is typically used. The Eurocode 5 strength degradation models also appear conservative compared with the experimental datasets on solid timber specimens (Garcia-Castillo, Gernay and Paya-Zaforteza, 2023). Despite these limitations, the mechanical properties defined in Eurocode 5 have been successfully applied to simulate the fire behaviour of loaded CLT panels with reasonable accuracy. However, where CLT is susceptible to delamination, the temperature-dependent behaviour of the adhesive bond lines must also be considered in the mechanical model (Wang *et al.*, 2020).

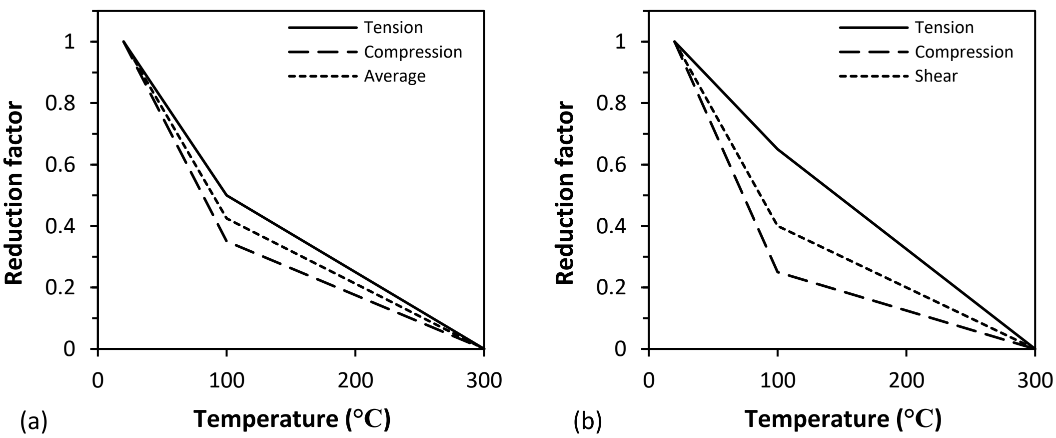

Figure 2.6: Temperature-dependent reduction factors for (a) stiffness and (b) strength of timber

2.2.4 Structural Steel as a Material in Fire

Steel structures subjected to fire experience significant changes in material properties and structural behaviour. Elevated temperatures reduce stiffness and strength, while restrained thermal expansion can induce additional member forces and compromise stability. Furthermore, non-uniform temperature distribution across the cross-section of a steel member can lead to thermal bowing due to differential expansion. Design must account not only for material degradation and high-temperature creep but also for potential instability, thermal gradients, connection behaviour, and support conditions, as these factors collectively govern the failure mechanisms of steel members under fire exposure (Usmani *et al.*, 2001; Wang *et al.*, 2012).

2.2.5 Thermal Properties of Steel

The thermal response of steel in fire is governed by its thermal conductivity, specific heat capacity, and thermal expansion, all of which are temperature-dependent. Figure 2.7 illustrates these temperature-dependent properties for carbon structural steel based on BS EN 1993-1-2 (2005). Thermal conductivity controls the rate of heat transfer within the material and generally decreases with increasing temperature. In contrast, the specific heat capacity increases with temperature and exhibits a pronounced peak around 735 °C associated with phase transformations, which slows the rate of temperature rise by absorbing a significant amount of latent heat. The higher the specific heat of a material, the more slowly it tends to heat up. The density of steel is typically assumed constant in structural fire analysis, while thermal expansion is considered separately as a mechanical strain, influencing the development of thermal strains and fire-induced internal forces in restrained members.

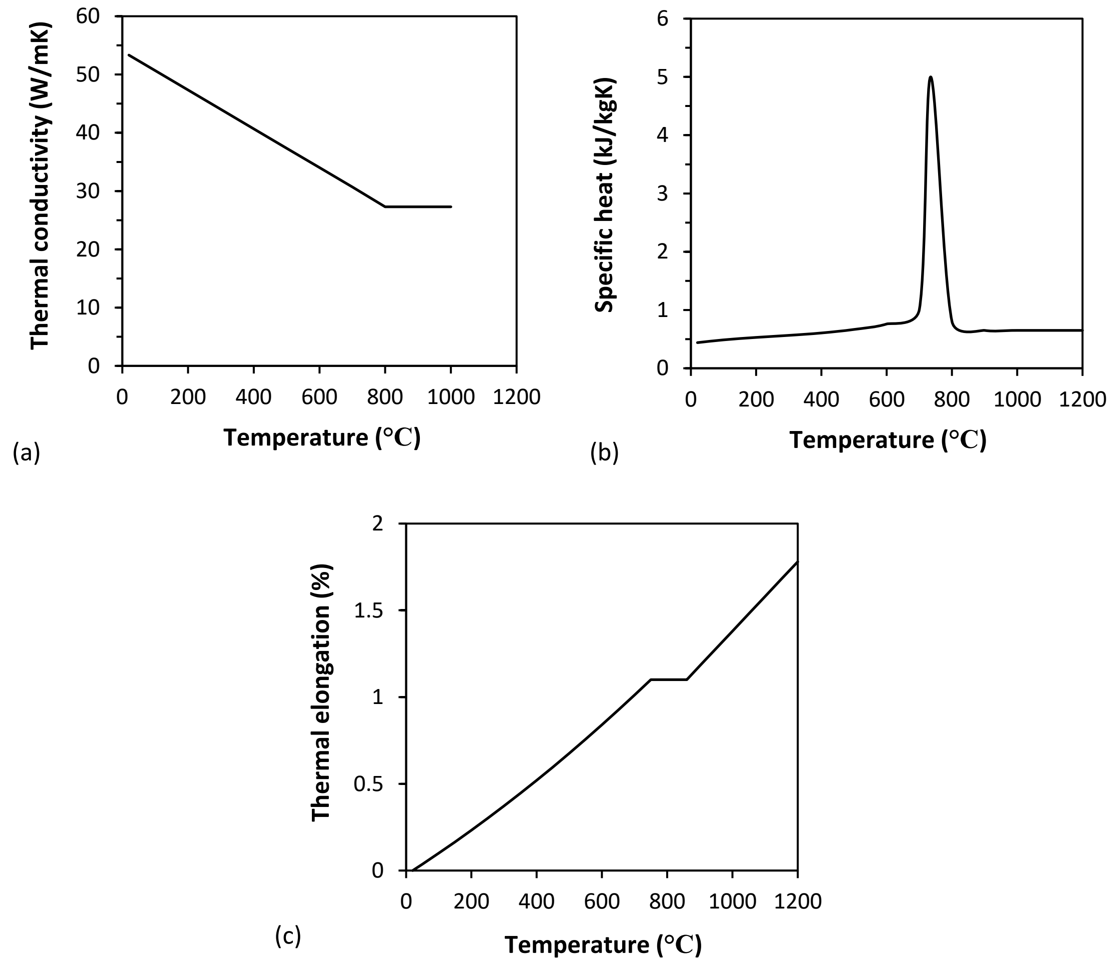

Figure 2.7: (a) Thermal conductivity, (b) specific heat capacity, and (c) thermal elongation of steel

2.2.6 Mechanical Properties of Steel

The mechanical performance of structural steel at elevated temperatures is characterised by significant reductions in both modulus of elasticity and yield strength. As temperature increases, the stress-strain response becomes increasingly elliptical, losing the distinct linear-elastic region and yield plateau observed at ambient conditions. Accurate representation of this behaviour requires non-linear constitutive models, such as the temperature-dependent stress-strain relationships provided in Eurocode 3 or Ramberg-Osgood formulations (Wang *et al.*, 2012). The Eurocode model, as illustrated in Figure 2.8, incorporates temperature-dependent reduction factors for stiffness and strength and implicitly accounts for time-dependent creep effects at elevated temperatures.

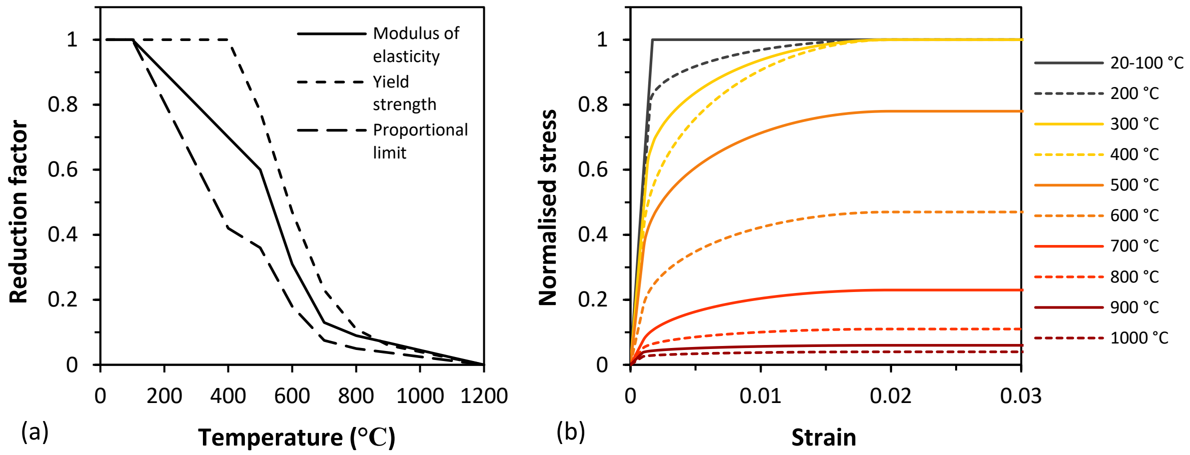

Figure 2.8: (a) Temperature-dependent reduction factors and (b) normalised stress-strain curves for steel

2.3 Structural Response of CLT Floor and Steel Beams in Fire

Steel-CLT hybrid structures exhibit complex thermo-mechanical behaviour in fire, as timber undergoes charring while steel is highly sensitive to restrained thermal expansion, which can trigger instability failures. Understanding the elevated-temperature behaviour of each component in isolation is therefore essential for evaluating the response of hybrid systems.

2.3.1 CLT Floor Response in Fire

Cross-laminated timber floor systems are widely used as load-bearing elements in mass timber buildings. When exposed to fire, their structural response is governed primarily by the charring of exposed timber surfaces, which reduces the effective load-bearing cross-section. As the char layer develops, it provides thermal insulation to the underlying timber, slowing heat penetration. However, the remaining uncharred section must carry the applied loads with diminished stiffness and strength, leading to increased deflection and a gradual loss of load-bearing capacity as fire exposure continues (Lineham *et al.*, 2016).

A critical aspect of CLT floor performance is the risk of heat-induced delamination at the glue line, occurring when adhesive bonds degrade at elevated temperatures behind the charring front. If delamination occurs, outer charred layers can detach and expose fresh timber to re-ignition, accelerating charring and altering both the thermal and structural response of the panel. Repeated delamination can expose successive layers, increasing heat release and contributing to fire regrowth, with the extent depending on adhesive type, lamella thickness, moisture content, loading, and fire severity (Liu and Fischer, 2022; Bøe *et al.*, 2023).

The fire performance of CLT floors is also influenced by whether the timber surfaces are exposed or protected. Encapsulation using fire-resistant linings can delay the onset of charring and extend the period during which the structural element retains its full cross-section. Once protective linings fail, the panel may transition rapidly from protected to exposed behaviour, leading to accelerated section loss (Hadden *et al.*, 2017). In contrast, fully exposed CLT elements can increase the compartment fire load and prolong the duration of burning, affecting both the structural response and the fire dynamics, with the extent depending on exposed timber surface area, ventilation conditions, and available fuel (Liu and Fischer, 2022).

Figure 2.9 schematically illustrates the potential development of fire in timber compartments, including thermal feedback between exposed CLT surfaces.

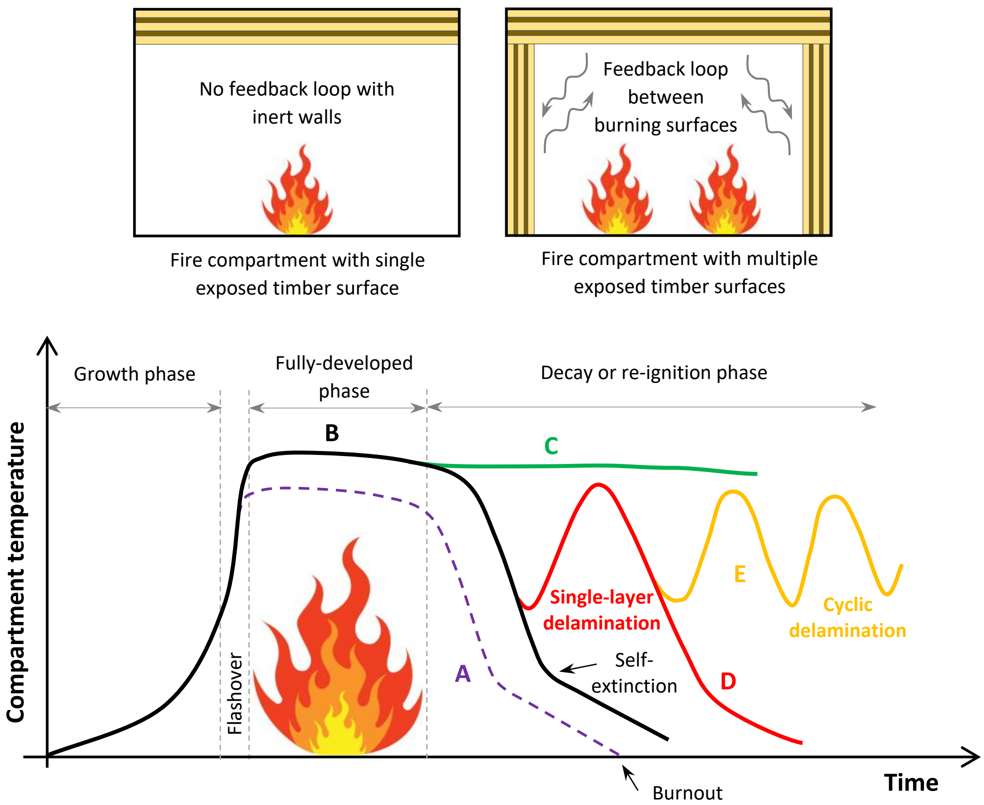

A: Non-combustible compartment or fully encapsulated timber structure
B: Exposed or partially protected timber structure with self-extinction (no delamination)
C: Exposed or partially protected timber structure without self-extinction (exposed timber continues to contribute to fire e.g. multiple burning surfaces creating a self-sustaining feedback loop)
D: Fire regrowth due to single-layer delamination exposing fresh timber surfaces
E: Fire regrowth due to cyclic delamination exposing successive timber layers

Figure 2.9: Schematic representation of possible compartment fire development in timber structures based on experiments by Hadden *et al.* (2017) and Bartlett *et al.* (2020)

Under certain conditions, exposed timber elements may exhibit self-extinction, a phenomenon in which flaming combustion ceases when the external heat flux is removed or drops below a critical threshold required to sustain pyrolysis and gas-phase combustion. While self-extinction is a recognised mechanism for enhancing the fire safety of mass timber buildings, it is associated with significant uncertainty and is typically demonstrated under simple and well-controlled configurations. In CLT, delamination can re-expose virgin timber, increase heat release, and sustain flaming combustion, potentially preventing self-extinction under certain conditions. Even when flaming ceases, smouldering combustion may persist, which can lead to continued degradation and potential structural failure at later stages (Bartlett *et al.*, 2017; Xu *et al.*, 2022; Wiesner *et al.*, 2025).

2.3.2 Simply Supported Steel Beam in Fire

The structural response of simply supported steel beams subjected to fire has historically been characterised through isolated member testing under standard fire conditions (Bisby, Gales and Maluk, 2013). In this idealised, statically determinate configuration, the beam is free to expand axially and does not interact with adjacent structural components. Heating is typically applied according to a standard fire curve, such as ISO 834 or ASTM E119. These curves represent continuously increasing furnace temperatures and do not include a cooling phase.

The structural response in this scenario is governed primarily by temperature-dependent degradation of material properties and non-uniform thermal gradients through the cross-section. According to Eurocode 3, both the elastic modulus and yield strength reduce significantly with temperature, with stiffness loss preceding strength reduction. Thermal expansion also produces additional sagging curvature, particularly when non-uniform heating causes the bottom flange to expand more rapidly than the top flange, resulting in thermal bowing. This curvature develops while generating only negligible axial forces, as longitudinal expansion is effectively unrestrained. The temperature-deflection response typically progresses from an initial stiffness-controlled phase to a non-linear yielding phase, and ultimately to a runaway deflection phase in which small temperature increases produce disproportionately large displacements (Buchanan *et al.*, 2004). In some cases, the load-bearing limit is reached before the runaway phase occurs.

In standard fire-resistance testing, simply supported steel beams are primarily assessed against the load-bearing (R) criterion. A beam may fail through loss of load-bearing capacity, typically associated with plastic hinge formation or structural instability such as lateral–torsional buckling. Failure may also occur when vertical deflection exceeds the allowable limit specified in the test standard, even if the member is still capable of sustaining the applied load.

In addition, an excessive rate of deflection is recognised as an indicator of impending runaway behaviour and constitutes a separate failure criterion, as defined in BS EN 1363-1 (2020). As axial expansion is largely unrestrained in a simply supported beam, failure is governed by flexural softening rather than thermally induced compression. The reported fire resistance therefore corresponds to the time or temperature at which the first of the prescribed failure limits is reached, distinguishing between ultimate (load-bearing) failure and deflection-based criteria.

2.3.3 Axially Restrained Steel Beam in Fire

In real structures, steel beams do not behave as isolated members. Interaction with surrounding structural components, including slabs, connections, and adjacent framing, introduces varying degrees of axial and rotational restraint. Axial restraint fundamentally alters their fire behaviour compared with simply supported beams. When thermal expansion is restrained, axial forces develop, which may be compressive during early heating and tensile at large deflections or during cooling (Wang, 2002). Rotational restraint is neglected here for simplicity, as typical simple construction connections provide limited rotational stiffness and bending resistance reduces significantly once catenary action develops.

Figure 2.10 compares the typical fire-induced behaviour of simply supported and axially restrained steel beams with temperature. The behaviour of axially restrained beams under fire can be described using a three-stage response, based on the assumption that they are adequately restrained against lateral-torsional buckling (Liu, Fahad and Davies, 2002). In the initial compression phase, restrained thermal expansion generates increasing compressive axial force while deflections remain relatively small, though generally comparable to or slightly greater than those in unrestrained beams. Non-uniform heating can also result in thermal bowing due to a cooler top flange. This is followed by a transition phase which is characterised by rapid increases in deflection and a reduction in compressive axial force due to material softening. At larger deflections, the structural behaviour transitions into a catenary phase, where bending resistance has significantly degraded and load is carried primarily through axial tension in a cable-like manner despite severe material degradation and large vertical deflections. Ultimate failure typically occurs when the tensile capacity of either the member or its connections is exceeded. Although catenary action can enhance the load-carrying capacity of a restrained beam, its development requires large deformations that can trigger slab integrity failure or local failures at the connections, so it cannot generally be relied upon in conventional design (Wang and Yin, 2006). Thermal expansion of heated members can also affect the displacement of adjacent members inside or outside a fire compartment. Chapters 3 and 4 further explore the influence of axial restraint within hybrid systems.

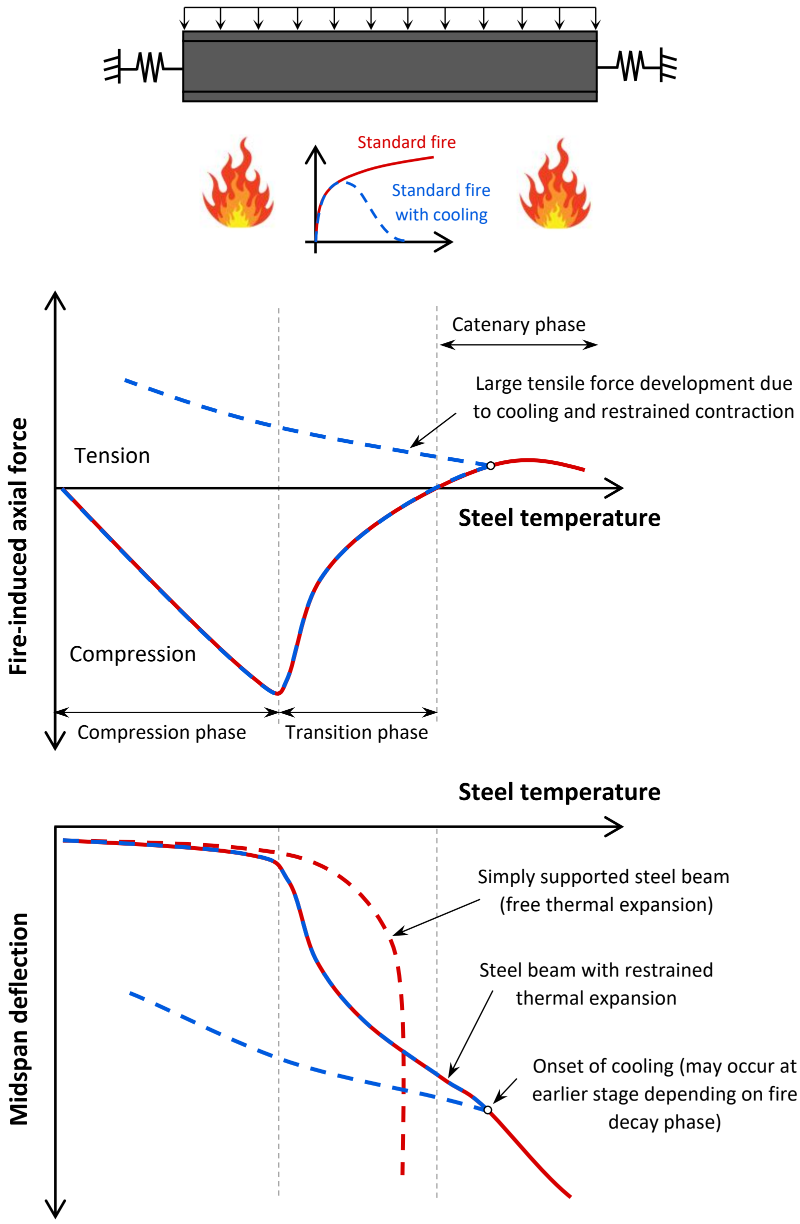

Figure 2.10: Comparison of thermo-mechanical response of simply supported and axially restrained steel beams during heating and cooling phases

While catenary action can provide additional load-carrying capacity during heating, further tensile forces may develop during the cooling phase of a fire, a behaviour that is not captured in standard furnace tests (Li and Guo, 2008). As the beam cools and attempts to contract, restraint to thermal shortening can generate significant tensile forces, even if the beam was previously in compression during heating. These forces may exceed the capacity of connections or supporting columns, leading to connection fracture or pull-in failures in which the contracting beam draws the supporting columns inward. Such cooling-phase effects highlight the importance of connection performance in maintaining frame stability throughout the fire event.

Experimental and numerical studies indicate that bare steel beams and steel-concrete composite beams exhibit broadly similar fire-induced behaviour, with both systems following the same overall pattern of response under elevated temperatures (Bailey, 1998; Liu, Fahad and Davies, 2002; Buchanan *et al.*, 2004). Evidence from the Cardington full-scale fire tests demonstrated that composite beam systems can survive steel temperatures exceeding 1000 °C, far above those considered critical in isolated member tests, indicating large reserves of fire resistance. Tensile membrane action in the slabs at large displacements allowed unprotected secondary beams to sustain loads well beyond traditional fire-resistance limits by developing alternative load paths (British Steel, 1999). The columns and primary beams were fire-protected to maintain overall frame stability and load redistribution during fire exposure.

Overall, these findings indicate that the beam behaviour observed in the Cardington tests broadly reflected the restrained fire-induced response identified in smaller-scale beam studies. However, the tensile membrane action characteristic of reinforced concrete composite floors is unlikely to develop in steel-CLT floor systems without a reinforced concrete topping, as CLT slabs lack continuous ductile reinforcement capable of sustaining large in-plane tensile forces.

2.4 Thermo-Mechanical Behaviour of Steel-CLT Hybrid Structures in Fire

In fire, the contrasting thermal responses of steel and timber lead to complex thermo-mechanical interactions in hybrid systems. A clear understanding of these mechanisms and the associated fire safety principles is therefore essential for evaluating structural stability and composite behaviour at elevated temperatures.

2.4.1 Fire Safety Principles for Steel-Timber Hybrid Structures

Fire safety in England is regulated by the statutory functional requirements of Part B of the Building Regulations, which comprise means of warning and escape (B1), internal fire spread through linings (B2), internal fire spread through the structure (B3), external fire spread (B4), and access and facilities for the fire service (B5) (The Building Regulations 2010). These requirements apply to all construction materials, whether combustible (e.g. timber) or non-combustible (e.g. steel and concrete). Compliance with the functional requirements may be demonstrated using either prescriptive or performance-based design approaches.

In a prescriptive approach, compliance is achieved by adhering to predefined rules set out in practical guidance such as Approved Document B (HM Government, 2019). These rules specify minimum fire resistance ratings for structural and compartment elements, based on factors such as building height, occupancy, and provisions for firefighting (e.g. sprinklers). Fire resistance is classified in terms of load-bearing capacity (R), integrity (E), and insulation (I). While structural elements (e.g. beams and columns) must typically maintain R for a specified period, elements serving as both load-bearing and compartmentation (e.g. floors and walls) must achieve REI performance for the required duration to maintain stability and prevent fire spread. This is illustrated for steel-timber hybrid buildings in Figure 2.11. While prescriptive methods are straightforward to apply, they can be restrictive for complex buildings or the use of materials such as timber, where design must also account for charring rates, section loss, and potential delamination. Where prescriptive provisions are not directly applicable or are insufficient to demonstrate compliance, the functional requirements of the Building Regulations may instead be satisfied using performance-based design.

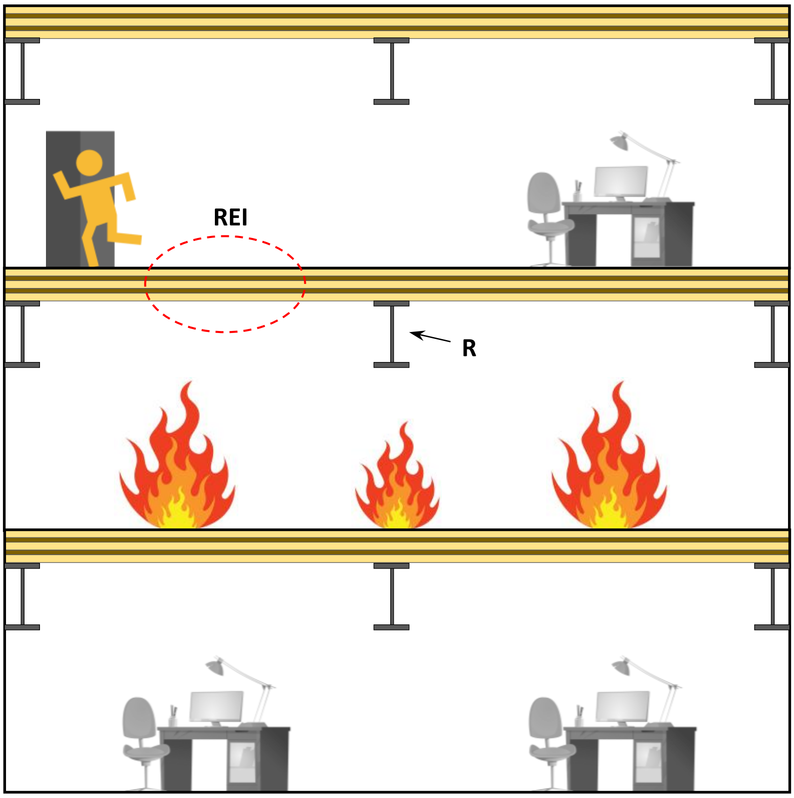

Figure 2.11: Schematic of a steel-timber hybrid building under fire, showing performance requirements for load-bearing capacity (R), integrity (E), and insulation (I)

Performance-based design is a methodology to achieve specified fire safety objectives and performance criteria through the application of scientific and engineering principles. Compliance is demonstrated by directly assessing whether the building satisfies the functional requirements under project-specific fire scenarios, rather than relying on prescriptive rules. This approach evaluates the building's response using analytical, numerical, or experimental methods. This includes, for example, modelling fire dynamics in compartments, smoke and heat transport, egress analysis for occupant evacuation, and thermal and mechanical response of structural elements. Performance is assessed against defined acceptance criteria, such as maintaining structural stability for the required duration or until burnout, ensuring tenable conditions for safe evacuation, and limiting fire and smoke spread (Gernay, 2024).

A key consideration in mass timber design is whether structural timber elements are exposed to fire. Fire strategies vary with building height and occupancy. Lower consequence buildings only require structural stability for a prescribed fire resistance period (e.g. 60 minutes) to facilitate safe evacuation and firefighting intervention. Conversely, higher consequence buildings must satisfy a burnout criterion; timber elements must either be fully encapsulated to prevent fuel contribution during the design fire resistance period, or be designed to achieve self-extinction while maintaining stability during and after the fire (STA, 2023).

Figure 2.12 shows the compliance routes for timber buildings to achieve structural stability in fire. Low-rise buildings may allow exposed or partially protected timber and adopt a strategy accepting structural failure after the required fire resistance period, whereas medium- and high-rise buildings typically require encapsulation or demonstrated self-extinguishing behaviour to survive burnout. Consequently, performance-based approaches are often required for taller or higher-consequence buildings (STA, 2023; Built by Nature, 2026).

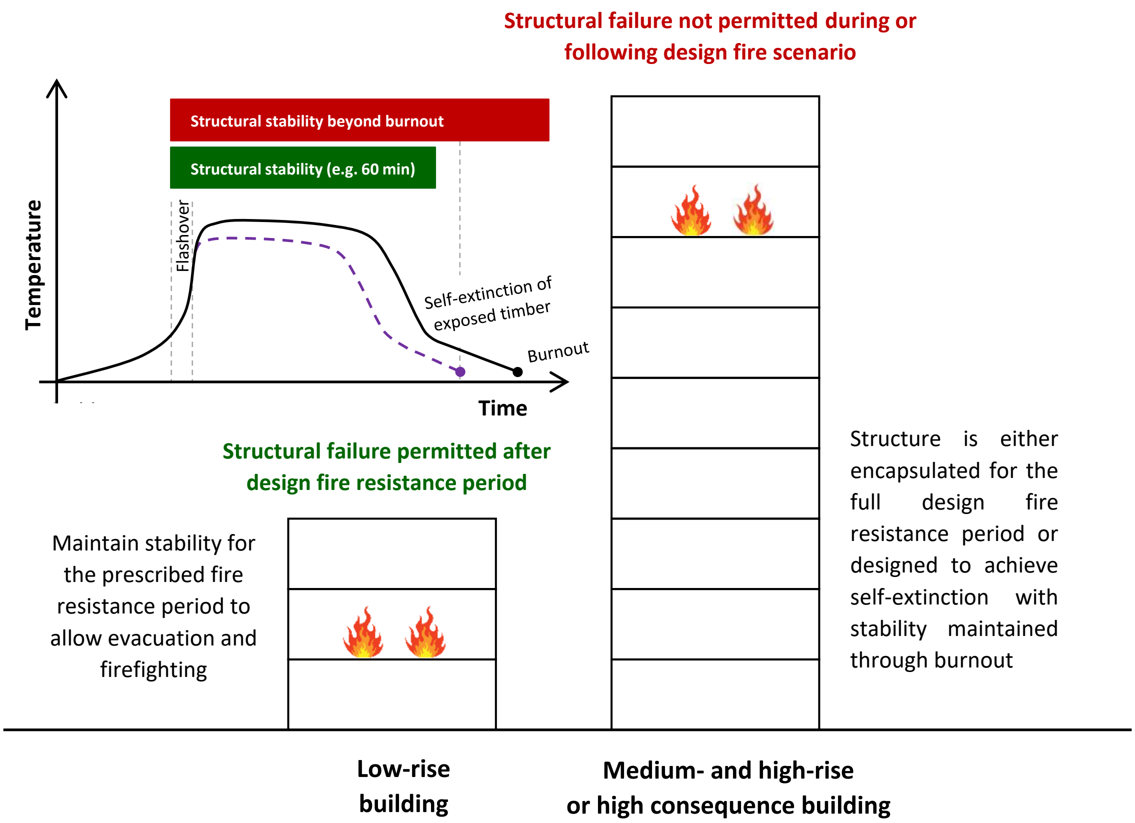

Figure 2.12: Illustration of compliance routes for timber buildings to achieve structural stability in fire

However, there is currently no international consensus, with fire design strategies varying across regional practices (Östman, Brandon and Frantzich, 2017), particularly regarding encapsulation, the extent of CLT exposure, and the thermal performance of adhesives, all of which influence delamination behaviour and the potential for self-extinction. In steel-timber hybrid buildings, restricting exposed timber to the ceiling surface may limit the participation of timber in compartment fire development when compared with mass timber buildings incorporating more extensive exposed timber surfaces, thereby increasing the likelihood of self-extinction (Bøe *et al.*, 2023; Ali Awadallah, Hadden and Law, 2024; Arup, 2024).

2.4.2 Interaction between Steel and CLT in Fire

The fire performance of steel-CLT hybrid systems is governed by the interaction between materials with significantly different thermal and mechanical properties. Steel heats rapidly when exposed to fire due to its high thermal conductivity, whereas timber experiences a slower temperature rise because of its inherently lower thermal conductivity. The formation of an insulating char layer during fire exposure further reduces heat flux into the remaining wood core. Consequently, hybrid assemblies may develop non-uniform temperature distributions, particularly where CLT panels partially shield the top flange of steel beams from direct fire exposure (Barber, Roy-Poirier and Wingo, 2021; Godoy Dellepiani *et al.*, 2023).

Although the CLT slab may protect the upper flange from direct flame exposure, the steel beam can act as a thermal bridge that conducts heat toward the steel-timber interface. Heat transferred through the steel flange may therefore cause localised heating and charring of the timber directly above the beam. Most experimental studies of steel-timber hybrid floor systems in fire have focused on slim-floor configurations, where the steel beam is partially embedded within the floor depth (Malaska *et al.*, 2023; Dumler *et al.*, 2025; Aprisa *et al.*, 2026). As a result, the thermal behaviour of downstand steel beams supporting CLT panels is less frequently discussed in the literature. Nevertheless, furnace tests on slimfloor systems have demonstrated that steel sections can conduct heat into the supported timber region, not only from below but also laterally via the web, initiating localised charring near the beam-timber interface.

Mechanical connectors used to join CLT panels to steel beams can further influence the interaction between the materials. Screws or fasteners may provide additional conductive pathways, locally increasing heat transfer within the connection region (Létourneau-Gagnon, Dagenais and Blanchet, 2021; Kinnersley *et al.*, 2026). The char layer at the timber surface has limited mechanical strength and may locally crush under vertical load on the top flange. Differential thermal expansion between steel and timber can affect the interface behaviour, particularly when the timber remains relatively cool and restrains expansion of the heated steel beam, generating local thermal stresses. Similar effects may also occur in timber-concrete composite systems due to differential thermal elongation (Iwase *et al.*, 2025). Under fire conditions, degradation of the timber and connectors may modify the interface, potentially altering local contact conditions and heat transfer across the steel-CLT interface.

Understanding these local thermal and mechanical interactions at the steel-CLT interface provides the basis for assessing the stability and composite behaviour of downstand hybrid beams under fire. Unlike steel-concrete beams, where the concrete generally maintains reliable lateral restraint and composite action at elevated temperatures, the performance of steel-CLT systems may be more sensitive to connector and timber degradation, influencing beam stability and load sharing between components. These effects are further explored in Chapters 3 and 4 in the context of structural stability, and in Chapter 5 for composite action.

2.4.3 Lateral-Torsional Buckling in Fire

Lateral-torsional buckling (LTB) is a global instability phenomenon that may occur in steel beams at both ambient and elevated temperatures. It arises when the compression flange of a beam subjected to bending is insufficiently restrained, causing lateral displacement of the compression flange accompanied by torsional rotation of the cross-section (Timoshenko and Gere, 1961; Trahair, 1993). This coupled lateral-torsional response, as illustrated in Figure 2.13, may lead to instability before the beam reaches its full plastic moment resistance, making LTB an important consideration in steel beam design.

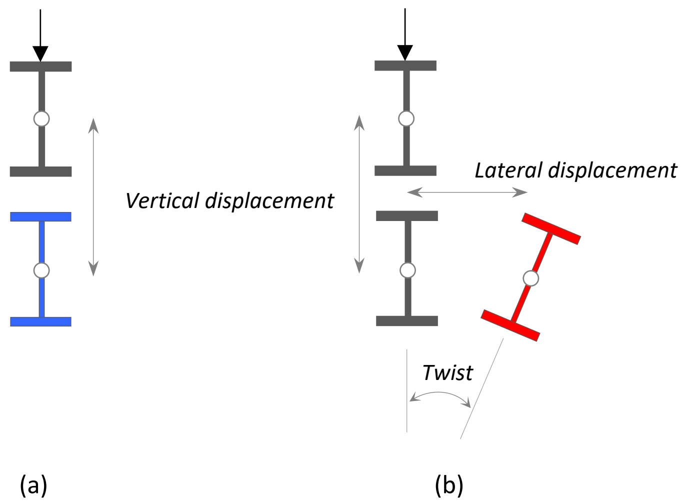

Figure 2.13: Schematic representation of steel beam deformation showing (a) fully restrained case with vertical displacement only, and (b) beam undergoing lateral-torsional buckling with lateral displacement and twist

Under fire conditions, the susceptibility of steel members to LTB increases because material properties degrade at elevated temperatures. As the temperature rises, the elastic modulus decreases, reducing the flexural and torsional stiffness of the member and lowering the critical lateral-torsional buckling moment. At the same time, the yield strength decreases, reducing the plastic moment resistance of the section. Together, these effects make the beam more prone to instability during fire exposure (Bailey, Burgess and Plank, 1996; Mesquita *et al.*, 2005).

In conventional steel-concrete composite construction, the top flanges of downstand steel beams are typically assumed to be fully restrained laterally by the concrete slab. This restraint is achieved through interfacial shear transfer, primarily provided by mechanical connectors and, where applicable, frictional interlock between the slab and the steel flange. In the absence of these connectors, the beam may behave as an unbraced member; while interfacial friction offers a nominal degree of restraint, it is generally considered insufficient and unreliable for design purposes (SCI, 2011).

In steel-CLT hybrid systems, lateral restraint is governed primarily by the in-plane stiffness of the timber panels and the lateral stiffness of the steel-to-timber connections, which control the onset of LTB. Although rotational stiffness in the connections can theoretically improve resistance to twisting (Gao and Moen, 2012), this effect is likely limited in screw-type fasteners due to local bending of the screws and timber embedment deformations in fire. Consequently, lateral stiffness is considered the primary contributor to suppressing LTB. Elevated temperatures degrade timber embedment and overall connection stiffness, progressively weakening lateral and any rotational restraint and thereby increasing the risk of LTB. The influence of screw load-slip behaviour, with particular attention to slip modulus, is further evaluated in Chapters 3 and 4.

Overall, lateral-torsional buckling behaviour of steel-CLT hybrid beams in fire is governed by the complex interaction between material degradation and the evolving restraint provided by the connectors and timber panels. Due to the lack of experimental evidence for downstand configurations, the reliability of lateral restraint under fire remains uncertain, emphasising the importance of considering LTB in the design and assessment of hybrid systems (AISC, 2022; SCI, 2024).

2.4.4 Composite Action in Fire

Composite action in steel-CLT hybrid systems refers to the structural interaction between a timber slab and a supporting steel beam, whereby the combined section exhibits enhanced stiffness and strength compared to the individual components acting independently. This interaction is governed by the transfer of longitudinal shear forces at the interface, typically achieved through mechanical fasteners or adhesive bonding. The performance of these systems is bounded by two theoretical limits: full interaction, characterised by zero interfacial slip and complete strain compatibility, and zero interaction, where the components act independently. In practice, most hybrid systems exhibit partial composite action, in which the degree of shear transfer is controlled by the load-slip behaviour and spatial distribution of the connectors (SCI, 2015).

Under fire conditions, the effectiveness of composite action is significantly influenced by the degradation of materials and connectors. Elevated temperatures reduce the stiffness and strength of steel, while timber undergoes charring and progressive loss of cross-section. Simultaneously, deterioration in the stiffness and capacity of mechanical fasteners promotes interfacial slip and increases the demand on the heated steel beam. Once charring reaches the vicinity of the fasteners, the embedment strength of the timber can decrease significantly, leading to a reduction in connector performance and shear transfer capacity (Barber, Roy-

Poirier and Wingo, 2021). Differential thermal expansion between the rapidly heating steel beam and the CLT slab can further contribute to interfacial slip.

Unlike steel-concrete composite beams, where the concrete slab generally retains some capacity to transfer shear over a significant portion of the fire exposure (Huang, Burgess and Plank, 1999), steel-CLT systems may not exhibit the same level of thermo-mechanical robustness at the interface. Localised heating can lead to charring of the timber above the flange and subsequent crushing of the char layer, along with degradation of the shear connectors. These effects may increase interfacial slip and result in a transition towards non-composite behaviour. Figure 2.14 illustrates this contrast in fire performance, showing the integrity of the concrete slab and the development of timber charring and interface degradation in the CLT slab.

Given the absence of experimental data for steel-CLT composite systems in fire, particularly for downstand configurations, current understanding of composite action degradation is largely inferred from numerical modelling and analogy with steel-concrete systems. The study by Godoy Dellepiani *et al.* (2023) indicates that composite action may not persist throughout the full duration of a fire. A detailed review of composite action at both ambient and elevated temperatures, including the limitations of existing numerical work, is provided in Chapter 5. Despite these contributions, the literature has not yet established how composite action evolves during fire exposure and this remains an important area for further investigation.

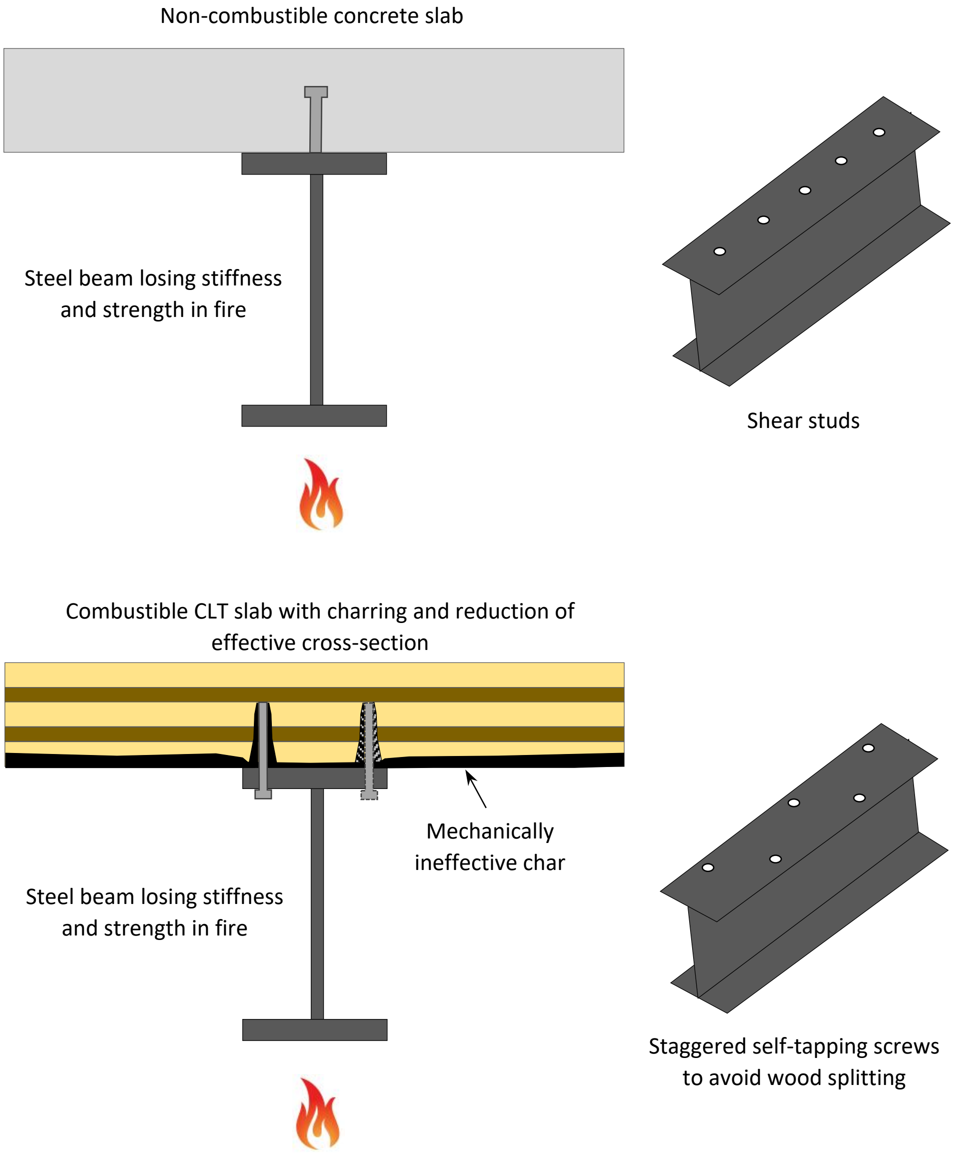

Figure 2.14: Comparative fire response of composite beams showing a non-combustible concrete slab and a reduced CLT slab due to charring, potentially compromising composite action at the shear interface

2.5 Numerical Modelling of Steel-CLT Hybrid Structures in Fire

Numerical modelling can provide an effective means of investigating the fire performance of steel-CLT hybrid structures, particularly given the lack of experimental data for downstand systems. Finite element (FE) analysis enables detailed assessment of thermal and mechanical behaviour at elevated temperatures, including temperature development, material degradation, deformation patterns, and overall structural response. Numerical approaches, which underpin the analyses presented in Chapters 4 and 5, also allow parametric studies that are impractical to achieve experimentally.

2.5.1 Modelling Frameworks

Modelling frameworks for steel-CLT hybrid structures under fire conditions vary in complexity, reflecting the need to capture both thermal and mechanical behaviour within a unified numerical approach. Two principal modelling strategies are reported in the literature: sequentially coupled and fully coupled thermo-mechanical analyses. In sequential models, the temperature field is first obtained from a thermal analysis on the initial undeformed state and subsequently applied to the mechanical model, offering computational efficiency and therefore widespread use in fire engineering (Franssen and Gernay, 2017; Godoy Dellepiani *et al.*, 2023). While this approach is generally appropriate for non-combustible materials, it represents a simplified approximation for timber components. It overlooks critical feedback mechanisms in timber fire dynamics, where damage phenomena such as cracking and delamination can alter heat transfer and expose fresh timber layers to the fire environment. A coupled analysis to capture these phenomena adds significant complexity and is therefore beyond the scope of this study. Fully coupled models, although less common due to their significantly higher computational cost, solve the thermal and mechanical fields simultaneously, capturing interaction effects arising from the coupling between temperature and deformation.

A further distinction exists between modelling scales, namely global and local approaches. Global models employ beam, shell, or solid elements to represent the steel-CLT assembly, using simplified connector or contact formulations to evaluate system-level performance efficiently (Xu, Hofmeyer and Maljaars, 2024). In contrast, local models typically employ solid elements with mesh refinement at critical regions to capture detailed behaviour, albeit at a significantly higher computational cost. These modelling choices inevitably involve trade-offs, often requiring simplifying assumptions such as idealised or simplified boundary conditions. The selected modelling scale also influences the level of detail achievable in both thermal and mechanical analyses, particularly when representing complex phenomena such as charring, delamination, and failure modes.

Regardless of the scale or coupling strategy, rigorous validation against experimental data remains essential. However, datasets for integrated steel-CLT systems remain scarce, with most existing work on either mass timber assemblies or isolated steel elements, highlighting a key limitation in current modelling practice. Consequently, many modelling assumptions cannot yet be validated comprehensively, requiring FE frameworks to rely on calibration and sensitivity analyses to account for uncertainties. These constraints necessitate a cautious interpretation of numerical results and reinforce the importance of continued experimental research to support the development of advanced modelling approaches (Malaska *et al.*, 2023).

The general workflow for FE modelling of structures in fire is summarised in Figure 2.15; thermal analysis is typically driven by heat fluxes derived from temperature-time curves via convection and radiation. In some cases, an iterative or fully coupled approach may be required, particularly where mechanical damage (e.g. cracking and delamination) significantly alters the thermal boundary conditions during the simulation.

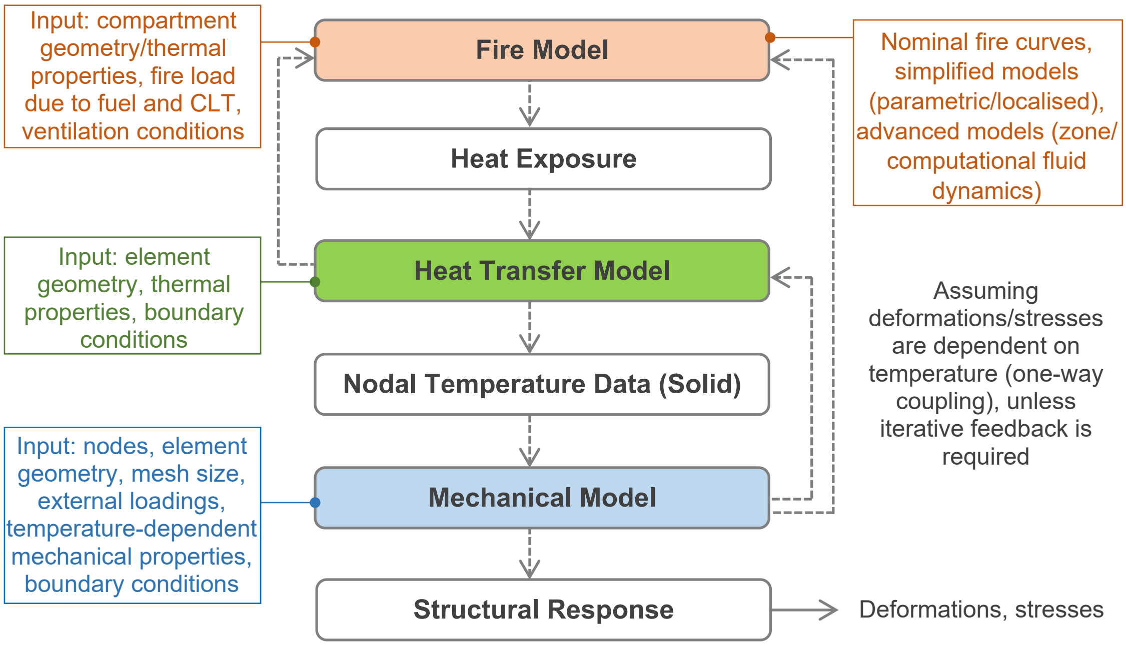

Figure 2.15: Finite element framework for modelling structures in fire

2.5.2 Thermal Modelling

Thermal modelling provides the temperature field required for subsequent mechanical analysis and is therefore a critical component of FE simulations in fire. The thermal response of steel-CLT assemblies is governed by conduction within the materials and convection and radiation at exposed surfaces, typically defined using standard or advanced fire models. Convective heat transfer coefficients and surface emissivity are key parameters influencing the rate of heat input and are often sources of uncertainty in thermal predictions.

Steel components are generally modelled using temperature-dependent thermal properties, with particular attention to heat transfer at steel-timber interfaces. For CLT, thermal modelling must account for timber degradation and progression of the char front. Notably, phenomena such as timber combustion and moisture migration are not typically simulated as explicit thermochemical reactions; instead, their effects are implicitly accounted for through the use of effective temperature-dependent thermal properties (König, 2006). In some cases, additional mechanisms such as lamination fall-off or adhesive failure may be included through element removal or modified boundary conditions. However, these phenomena are often simplified due to their complexity and limited experimental validation (Malaska *et al.*, 2023; Aprisa *et al.*, 2026).

The accuracy of thermal predictions is influenced by uncertainties in material properties, moisture content, and boundary conditions. As a result, calibration against available fire tests is often required, and sensitivity studies are commonly performed to assess the influence of uncertain parameters (e.g. emissivity) on predicted temperature fields (Wang *et al.*, 2012). While thermal analysis defines the temperature field within hybrid systems, the resulting structural response is typically governed by the temperature-dependent degradation of mechanical properties.

2.5.3 High Temperature Mechanical Analysis

Mechanical analysis at elevated temperatures evaluates the structural response of steel-CLT hybrid assemblies under temperature fields obtained from thermal modelling. It considers the temperature-dependent degradation of material properties, geometric changes, and interaction effects between components under fire conditions. Fire-induced deformations such as thermal bowing and differential expansion between materials must also be captured within the mechanical model.

In FE simulations, defining temperature-dependent constitutive models is essential for capturing structural response during fire exposure. For steel components, the material model must account for reductions in elastic modulus, yield strength, and post-yield hardening, alongside the effects of thermal expansion. Conversely, CLT requires a more sophisticated approach due to its inherent orthotropy and the thermo-chemical decomposition of timber. Beyond the geometric loss of cross-section through charring, the material model must accurately represent the thermally affeacted zone beneath the char front. Within this region, mechanical properties undergo non-linear degradation, transitioning from negligible capacity at the char-line interface to the full performance values of virgin timber at the cooler core (Chen, Tung and Karacabeyli, 2022).

Furthermore, a robust constitutive model for timber must account for the ductile response in compression and the abrupt brittle failure in tension. While general-purpose FE software packages are ubiquitous in structural analysis, the literature frequently highlights the necessity of user-defined subroutines to accurately implement these complex, orthotropic constitutive laws (Christoforo *et al.*, 2025). Nevertheless, computational simplifications are often permissible in specific cases by adopting elastic, elasto-plastic or elasto-brittle stress-strain relationships (Quiquero *et al.*, 2020; Chen, Tung and Karacabeyli, 2022; Godoy Dellepiani *et al.*, 2023). For global structural analyses or large-scale fire simulations, these simplifications facilitate a balance between numerical convergence and physical accuracy, particularly when modelling objectives are limited to predicting overall load-bearing capacity rather than localised failure mechanisms.

Connections and interfaces between steel and CLT components also significantly influence the structural response under fire conditions. Load transfer between the materials depends on the load-slip behaviour of the fasteners and the performance of adhesive layers between lamellae, both of which degrade at elevated temperatures. However, in large-scale numerical studies, the temperature-dependent degradation of fasteners and adhesives is often omitted or represented in a highly simplified manner, as explicitly modelling each fastener, adhesive layer, and complex contact interaction requires substantial computational effort. Such simplifications are commonly adopted to ensure numerical stability and computational efficiency, enabling the analysis to focus on the macro-scale structural behaviour (Xu, Hofmeyer and Maljaars, 2024).

In practice, the level of mechanical detail adopted in fire simulations must therefore reflect the intended purpose of the analysis. When the objective is to capture global deformation and load-bearing capacity, simplified constitutive laws and idealised interaction assumptions are generally sufficient. These modelling choices allow large-scale simulations to remain computationally feasible while still capturing the dominant structural mechanisms of steel-CLT hybrid systems, without the need for detailed modelling of localised behaviour.

2.6 Synthesis of Literature and Identification of Research Gaps

The literature reviewed in this chapter demonstrates that while the behaviours of steel and timber under fire are well established individually, their interaction within hybrid systems remains poorly characterised. This is particularly true for downstand steel beams supporting CLT slabs. Existing structural fire design frameworks are predominantly derived from isolated steel members or steel-concrete composite systems, where thermal response, restraint conditions, and interface mechanics differ fundamentally from those governing steel-CLT assemblies. Consequently, the direct application of current design provisions to hybrid systems is not supported by sufficient experimental evidence.

A key theme emerging from the literature is the limited understanding of steel beam stability under fire conditions. Conventional fire design approaches typically idealise beams as either fully laterally restrained or unrestrained, providing little guidance for intermediate lateral restraint scenarios that are common in practice. Moreover, the combined influence of lateral and axial restraint on lateral-torsional buckling behaviour remains poorly understood, particularly at elevated temperatures.

In parallel, this review highlights a substantial knowledge gap in the fire performance of steel-CLT composite systems. Although the mechanics of composite action at ambient temperature are reasonably characterised, its evolution during fire exposure remains insufficiently explored. Elevated temperatures degrade shear connectors, reduce timber embedment strength, and promote interfacial slip through differential thermal expansion. These effects collectively diminish the ability of the interface to transfer longitudinal shear and may lead to an abrupt loss of composite action; however, the mechanisms governing this transition remain largely unknown.

The literature therefore reveals two key and interrelated research gaps:

1) The lateral-torsional buckling behaviour of steel beams under combined partial lateral and axial restraint during fire exposure is not adequately understood, limiting the ability to predict instability in hybrid systems.

2) The composite behaviour of steel-CLT assemblies under fire, particularly the degradation of longitudinal shear transfer, remains under-researched, creating uncertainty about the evolution of composite action in hybrid systems.

These gaps directly motivate the analytical and numerical investigations undertaken in this thesis. The research presented in Chapters 3 to 5 examines how restraint conditions and composite behaviour influence the structural fire performance of downstand steel-CLT hybrid systems, with each chapter addressing a distinct and complementary study. Addressing these challenges is essential for the safe, wider adoption of steel-timber hybrid structures in low-carbon construction.

3

Influence of Continuous Elastic Lateral Restraints on Steel Beams and Beam-Columns in Fire

Summary

This chapter investigates the lateral-torsional buckling resistance of steel beams with partial lateral restraint at elevated temperatures. Analytical methods are used to evaluate the adequacy of existing fire design assumptions and quantify the influence of lateral restraint stiffness on instability behaviour, providing the foundational understanding for the numerical investigation presented in Chapter 4. Based on existing literature, the continuous elastic lateral stiffness available to restrain the beam at the fire limit state is estimated to range from approximately 500 kN/m/m to 2000 kN/m/m. Using this range of restraint stiffness, a parametric study was conducted using the Eurocode 3 design buckling resistance equations for 9 m simply supported steel beams and beam-columns with span-to-depth ratios of approximately 10, 15, 20 and 25. The results indicate that assuming full lateral restraint under fire conditions may lead to unrealistic design assumptions and potentially unsafe structures. While this chapter addresses Objective 1 of the research by examining the influence of partial lateral restraint using analytical methods, Chapter 4 extends the investigation through validated thermo-mechanical finite element modelling to examine the interaction between lateral and axial restraint under fire conditions.

Keywords: Steel-timber hybrid structures; Lateral-torsional buckling; Continuous elastic restraints; Parametric study; Fire

3.1 Introduction

Steel-timber hybrid structures are innovative structural solutions that are being adopted for commercial office and mixed-use developments. This type of construction consisting of mass-timber cross-laminated timber (CLT) panels with non-combustible steel frames offer benefits such as sustainability with low embodied carbon impacts, dry construction, off-site fabrication, lightness, biophilic design, and long beam spans. However, the fire performance of such systems is a concern and there is uncertainty among industry practitioners regarding the susceptibility of the steel beams to lateral-torsional buckling instability in fire conditions (Barber, Roy-Poirier and Wingo, 2021; AISC, 2022), which is further exacerbated by the development of axial compression due to restrained thermal expansion (Li and Guo, 2008).

In this type of structural system, the CLT panels are connected to steel beams using closely spaced self-tapping screws and from a structural perspective, these beams can be assumed to be supported laterally by a linear elastic foundation with uniform continuous stiffness k located at a distance a from the centroid of the section, as shown in Figure 3.1. Researchers such as Flint (1951), McCann, Gardner and Wadee (2013), and Belaid, Ammari and Adman (2018) have shown improvement of the lateral-torsional buckling behaviour of steel beams with different types of restraints but studies with continuous elastic restraints in fire are lacking. This is because in conventional steel-concrete composite construction, the steel beams are normally assumed to be fully restrained by the concrete slab and restraints in other types of steel construction are generally discrete and at large spacings. Compared to unrestrained beams, which fail at moments close to the critical elastic moment, beams with continuous or closely spaced restraints and sufficient lateral stiffness capacity can achieve full plastic moment resistance (Vila Real *et al.*, 2004). Hence, the aim of this study is to investigate the influence of uniform continuous elastic restraints on steel beams and beam-columns in steel-timber hybrid structures at elevated temperatures. The objectives are: (i) to review the current lateral-torsional buckling resistance equations for partially restrained members, (ii) to assess the level of lateral stiffness mobilised by self-tapping screws based on existing literature, and (iii) to perform a parametric study to determine the influence of continuous restraints on heated beams and beam-columns.

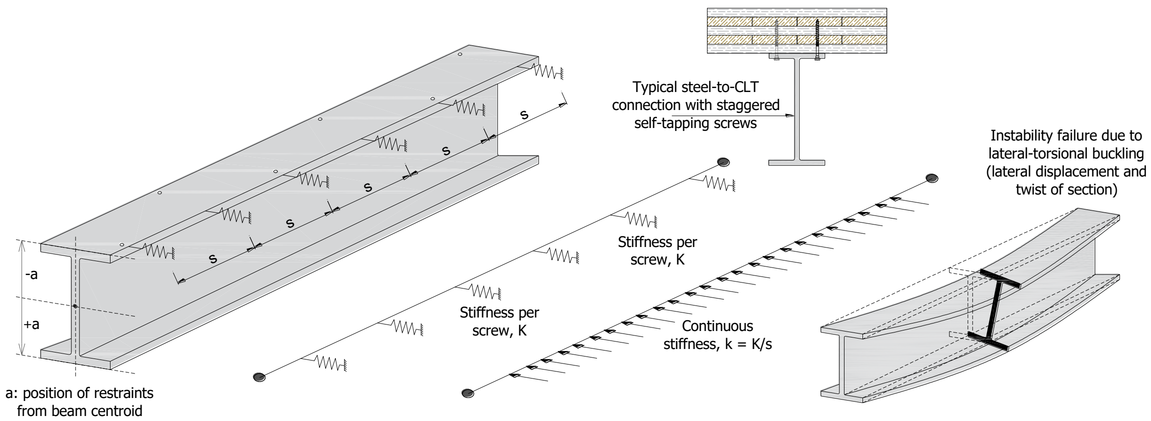

Figure 3.1: Beam supported laterally by a continuous elastic medium

3.2 Theoretical Background

This section provides an overview of the theoretical framework for the verification of lateral-torsional buckling of steel beams and beam-columns with uniform continuous elastic restraints at high temperature using current design equations in BS EN 1993-1-2 (2005). Existing analytical methods to determine the critical elastic moment and critical elastic load for both cases are also presented. A background knowledge of steel section classification with respect to slenderness, local buckling and plastic/elastic capacity is required to understand this section and a detailed explanation can be found in Franssen and Vila Real (2015).

3.2.1 Lateral-Torsional Buckling Resistance of Beams in Fire

The design lateral torsional buckling resistance moment $M_{b,fi,t,Rd}$ at time t of a laterally unrestrained steel beam at elevated temperatures with a Class 1 or 2 cross-section can be determined from:

$$M_{b,fi,t,Rd} = \frac{\chi_{LT,fi} W_{pl,y} k_{y,\theta,com} f_y}{\gamma_{M,fi}} \tag{3.1}$$

where $\chi_{LT,fi}$ is the reduction factor for lateral torsional buckling in fire, $W_{pl,y}$ is the plastic modulus of the section, $k_{y,\theta,com}$ is the reduction factor for the yield strength at the maximum steel temperature in the compression flange, f_y is the yield strength of the steel section, and $\gamma_{M,fi}$ is the partial safety factor for material properties in fire, which is usually taken as 1.0.

The value of $\chi_{LT,fi}$ is determined using the following equation:

$$\chi_{LT,fi} = \frac{1}{\phi_{LT,\theta,com} + \sqrt{(\phi_{LT,\theta,com})^2 - (\bar{\lambda}_{LT,\theta,com})^2}} \tag{3.2}$$

with
$$\phi_{\mathrm{LT,\theta,com}} = 0.5\left[1 + \alpha\bar{\lambda}_{LT,\theta,com} + (\bar{\lambda}_{LT,\theta,com})^2\right] \tag{3.3}$$

The imperfection factor α, which is a function of the steel yield strength, and the non-dimensional slenderness $\bar{\lambda}_{LT,\theta,com}$ at high temperature are given by:

$$\alpha = 0.65\sqrt{\frac{235}{f_y}} \tag{3.4}$$

$$\bar{\lambda}_{LT,\theta,com} = \bar{\lambda}_{LT}\sqrt{\frac{k_{y,\theta,com}}{k_{E,\theta,com}}} \tag{3.5}$$

where $k_{E,\theta,com}$ is the reduction factor for the modulus of elasticity at the maximum steel temperature in the compression flange.

The non-dimensional slenderness $\bar{\lambda}_{LT}$ at room temperature is given by:

$$\bar{\lambda}_{LT} = \sqrt{\frac{W_{pl,y} f_y}{M_{cr}}} \tag{3.6}$$

where M_{cr} is the critical elastic moment at room temperature which causes stability failure due to lateral-torsional buckling.

Eurocode 3 does not provide any guidance on how to calculate M_{cr} and this is left entirely at the designer's discretion. The calculation of this value should take into consideration all the parameters such as the loading type and position, end boundary conditions and effect of lateral restraints to represent the actual structure being investigated. Section 3.2.2 addresses this situation for steel-timber hybrid structures with continuous elastic lateral restraints.

3.2.2 Critical Elastic Moment of Beams with Continuous Lateral Restraints

According to Timoshenko and Gere (1961), the critical elastic buckling moment M_{cr} of a simply supported beam with doubly-symmetric cross-section under pure bending can be determined using the classical Equation (3.7). In this case, it is assumed that the ends of the beam are prevented from lateral translation and twist, but are free to warp and rotate laterally. Similarly, the critical elastic buckling moment M_{cr} of a beam with continuous elastic restraints can be determined using Equation (3.8) under the same loading and end boundary conditions, the derivation of which can be found in Trahair (1993).

$$M_{cr} = \frac{n^2\pi^2 EI_z}{L^2}\sqrt{\frac{I_w}{I_z} + \frac{L^2 GI_t}{n^2\pi^2 EI_z}} \; or \; \sqrt{\frac{n^2\pi^2 EI_z}{L^2}\left(GI_t + \frac{n^2\pi^2 EI_w}{L^2}\right)} \tag{3.7}$$

$$\left[M_{cr} + \frac{kaL^2}{n^2\pi^2}\right]^2 = \left[\frac{n^2\pi^2 EI_z}{L^2} + \frac{kL^2}{n^2\pi^2}\right]\left[GI_t + \frac{n^2\pi^2 EI_w}{L^2} + \frac{kaL^2}{n^2\pi^2}\right] \tag{3.8}$$

In the above equations, I_z is the moment of inertia about the minor z-z axis, L is the laterally unbraced length, E is the elastic modulus of steel, G is the shear modulus of steel, I_w is the warping constant of the section, I_t is the torsional constant of the section, n is the mode of buckling, k is the uniform continuous elastic restraint stiffness, and a is the position of the restraint measured from the centroid of the section (restraints located above the centroidal axis towards compression flange are negative and those below are positive (Trahair, 1993)). It is important to note that the critical buckling mode of a continuously restrained beam is dependent on the degree of lateral restraint stiffness in contrast to an unrestrained beam for which the first mode gives the most critical situation for lateral-torsional buckling. Hence, several trials are required to determine the buckling mode which gives the lowest buckling moment for continuously restrained beams.

3.2.3 Lateral-Torsional Buckling Resistance of Beam-Columns in Fire

Steel beams, which are axially restrained at their ends as a result of the support conditions or the presence of adjacent members in a structure, develop axial compression due to restriction of the thermal expansion during the heating phase of a fire (Li and Guo, 2008). Members with a Class 1 or 2 cross-section that are subjected to combined uniaxial bending about the major axis $M_{y,fi,Ed}$ and axial compression $N_{fi,Ed}$ behave as beam-columns and should satisfy the following interaction equation:

$$\frac{N_{fi.Ed}}{\chi_{z,fi} A k_{y,\theta} \dfrac{f_y}{\gamma_{M,fi}}} + \frac{k_{LT} M_{y,fi,Ed}}{\chi_{LT,fi} W_{pl,y} k_{y,\theta} \dfrac{f_y}{\gamma_{M,fi}}} \leq 1 \tag{3.9}$$

where $\chi_{z,fi}$ is a reduction factor for flexural buckling in fire situation, A is the area of the cross-section, and k_{LT} is an interaction factor for lateral-torsional buckling. $W_{el,y}$ should be used for Class 3 sections (see Section 3.2.1 for other repeated notations).

The value of $\chi_{z,fi}$ is determined using the following equation:

$$\chi_{z,fi} = \frac{1}{\phi_\theta + \sqrt{\phi_\theta - \bar{\lambda}_\theta^2}} \tag{3.10}$$

with $$\phi_\theta = 0.5\left[1 + \alpha\bar{\lambda}_\theta + (\bar{\lambda}_\theta)^2\right] \tag{3.11}$$

The imperfection factor α is similar to that in Equation (3.4) and the non-dimensional slenderness $\bar{\lambda}_\theta$ at high temperature is given by:

$$\bar{\lambda}_\theta = \bar{\lambda}\sqrt{\frac{k_{y,\theta}}{k_{E,\theta}}} \tag{3.12}$$

The non-dimensional slenderness $\bar{\lambda}$ at room temperature is given by:

$$\bar{\lambda} = \sqrt{\frac{Af_y}{N_{cr}}} \tag{3.13}$$

where N_{cr} is the critical elastic buckling load at room temperature which causes stability failure and can be determined as explained later in Section 3.2.4.

The value of k_{LT} is found using the following equation:

$$k_{LT} = 1 - \frac{\mu_{LT} N_{fi,Ed}}{\chi_{z,fi} A k_{y,\theta} \dfrac{f_y}{\gamma_{M,fi}}} \leq 1 \tag{3.14}$$

with

$$\mu_{LT} = 0.15 \bar{\lambda}_{z,\theta} \beta_{M,LT} - 0.15 \leq 0.9 \tag{3.15}$$

The value of $\beta_{M,LT}$ is equal to 1.1 for beams with pure bending with equal and opposite end moments, and 1.3 for beams with a uniformly distributed load.

3.2.4 Critical Elastic Load of Columns with Continuous Lateral Restraints

For a doubly-symmetric column with shear centre continuous elastic restraints *k*, the critical elastic load to cause lateral-torsional buckling can be determined using Equations (3.16) to (3.18), the derivation of which can be found in Trahair (1993). In this case, there are three possible buckling modes: flexure about the major y-y axis at $N_{cr,y}$, flexure about the minor z-z axis at $N_{cr,z}$, and torsion about the longitudinal x-x axis at $N_{cr,x}$. The actual buckling load N_{cr} will be the lowest of the three. In the equations, I_y is moment of inertia about the major y-y axis (see previous sections for other repeated notations).

$$N_{cr,y} = \frac{n^2 E I_y}{L^2} \tag{3.16}$$

$$N_{cr,z} = \frac{n^2 E I_z}{L^2} + \frac{k L^2}{n^2 \pi^2} \tag{3.17}$$

$$N_{cr,x} = \frac{G I_t + \dfrac{n^2 \pi^2 E I_w}{L^2}}{r^2} \quad , with \;\; r^2 = \frac{I_y + I_z}{A} \tag{3.18}$$

For a doubly-symmetric column with continuous elastic restraints *k* acting at a distance *a* from the centroid of the section, a number of trials must be made to find the lowest buckling load N_{cr} using the general but more complex Equation (3.19). In many cases, the lowest solution will correspond to the flexural-torsional buckling mode in which the section twists and translates about the two axes (Trahair, 1993).

$$N_{cr} = \min\left[\frac{n^2\pi^2 EI_y}{L^2};\frac{(Ar^2+B)\pm\sqrt{(Ar^2+B)^2-4r^2(AB-C^2)}}{2r^2}\right] \tag{3.19}$$

with

$$A = \frac{kL^2}{n^2\pi^2}+\frac{n^2\pi^2 EI_z}{L^2}\ ;\ B = \frac{ka^2L^2}{n^2\pi^2}+GI_t+\frac{n^2\pi^2 EI_w}{L^2}\ ;\ C = -\frac{kaL^2}{n^2\pi^2} \tag{3.20}$$

3.3 Lateral Restraint of Steel-to-CLT Connections

In current steel-timber hybrid construction, CLT floor panels are fixed to steel beams using regularly spaced self-tapping screws at spacings not exceeding 600 mm and in a staggered manner to prevent the potential for wood splitting during installation of the mechanical fasteners. The proprietary screws adopted in mass-timber connections are either partially threaded or fully threaded (AISC, 2022). These screws offer a certain degree of lateral stiffness which can potentially prevent beam lateral-torsional buckling in both ambient and fire conditions. For conservatism in design, the steel beams can be designed as laterally unrestrained due to the uncertainty among designers on the current practice regarding the degree of lateral restraint offered by the screws, particularly under fire exposure. Merryday *et al.* (2023) conducted a four-point bending test on a simply supported steel-CLT composite beam and reported that lateral-torsional buckling is not a concern at ambient temperature even with a narrow CLT slab width.

Over the years, numerous experimental tests have been carried out for timber-to-timber connections and several semi-empirical equations have been developed to predict their mechanical behaviour as given in design standards such as BS EN 1995-1-1:2004+A2 (2014). Conversely, experimental programmes for steel-to-timber connections using self-tapping screws are less established, especially under elevated temperatures in which most of the studies investigated connections made with bolts and dowels (Létourneau-Gagnon, Dagenais and Blanchet, 2021; Marcolan Júnior and Dias de Moraes, 2022). Researchers such as Hassanieh, Valipour and Bradford (2016), Loss, Piazza and Zandonini (2016), Hassanieh, Valipour and Bradford (2017a), Yang *et al.* (2020) and Ling, Rong and Xiang (2021) present several ambient temperature tests on various types of steel-to-timber connections, but these are generally not representative of the typical connection system adopted in current large-scale steel-timber hybrid construction. More realistic monotonic push-out tests using self-tapping screws to connect steel-CLT specimens have been carried out by MTC Solutions (2019) and Merryday, Sener and Roueche (2023), but these mainly focused on the connection strength rather than the lateral stiffness characteristics. On the other hand, Létourneau-Gagnon, Dagenais and Blanchet (2021) investigated the pull-out resistance of self-tapping screws via high temperature pull-out tests and also reported that limited information is available on the fire performance of such modern mass timber fasteners.

The load-slip relationship of steel-to-CLT connections using self-tapping screws is highly complex and is generally characterised by a non-linear behaviour at ambient temperature as shown in Figure 3.2. For design purposes, the lateral stiffness offered by screws is defined in terms of the slip modulus for different limit states: K_{ser} for the serviceability limit state, K_u for the ultimate limit state and K_{fi} for the fire limit state. In accordance with BS EN 26891 (1991), the slip modulus K_{ser} can be determined experimentally using Equation A as given in Table 3.1. Other semi-empirical expressions for stiffness can also be used to predict K_{ser} using Equations B, C, D1 and D2 in Table 3.1, and more detailed information on these equations can be found in Jockwer and Jorissen (2018) and Jockwer, Caprio and Jorissen (2022). The determination of the slip modulus K_u is not specified in BS EN 26891 (1991) and is taken as two-thirds of K_{ser} as per BS EN 1995-1-1:2004+A2 (2014). The slip modulus K_{fi} under fire condition should be taken as 20% of K_u in line with BS EN 1995-1-2 (2004). This indicates that in fire, a single value of K_{fi} is applicable and no consideration is given to the connector degradation at different temperatures, as illustrated in Figure 3.3. The degradation curve shown is only for the purpose of illustration (based on the general shape of shear connector strength reduction in steel-concrete composite structures) as there is a lack of experimental studies on the behaviour of such type of connection system in fire. High-temperature push-out tests are required to characterise the curve-shape, which will be influenced by the material degradation/failure criterion of the individual components of the connection. However, this connection design assumption can be problematic if it is a non-conservative simplification in terms of structural behaviour and should therefore be explicitly verified by fire testing, as the joint behaviour influences the force distribution and deformation of a structure.

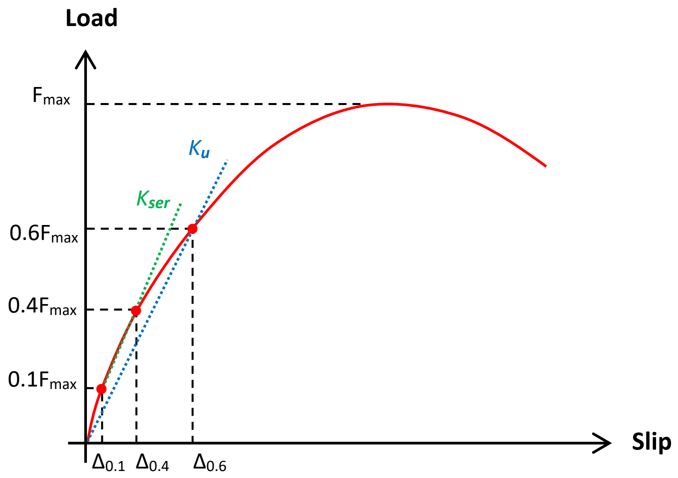

Figure 3.2: Typical load-slip curve for steel-timber connection with self-tapping screws

Table 3.1: Equations to calculate K_{ser}, K_u, and K_{fi} in N/mm

	Equations	Reference
A	$K_{ser} = \dfrac{0.4F_{max}}{\frac{4}{3}(v_{04} - v_{01})}$	BS EN 26891 (1991)
B	$K_{ser} = \dfrac{\rho_m^{1.5} d}{23}$ (*may be multiplied by* 2.0)	BS EN 1995-1-1:2004+A2 (2014)
C	$K_{ser} = \dfrac{\rho_k^{1.5} d}{30}$	Ehlbeck and Larsen (1993)
D1	$K_{ser,0} = 6\rho_k^{0.5} d^{1.7}$	SIA 265 (2012)
D2	$K_{ser,90} = 3\rho_k^{0.5} d^{1.7}$	
E	$K_u = \dfrac{2}{3} K_{ser}$	BS EN 1995-1-1:2004+A2 (2014)
F	$K_{fi} = 0.2K_u$	BS EN 1995-1-2 (2004)

Where F_{max} is the maximum load
v_{04} and v_{01} are the slip at 40% and 10% of the maximum load, respectively
ρ_m is the mean density in kg/m³
ρ_k is the characteristic density in kg/m³
d is the nominal diameter of the screw in mm

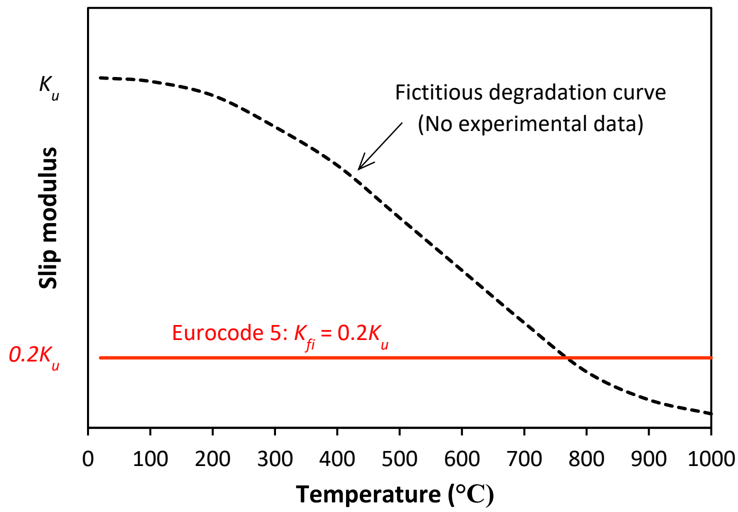

Figure 3.3: Fictitious degradation curve of screws in fire and Eurocode 5 guidance

For this study, the load-slip curves from the two aforementioned papers (MTC Solutions, 2019; Merryday, Sener and Roueche, 2023) were used to determine the slip modulus K_{ser}, as shown in Figure 3.4. The results show that K_{ser} varies approximately between 1.50 kN/mm and 3.50 kN/mm per screw for the 12 mm nominal diameter self-tapping screws. From Figure 3.5, it can also be observed that the experimental results obtained using Equation A generally deviate significantly from the predictions of Equations B, C, D1 and D2, with the exception of Equation C, which is reliable in some circumstances. Jockwer and Jorissen (2018) also concluded that the background of the equations for stiffness in Eurocode 5 is vague and based on simplified assumptions. Hence, further research is required to develop clear guidelines on the mechanical performance of steel-to-timber connections using self-tapping screws, particularly in fire conditions. The fire testing should consider parameters such as the type of screw (partially or fully threaded), screw diameter, screw embedment length, screw spacing, outer grain orientation, panel layup and lamella thickness. This would enable designers to predict the lateral stiffness K_{fi} at various temperatures, which could subsequently be used to check the lateral-torsional buckling resistance of heated beams. At this stage of the present study, it is proposed to use Equation (3.21) to estimate the serviceability slip modulus in the absence of more rigorous tests from screw manufacturers, from which K_{fi} could then be estimated. Equation (3.21) is based on Equation C in Table 3.1 but with the application of a correction factor of 0.5 to ensure conservatism in the absence of more definitive experimental or numerical data.

$$K_{ser} = \frac{\rho_k^{1.5} d}{60} \tag{3.21}$$

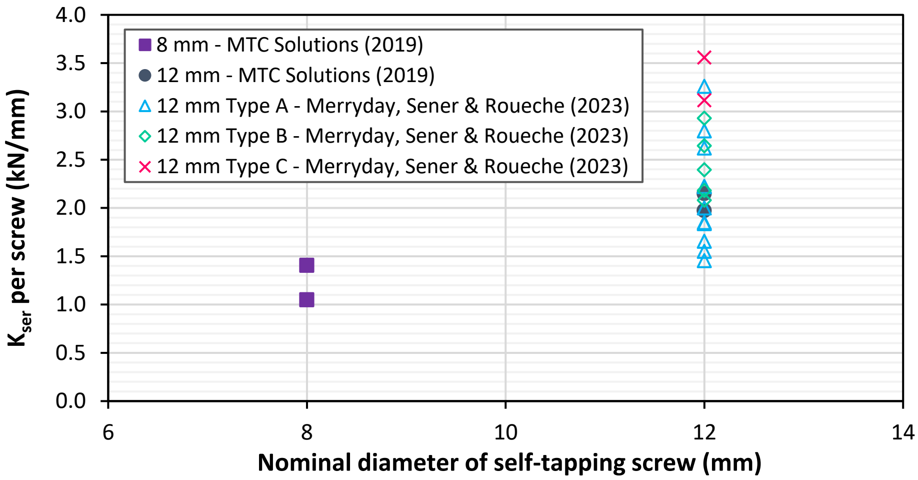

Figure 3.4: Variation of K_{ser} with nominal diameter of self-tapping screws

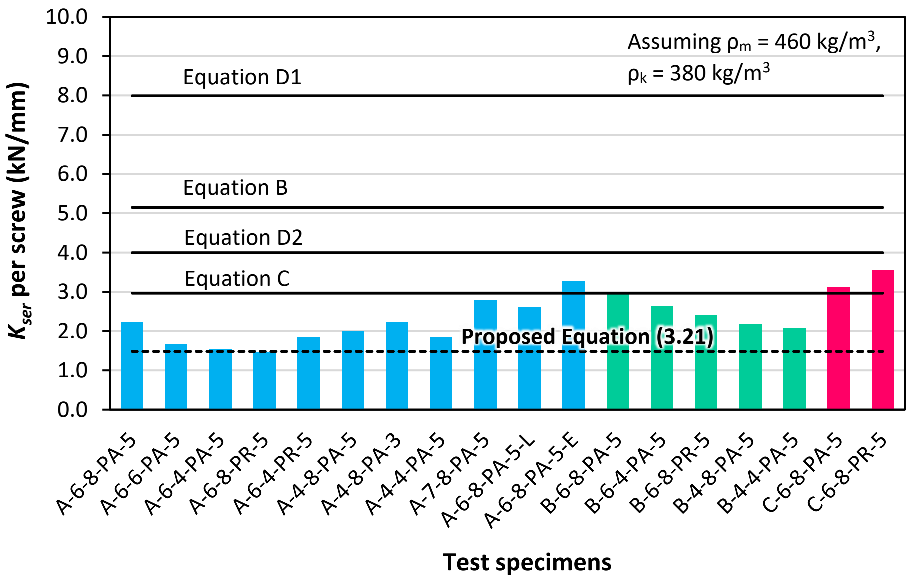

Figure 3.5: Experimental and predicted K_{ser} for different test specimens in Merryday, Sener and Roueche (2023)

Table 3.2 shows the variation of the continuous lateral stiffness k_{fi} for the fire limit state with spacing of staggered self-tapping screws varying from 200 mm to 500 mm. These values have been determined for the range of slip modulus K_{ser} (1.50 kN/mm to 3.50 kN/mm) observed in the push-out tests. From the tabulated data, it can be inferred that k_{fi} has lower- and upper-bounds of approximately 500 kN/m/m and 2000 kN/m/m, respectively. These values represent the practical range of continuous lateral stiffness likely to be mobilised in steel-timber hybrid structures based on current design guidance and test datasets, which must evidently be validated with further fire experimentation.

Table 3.2: Continuous lateral stiffness k_{fi} in fire for different screw spacings

K_{ser} (kN/mm)	1.50	2.00	2.50	3.00	3.50
K_u (kN/mm)	1.00	1.33	1.67	2.00	2.33
K_{fi} (kN/mm)	0.200	0.267	0.333	0.400	0.467
Spacing (mm)	**Continuous lateral stiffness, k_{fi} (kN/m/m)**				
200	1000	1333	1667	2000	2333
250	800	1067	1333	1600	1867
300	667	889	1111	1333	1556
350	571	762	952	1143	1333
400	500	667	833	1000	1167
450	444	593	741	889	1037
500	400	533	667	800	933

Note: The continuous lateral stiffness k_u at ambient temperature can be obtained by multiplying the tabulated values of k_{fi} by 5.

3.4 Parametric Study for Downstand Steel-Timber Hybrid Systems

This section presents a parametric study performed on four steel beams and beam-columns in a downstand arrangement to investigate analytically the potential for lateral-torsional buckling under high temperatures. In line with current practice, it is assumed that the steel members carry all the applied loading and any form of composite action offered by the CLT slab is neglected because the degree of composite action mobilised in fire is not yet clearly understood. Hot-rolled structural steel members with a simply supported span of 9 m, steel grade S355, and span-to-depth ratios (L/H) of approximately 10, 15, 20 and 25 were selected for the present study. The 9 m span was chosen to reflect typical steel framing schematics with 9 m x 9 m column grids. Some of the key sectional and material properties of the steel cross-sections adopted are summarised in Table 3.3. Section classification was carried out for pure bending and for combined bending with axial compression for the fire limit state.

LTBeamN (2023), which is a free finite element software and developed by CTICM, was used for the determination of the critical moment M_{cr} and critical load N_{cr} for various loading and continuous lateral restraint conditions. The software facilitates the calculation of the critical moment and load in complex situations not covered by standard expressions and the equations presented in Section 3.2.2 and 3.2.4 were verified by the output results under specific conditions. In all cases, it is assumed that the end boundary conditions of the steel members are prevented from lateral translation and twist, but are free to warp and rotate laterally. These values were then used as input to determine the lateral-torsional buckling resistance of the steel beams and beam-columns in the fire situation. The parametric study was performed using a range of constant continuous lateral stiffness k (Figure 3.1) from 100 kN/m/m to 50000 kN/m/m, representing the continuous lateral stiffness k_{fi} at the fire limit state as shown in Figure 3.3. In reality, K_{fi} (and therefore k_{fi}) will vary with the screw temperature and more representative non-linear load-slip response of the screws must be considered for different temperatures to capture the mechanical response. However, it is presumed that the lateral torsional buckling resistance of beams and beam-columns obtained using this constant value (K_{fi} = 0.2K_u) from Eurocode 5 guidance is conservative, until more high temperature research data are available to characterise such connection behaviour.

It must also be pointed out that the calculation methods presented in Section 3.2 can be applied under both uniform and non-uniform temperature distribution in the steel cross-section; BS EN 1993-1-2 (2005) notes that it can conservatively be assumed that the compression flange temperature is equal to the uniform temperature. Hence, it is assumed that the reference temperature in this study is the temperature of the steel web as numerical simulations by Godoy Dellepiani *et al.* (2023) have shown initial non-uniform temperature profile with a cooler compression flange in steel-timber hybrid structures until a relatively uniform temperature profile is achieved with increasing fire exposure time. This assumption is expected to lead to safe results at this stage of the study and future numerical investigations are required to assess the effect of non-uniform heating over the member cross-section on the response of such systems.

Table 3.3: Sectional and material properties of S355 steel members with 9 m span

Steel member	L/H	$W_{pl,y}$ (cm³)	$W_{el,y}$ (cm³)	f_y (MPa)
UB 914x305x253	9.80	10944	9503	355
UB 610x229x125	14.71	3673	3219	355
UB 457x152x74	19.51	1624	1408	355
UB 356x171x57	25.10	1009	896	355

3.4.1 Beams

Two different loading conditions were considered for the four selected simply supported steel beams with free axial expansion under high temperatures: one with uniform end moment located at the shear centre and the other with a uniformly distributed load on the top flange. In both circumstances, it is assumed that the continuous elastic restraints representing the screws act at the top flange of the section. All the sections were found to be of Class 1 under pure bending in fire.

Figure 3.6 illustrates the variation of the buckling moment resistance of the steel beams with increasing temperatures for different span-to-depth ratios. The upper- and lower-bound curves respectively represent a fully restrained beam with full plastic moment resistance and a laterally unrestrained beam with zero restraint. The shaded area between the two bounds with continuous lateral stiffness k of approximately 500 kN/m/m and 2000 kN/m/m represents the practical range of buckling moment resistance likely to be mobilised in steel-timber hybrid structures. Figure 3.7 provides a more accurate distinction in terms of the ratio of the buckling moment resistance of a uniformly loaded beam with continuous lateral restraints to that of an unrestrained beam (Figure 3.7a) or a fully restrained beam (Figure 3.7b) with different span-to-depth ratios and temperatures. It can be observed that the ratio varies between 1.80 and 5.99 for unrestrained beams and between 0.36 and 0.75 for restrained beams.

From the above findings and assuming fire is the governing limit state, it can be deduced that if steel beams are designed as unrestrained in fire conditions, they would have additional reserve strength at the fire limit state due to the presence of the continuous lateral restraints. As such, this may lead to material savings in steel and fire protection, subject to further investigations. However, if the beams are designed as fully restrained, they may fail by lateral-torsional buckling at a load much lower than the full plastic moment resistance assumed in the design. This means that relying entirely on the screws for full restraint conditions appears unrealistic and may result in unsafe structures in the event of a fire. Consequently, further experimental and/or numerical investigations are required to determine the applicability of the current design buckling resistance equations for steel members with continuous elastic restraints in fire. Such investigations are essential to establish the framework required for the design of steel-hybrid structures at elevated temperatures.

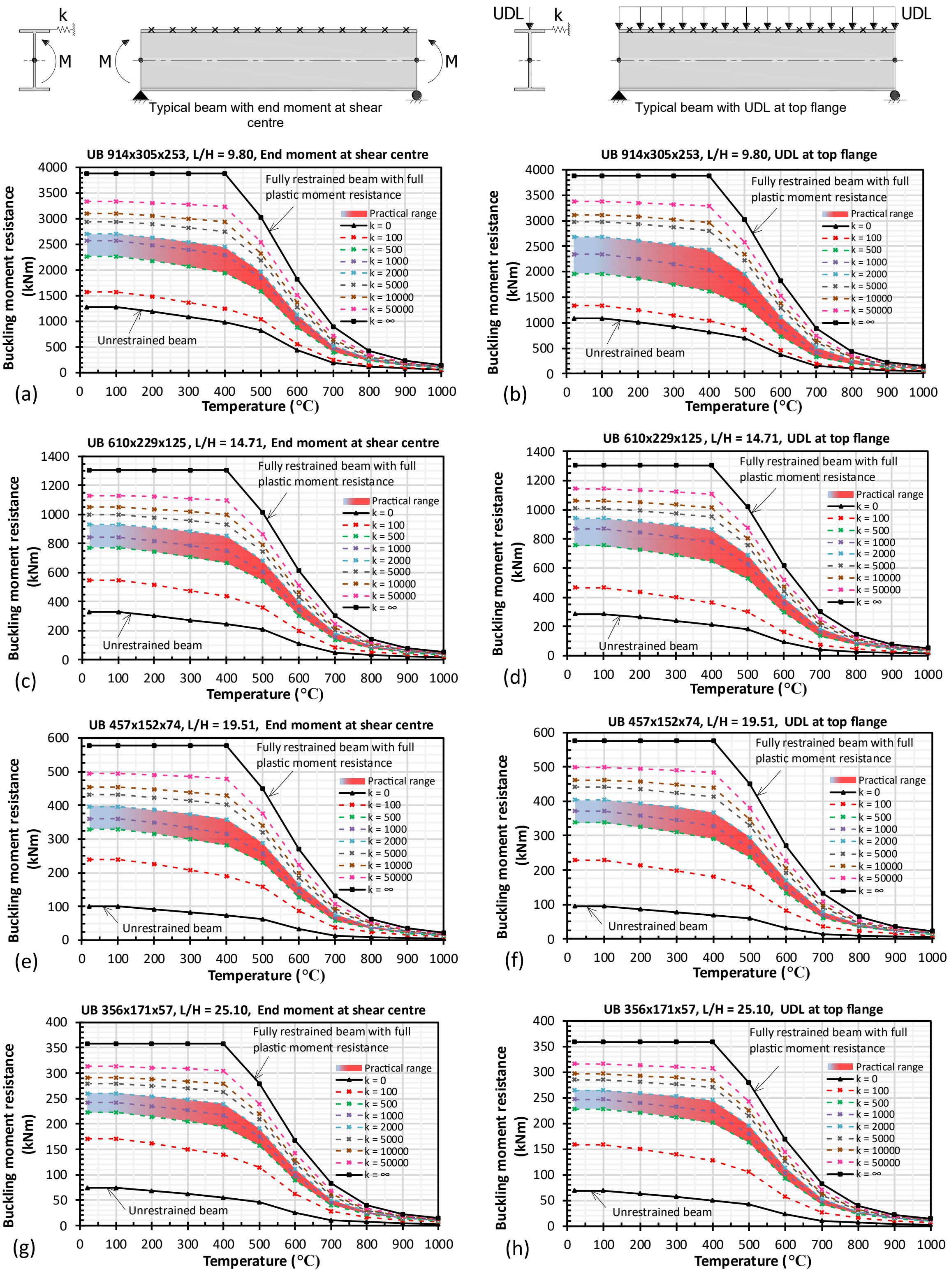

Figure 3.6: Variation of buckling moment resistance of beams with temperature for different degree of restraints with moment for span-to-depth ratios (a) 9.80, (c) 14.71, (e) 19.51, and (g) 25.10 and uniformly distributed load for span-to-depth ratios (b) 9.80, (d) 14.71, (f) 19.51, and (h) 25.10

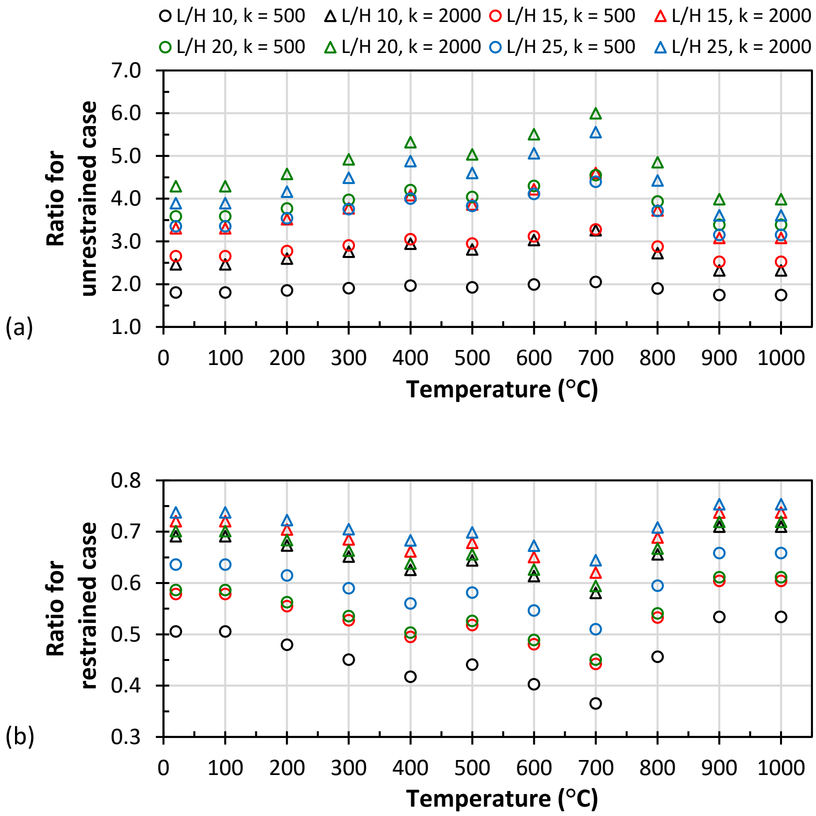

Figure 3.7: Ratio of buckling moment resistance of beam with continuous lateral restraints to that of (a) unrestrained beam and (b) fully restrained beam under uniformly distributed load with temperature

3.4.2 Beam-Columns (Beams with Axial Compression)

This section deals with axially restrained steel beams subject to uniaxial bending about the major axis $M_{y,fi,Ed}$ which develop axial compression $N_{fi,Ed}$ during heating. In this case, Equation (3.9) can be re-written as follows with axial and bending terms:

$$\frac{N_{fi.Ed}}{N_{b,fi,t,Rd}} + \frac{k_{LT} M_{y,fi,Ed}}{M_{b,fi,t,Rd}} \leq 1 \tag{3.22}$$

In Equation (3.22), $N_{b,fi,t,Rd}$ is the buckling resistance of a compression member, which is affected by the presence of continuous elastic restraints. This interaction formula reduces down to a beam problem when the axial compression is zero (as demonstrated previously in Section 3.4.1) and to a column with pure axial compression when there is no bending moment present. Hence, the influence of continuous elastic restraints on compression members must also be understood in order to account for combined bending and axial loading using Equation (3.22).

Figure 3.8 illustrates the variation of the compression buckling resistance of four simply supported steel columns with increasing temperatures under the effect of axial compression acting at the shear centre and continuous elastic restraints located at the top flange of the section. It can be observed that such columns are particularly sensitive to the restraints, with continuous lateral stiffness k of approximately 500 kN/m/m approaching a fully restrained section at the top flange. An extreme value of k equal to 1×10^{18} kN/m/m was used as input in *LTBeamN* (2023) to represent the situation with infinite lateral stiffness. As a result, such structural systems offer enhanced performance compared to unrestrained ones in terms of compression buckling resistance in fire conditions. It must be noted that the selected sections are Class 4 under pure compression and the equations described in Section 3.2.3 to determine $N_{b,fi,t,Rd}$ are not strictly applicable. On the contrary, these equations can still be used to verify buckling resistance for Class 1, 2 and 3 sections under combined bending and axial compression for a certain level of compression force.

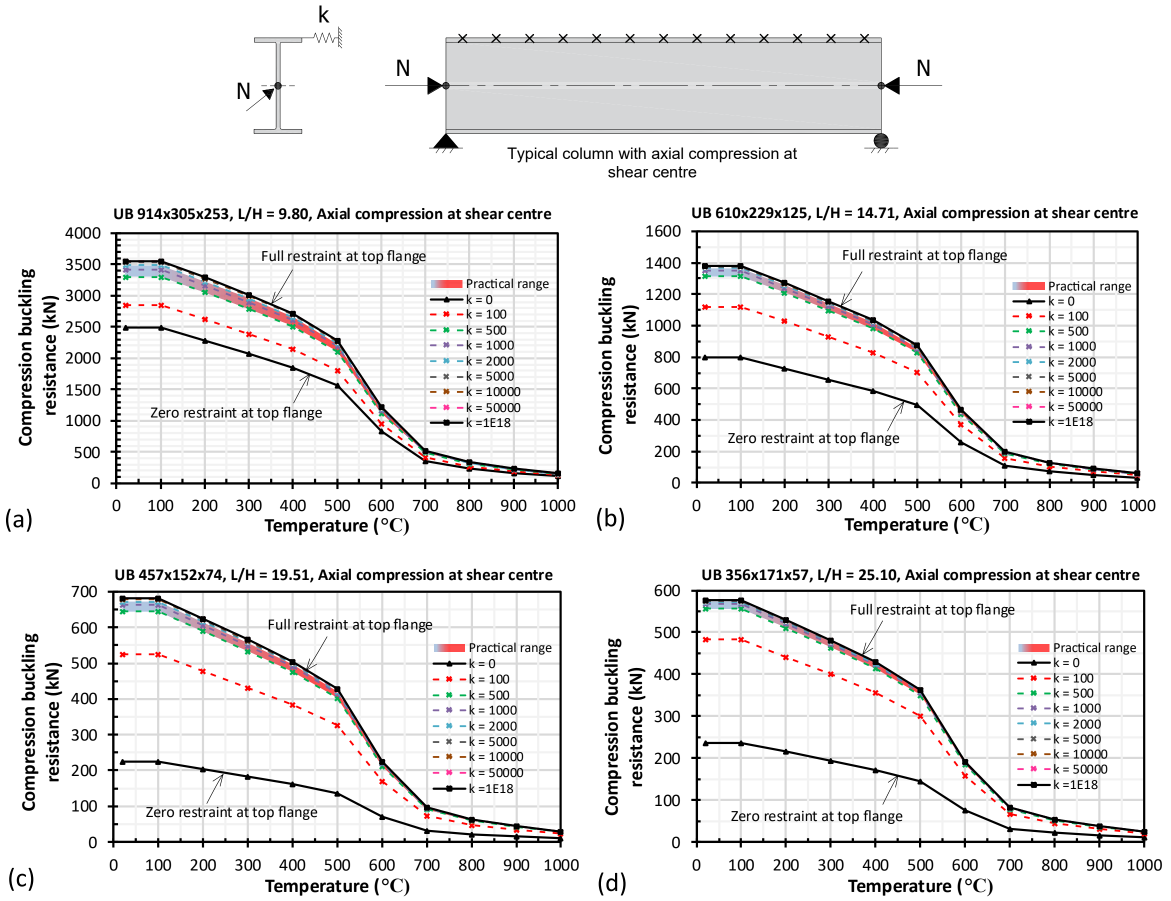

Figure 3.8: Variation of compression buckling resistance with temperature for different degree of restraints and span-to-depth ratios of (a) 9.80, (b) 14.71, (c) 19.51, and (d) 25.10

To evaluate both bending moment and axial compression in combination, the effect of continuous elastic restraints acting at the top flange of the section on four simply supported beam-columns was investigated at temperatures of 500 °C, 600 °C and 700 °C. The sections were found to be of Class 1, 2 and 3 in fire, with the section classification depending on the level of applied axial compression as shown in Table 3.4.

Table 3.4: Section classification based on maximum axial compression force

Steel member	L/H	Maximum axial compression (kN)			
		Class 1	Class 2	Class 3	Applied
UB 914x305x253	9.80	192	871	4683	2234
UB 610x229x125	14.71	161	482	2490	862
UB 457x152x74	19.51	203	412	1749	420
UB 356x171x57	25.10	223	372	1621	360

Figure 3.9 shows the interaction diagrams in terms of buckling moment resistance of the beam-columns with a uniformly distributed load on the top flange and axial compression acting at the shear centre of the section. The plotted curves define the failure envelope for all the possible combinations due to axial compression and bending for continuous lateral stiffness k of 0 kN/m/m, 500 kN/m/m and 2000 kN/m/m. The kink observed in Figure 3.9a and b, with sudden drop in buckling moment resistance, indicates a change in section class from Class 2 to Class 3. As mentioned previously, the sections become Class 4 under pure compression and the compression resistance on the interaction diagrams should be recalculated accordingly, which is outside the scope of this study. However, the purpose of this investigation is to illustrate the shift and improvement of moment-axial interaction diagrams for the practical range of 500 °C to 700 °C of steel beam-columns under the effect of continuous elastic restraints in comparison to an unrestrained case, with the value of k equal to zero. It can be observed that the beam-columns with continuous restraints offer enhanced structural fire performance.

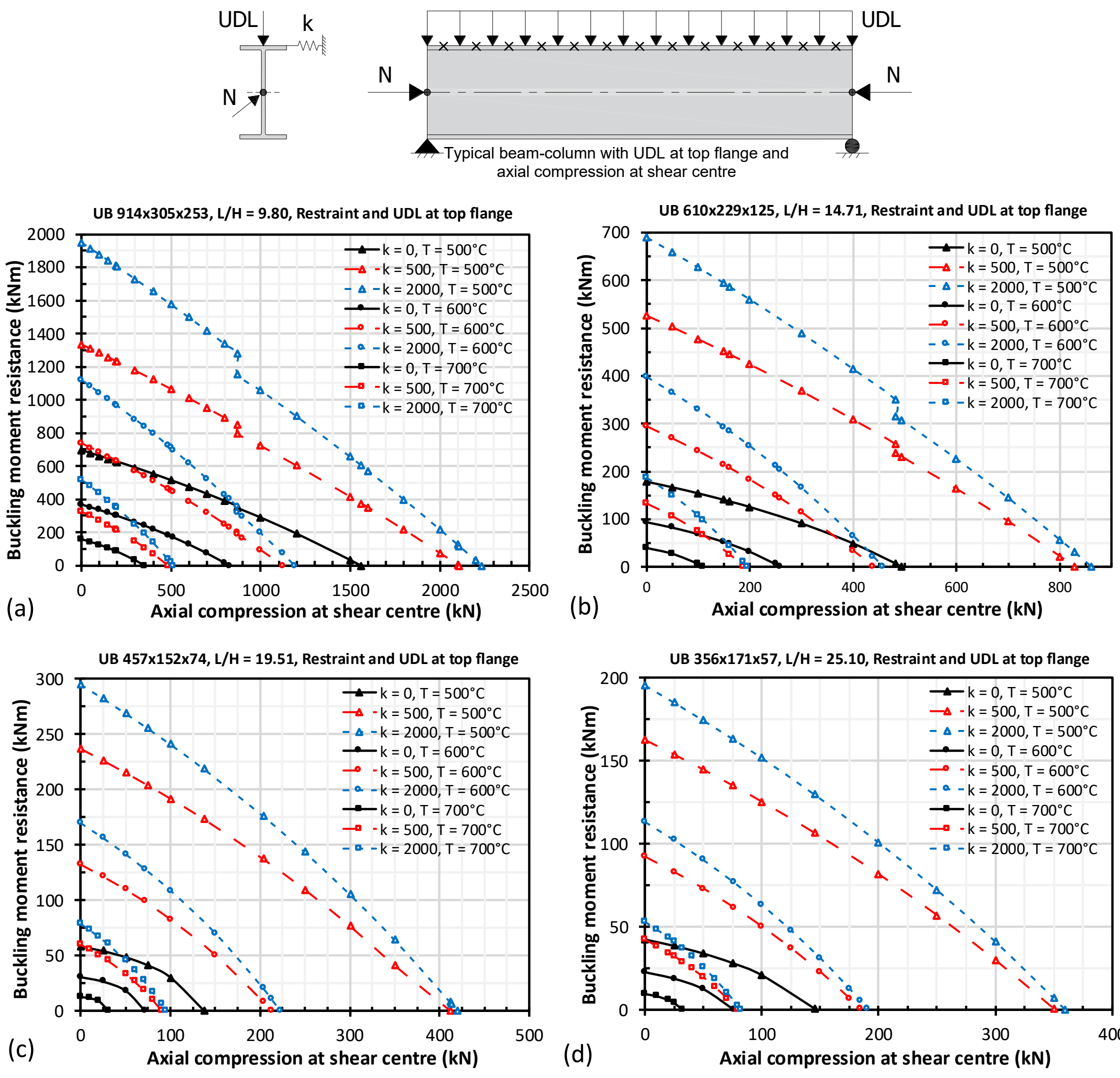

Figure 3.9: Interaction diagrams at 500, 600 and 700 °C for continuous lateral stiffness k of 0, 500 and 2000 kN/m/m for span-to-depth ratios (a) 9.80, (b) 14.71, (c) 19.51, and (d) 25.10

3.5 Conclusions

The influence of uniform continuous elastic restraints on steel beams and beam-columns in steel-timber hybrid structures at high temperature has been investigated. Based on the results of this investigation, the following conclusions can be drawn:

- Eurocode 3 provides design equations to check the lateral-torsional buckling resistance of steel beams and beam-columns at high temperatures. However, further experimental and/or numerical investigations are required to determine the applicability of these equations for steel members with continuous elastic restraints in fire and to identify whether they are overly conservative or unsafe.

- Prediction equations for the slip modulus of self-tapping screws at ambient temperature generally deviate significantly from experimental results and the assumption of 80% reduction of the slip modulus given in Eurocode 5 under fire conditions must be verified with further testing for steel-to-CLT connections using self-tapping screws, as also recommended in Barber, Roy-Poirier and Wingo (2021).
- If fire is the governing limit state, designing simply supported steel beams with free axial expansion as laterally restrained in fire conditions appears to be unrealistic and may lead to unsafe structures. On the other hand, designing beams as unrestrained indicates some reserve capacity, offering the possibility of material reduction in steel and fire protection.
- The presence of continuous lateral restraints in simply supported steel beam-columns shows an improvement of the moment-axial interaction diagrams at 500 °C, 600 °C and 700 °C compared to the unrestrained case.

This research has demonstrated that there is a significant lack of knowledge concerning steel-timber hybrid structures in fire. There is an urgent need for an experimental campaign of elevated temperature push-out tests to evaluate the longitudinal shear performance of modern screw connections in cross-laminated timber subjected to fire. With this data, a better understanding of steel-timber composite beams in fire can be developed using the tools outlined in this paper. To date, only numerical studies of steel-timber hybrid structures have been conducted in fire and there is a clear need for complementary experimental work as the demand for this hybrid topology is increasing in the built environment.

4

Behaviour of Heated Steel Beams with Lateral and Axial Restraint in Steel-Timber Hybrid Structures

Summary

Building on the analytical foundations established in Chapter 3, this chapter addresses Objective 2 of the research by examining the combined effects of lateral and axial restraint on the lateral-torsional buckling behaviour of steel beams in hybrid systems under fire conditions. Sequential thermo-mechanical finite element models were developed and validated to capture the thermal response, restrained thermal expansion, and subsequent instability of a 9 m unprotected steel beam with screws at 250 mm spacing under various levels of lateral restraint from the screws and axial restraint from the end connections. Parametric studies investigated different levels of lateral and axial restraint, as well as the influence of temperature on the compression flange. The results show that when axial restraint is present, the beam initially behaves similarly to a fully laterally restrained beam until the first screw fails in the midspan region, triggering lateral-torsional buckling. This chapter demonstrates how restraint interactions and connection failure influence the development of instability under fire conditions. The findings further demonstrate that it is unrealistic to assume full lateral restraint in fire design.

Keywords: Steel-timber hybrid structures; Lateral-torsional buckling; Fire; Parametric study; Thermo-mechanical modelling

4.1 Introduction

In recent years, steel-timber hybrid structures have emerged as a viable form of construction in response to the climate crisis and as demands for sustainability continue to escalate in the built environment. This hybrid approach to construction makes use of traditional steel frames integrated with cross-laminated timber (CLT) slabs, which are typically supported by the steel beams in downstand or slimfloor arrangements. In a downstand arrangement, the floor slab is supported on the top flanges of the beams, whereas the slimfloor arrangement makes it possible to support the floor directly on the wide bottom flanges of bespoke asymmetric beams. Steel-timber hybrid solutions offer several key environmental, structural and fabrication benefits over the widely used and well-established steel-concrete hybrid structures. However, the adoption of combustible timber structural elements in hybrid systems is beyond the scope of structural design guidance currently available for the fire limit state, particularly for the lateral-torsional buckling behaviour of the steel beams in a downstand arrangement at elevated temperatures (Barber, Roy-Poirier and Wingo, 2021; AISC, 2022). Additionally, the occurrence of end axial restraint from the surrounding structure can fundamentally change the response of the beams in fire as the development of compressive axial forces due to restrained thermal expansion can further increase their susceptibility to lateral-torsional buckling (Li and Guo, 2008). This is particularly important during the initial stages of a fire, when the beam response is predominantly elastic, and before very large deflections start to occur.

Over the last few decades, structural fire engineering approaches have been established for steel framed structures with concrete slabs (Wang *et al.*, 2012), and there is now an urgency to extend this knowledge and understanding to steel frames with CLT slabs. This is necessary to overcome the barriers faced by various construction stakeholders in adopting this relatively novel form of hybridisation, especially as the demand for this low-carbon topology continues to grow in the built environment as a response to the climate emergency. In conventional steel-concrete composite structures, the top flange of a downstand steel beam is normally assumed by designers to be fully restrained laterally under both ambient and fire conditions. In such cases, it is normally possible to achieve the full-in plane bending resistance of the beam. This may not be applicable to a steel-timber hybrid beam in fire, as lateral-torsional buckling instability may occur before the beam can attain its full moment capacity. Lateral restraint of the upper flange of the steel beam in steel-timber hybrid structures is traditionally achieved using closely-spaced self-tapping screws. Merryday *et al.* (2023) conducted a four-point bending test on a simply supported steel-CLT composite beam with self-tapping screws and reported that lateral-torsional buckling is not a concern at ambient temperature, even with a narrow width of CLT slab. This finding from a bending test indicates that the screws offer an adequate degree of lateral stiffness to prevent beam lateral-torsional buckling at ambient temperature, but this must also be verified under fire conditions due to degradation of the connectors at elevated temperatures.

Hence, the aim of this study is to investigate the behaviour of unprotected downstand steel beams in steel-timber hybrid structures against lateral-torsional buckling and restrained thermal expansion in fire. The objectives are: (i) to assess the level of lateral restraint mobilised by self-tapping screws based on existing literature, and (ii) to develop finite element modelling capacity to effectively investigate the lateral-torsional buckling behaviour of heated steel beams with top flange lateral restraint and end axial restraint. It must be noted that in this study the timber slab is not explicitly modelled for mechanical response but the connection between the steel beam and the timber slab is accounted for through the lateral stiffness provided by the fixings. There is little to no guidance on the design of steel-timber composite construction in current practice, so designers conservatively ignore any potential contribution of CLT panels to composite action and assume that the steel beams resist the full applied loading (AISC, 2022; Merryday *et al.*, 2023; Merryday, Sener and Roueche, 2023). The composite action of steel-timber beams has been investigated under ambient temperature conditions. CLT panels with a greater number of longitudinal layers aligned with the beam span have been shown to contribute more significantly to bending stiffness (Hassanieh, Valipour and Bradford, 2017b). However, the structural response of such systems under fire conditions remains largely unknown and represents an important area for future research. Therefore, this study deals with the case of steel beams without composite action with the timber slab, but the influence of the floor slab as a potential heat sink in the thermal response is considered. The assumptions made in this study with reference to the lateral restraints are conservative, and it is possible that partial composite action during a fire could result in higher flexural stiffness than that of a non-composite steel beam and a separate CLT slab; however, the extent of this effect is unknown.

4.2 Lateral Restraint of Self-Tapping Screws

This section provides an overview of the lateral stiffness characteristics of the self-tapping screws conventionally adopted in mass timber assemblies. Steel-timber hybrid structures can be designed with the connectors acting as lateral restraint to the top flange of the steel beam to prevent beam lateral-torsional buckling. In common practice, CLT panels are attached to steel beams using partially threaded or fully threaded self-tapping screws. The standard screw layout for steel-to-timber connections varies by project, but it is generally provided at spacings not exceeding 600 mm (AISC, 2022). Staggering of the screws is also recommended to reduce the possibility of wood splitting during installation of the fasteners and potentially to avoid overlapping of thermally affected areas of the timber in the vicinity of the screws, which might as a consequence affect the lateral shear resistance and pull-out resistance of the connectors in fire.

The screws, when loaded in shear, provide a degree of lateral stiffness against lateral-torsional buckling of the steel beam. For design purposes, the lateral stiffness offered by screws is defined in terms of the slip modulus for different limit states: K_{ser} for the serviceability limit state, K_u for the ultimate limit state, and K_{fi} for the fire limit state. The slip modulus for the serviceability limit state K_{ser} can be determined experimentally by means of push-out tests or using semi-empirical expressions. K_u is taken as two-thirds of K_{ser} as per BS EN 1995-1-1:2004+A2 (2014). For fire design in accordance with BS EN 1995-1-2 (2004), the slip modulus K_{fi} should be taken as 20% of K_u for screw connections and 67% of K_u for bolted connections. It must be noted that a single value of K_{fi} is adopted in fire and no consideration is given to the variation in connector properties at different temperatures. Figure 4.1 illustrates the procedure as set out in Eurocode 5 to determine the slip modulus of mechanical fasteners for different limit states. More detailed information on the lateral stiffness characteristics of steel-to-CLT connections using self-tapping screws can be found in Jeebodh *et al.* (2024).

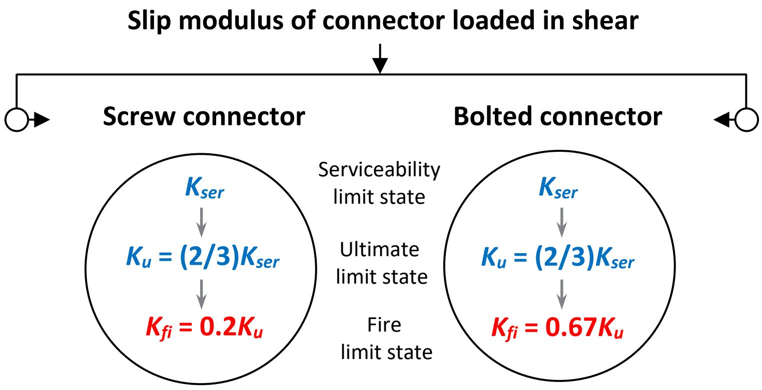

Figure 4.1: Flowchart for determination of slip modulus as per Eurocode 5 guidance

The load-slip relationship of steel-to-CLT connections using self-tapping screws is generally characterised by non-linear behaviour at ambient temperature. Experimental investigations to quantify the longitudinal shear capacity of the steel-timber connections with self-tapping screws in fire are lacking. Merryday, Sener and Roueche (2023) conducted several monotonic push-out tests to study the response of steel-to-CLT connections assembled using three brands of self-tapping screws of different geometries (Type A, B and C) at ambient temperature. The screws were subjected to shear at the interface plane between the steel beam and the timber slab.

Figure 4.2 shows the average load-slip behaviour of three laterally-loaded screw connection specimens with similar screw length, screw spacing, and CLT orientation, but with each specimen connected using a different brand of self-tapping screw. The remaining push-out performance for other test configurations can be found in Merryday, Sener and Roueche (2023). From the experimental results, it can be observed that the screws exhibited different stiffness, strength and ductility. The majority of Type A screws demonstrated ductile behaviour, while Type B and C screws showed more brittle behaviour. The load-slip results from the tests were used in this study to determine the serviceability slip modulus K_{ser} in accordance with BS EN 26891 (1991) equations. The serviceability stiffness K_{ser} varies approximately between 1500 N/mm and 3500 N/mm per 12 mm nominal diameter screw. Hence, K_{fi} can be assumed to vary approximately between 200 N/mm and 467 N/mm for the tested screws at the fire limit state according to Eurocode 5 guidance. As expected, slightly lower levels of stiffness for 10 mm screws in steel-to-CLT connections have been observed by Asiz and Smith (2011). However, the present study focuses on large diameter (12 mm) self-tapping screws which are likely to be more suitable for large-scale construction, as fabrication of small-diameter holes through thicker steel members may be difficult for the steel fabricator (Barber, Roy-Poirier and Wingo, 2021; AISC, 2022; Merryday, Sener and Roueche, 2023) and also to harness the benefits of higher slip modulus per screw.

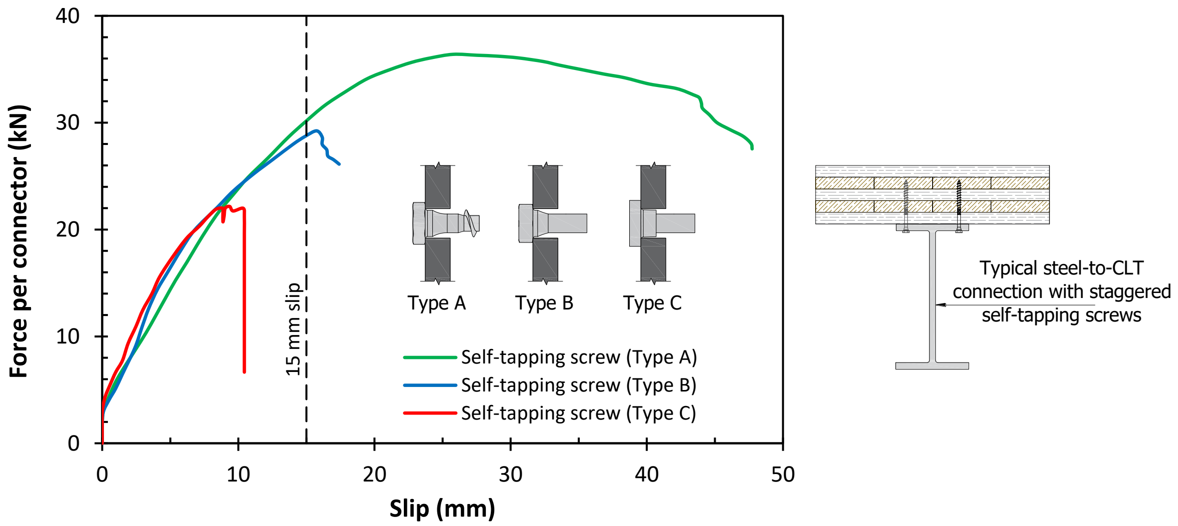

Figure 4.2: Average load-slip curves of push-out tests using three different screw brands (Merryday, Sener and Roueche, 2023)

4.3 Finite Element Modelling in Fire

The structural fire behaviour of steel-timber hybrid structures is mainly influenced by design decisions such as the beam-slab typology, type of connection, choice of adhesive, fire type, and the adopted fire safety strategy. As such, a better comprehension of the thermo-mechanical behaviour of such systems via experimental and/or numerical studies is essential to develop structural fire engineering approaches, with the aim of determining the best practices to design and construct robust steel-timber hybrid structures to resist fire conditions. This section presents the development of finite element models: (i) to capture the thermal response of steel beams supporting a timber flooring system in fire by heat transfer analysis, and (ii) to replicate the lateral-torsional buckling behaviour in the presence of axial restraint of heated steel beams using high temperature mechanical analysis. The numerical models were developed using the finite element analysis software *Abaqus* (Abaqus, 2021) and validated against experimental results from literature.

4.3.1 Development and Validation of Heat Transfer Model

Knowledge of heat transfer is essential to understand the thermal response of hybrid structures in fire. Whether in a fire compartment or a laboratory furnace, heat energy is transferred by the mechanisms of conduction, convection and radiation. When the top flange of a steel beam is attached to a timber or concrete flooring system and is immersed in the flames and hot gases of a fire, both the steel section and bottom surface of the floor receive thermal energy by convection from the hot gases and radiation by electromagnetic waves from the flames. Radiation is key as it is generally the dominant mechanism of energy transfer in large fire situations and is crucial for accurate temperature prediction in numerical models (Sacadura, 2005). In a downstand configuration, the beam is generally subjected to heating from three sides and as it begins to heat up, thermal energy is transferred through the steel material by conduction and eventually deeper into the upper floor which is in direct contact with the top flange of the beam.

In accordance with Eurocode 1 (BS EN 1991-1-2, 2002), the thermal action on a surface exposed to fire can be represented by a net heat flux $\dot{h}_{net}$, which is defined by the sum of convective $\dot{h}_{net,c}$ and radiative $\dot{h}_{net,r}$ flows as given by:

$$\dot{h}_{net} = \dot{h}_{net,c} + \dot{h}_{net,r} \tag{4.1}$$

The net convective heat flux component is determined using the following equation:

$$\dot{h}_{net,c} = \alpha_c(\theta_g - \theta_m) \tag{4.2}$$

where α_c is the coefficient of heat transfer by convection, θ_g is the gas temperature, and θ_m is the surface temperature of the member. In a heat transfer model, the code recommends α_c is taken as 25 W/m^{2}K on the fire-exposed surface to a standard fire and 9 W/m^{2}K on the unexposed side.

The net radiative heat flux component per unit surface area is given by:

$$\dot{h}_{net,r} = \phi \cdot \varepsilon_m \cdot \varepsilon_f \cdot \sigma\left[(\theta_r + 273)^4 - (\theta_m + 273)^4\right] \tag{4.3}$$

Where ϕ is the configuration factor, ε_m is the surface emissivity of the material, ε_f is the emissivity of the fire, σ is the Stefan-Boltzmann constant (5.67×10^{-8} W/m^{2}K^4), θ_r is the radiation temperature of the fire environment taken as equal to θ_g in the case of members fully engulfed in fire, and θ_m is the surface temperature of the member. The configuration factor ϕ is normally taken as 1.0 but a lower value can be used to take into consideration the shadow effects. $\varepsilon_m = 0.7$ for the surface of steel and concrete and $\varepsilon_m = 0.8$ for the surface of timber. The emissivity of the fire is in general taken as $\varepsilon_f = 1.0$.

In numerical simulations, the thermal boundary conditions of the surfaces of members exposed to convection and radiation must be realistically represented to obtain accurate temperature distributions. In fully developed compartment fires, radiation is generally acknowledged as the dominant mode of the total heat flux (Sacadura, 2005) and due to the complexity in determining the correct heat transfer parameters for the radiation flux on individual surfaces, Equation (4.3) has been simplified (Ghojel and Wong, 2005) using an equivalent emissivity of $\in_{eq}$, which takes into account the shadow effects of the incident radiation and emissivities of the fire and the steel member.

$$\dot{h}_{net,r} = \in_{eq} \cdot \sigma\left[(\theta_r + 273)^4 - (\theta_m + 273)^4\right] \tag{4.4}$$

with

$$\in_{eq} = \phi \cdot \varepsilon_m \cdot \varepsilon_f \tag{4.5}$$

For the bottom surface of a slab exposed to fire, the radiative shadowing can be ignored and the equivalent emissivity $\in_{eq}$ can be taken as equal to the emissivity of the floor material ε_m (i.e. assuming $\phi = 1.0$ and $\varepsilon_f = 1.0$). However, the shadow effects for a downstand steel section may not be neglected given that the surfaces between the two flanges will not be exposed to the same incident radiation as the soffit areas of the bottom flange. To allow for reduced incident radiation to these surfaces and considering that the emissivity of steel is temperature-dependent rather than a constant codified value, the equivalent emissivity $\in_{eq}$ can be varied in the numerical simulations until the results are consistent with the experimental fire test data (Franssen, Cooke and Latham, 1995; Ding and Wang, 2009). Figure 4.3 illustrates the shadow effects on an open I-section along with the typical boundary conditions that have been applied in this study for a hybrid system.

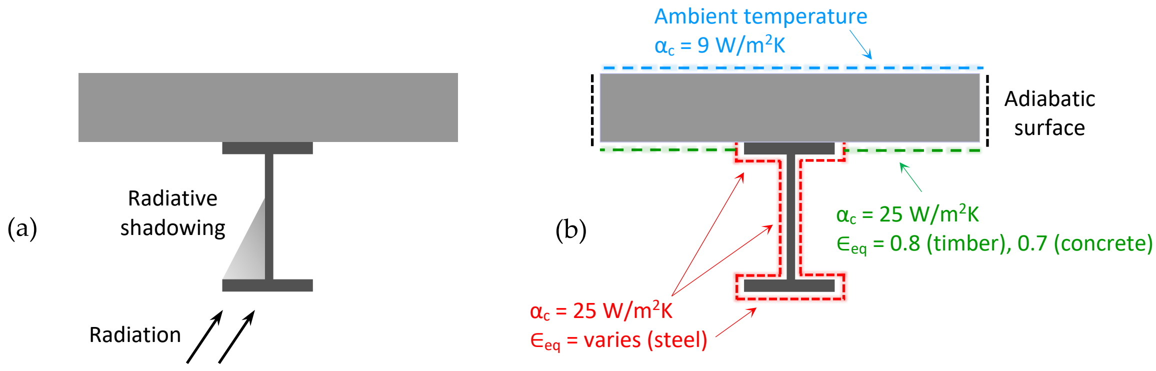

Figure 4.3: (a) Shadow effects on downstand steel beam, and (b) typical thermal boundary conditions of a hybrid beam for heat transfer simulation

There is currently a lack of experimental data on the thermal response of steel-timber hybrid beams in a downstand configuration. Fire test data for a slimfloor arrangement is available (Malaska *et al.*, 2023) but this is not particularly relevant to this study. Therefore, thermal models were initially developed and validated for standard furnace tests on a CLT floor (Fragiacomo *et al.*, 2013) and a steel-concrete beam (Zhang *et al.*, 2019) to predict the temperature distribution measured by thermocouples located at different depths in the test specimens. Subsequently, the concrete flooring was substituted by timber to investigate the temperature distribution in a steel-timber beam and the results were juxtaposed with other existing thermal models documented in literature (Barber, Roy-Poirier and Wingo, 2021; Godoy Dellepiani *et al.*, 2023). In all cases, the thermal behaviour of the heated specimens was captured by using two-dimensional elements, but assuming one-dimensional heat transfer. This study is focused on the thermo-mechanical behaviour of steel-timber systems in a downstand arrangement. In the absence of targeted fire testing, it is reasonable to draw upon existing data from an analogous steel-concrete downstand system and to apply engineering judgment – particularly when developing or calibrating thermal models where the primary interest is in the heating response of the steel beam, rather than the timber slab. The limitations of this approach are clearly acknowledged, especially given that the CLT component is expected to influence the thermal response in ways distinct from concrete due to its combustibility. To address this, the study has considered a range of heating regimes (cooler top flange, uniform temperature profile, and hotter top flange) to reflect possible variations in heat exposure arising from the timber's contribution to the fire dynamics. This approach provides a conservative and pragmatic basis for assessing steel performance in the early phases of model development, pending more targeted fire testing.

In regards to the fire exposure, a standard fire curve (ISO 834) has been selected on the basis that this is the most widely accepted benchmark available (Philion *et al.*, 2022). Standard fire curves have been known to be unscientific since their inception (Ingberg, 1928; Harmathy, 1981; Bisby, Gales and Maluk, 2013), and this is especially the case when the sample is combustible, as is the case for timber. This has been proven experimentally (Węgrzyński, Turkowski and Roszkowski, 2019; Lange *et al.*, 2020). Nonetheless, while other more scientifically sound methods exist – e.g. the compartment fire framework (Thomas and Heselden, 1972), Swedish curves (Pettersson, Magnusson and Thor, 1976), travelling fires (Stern-Gottfried and Rein, 2012), or large compartment fire framework (Gupta, 2021) – none of these are suitable for combustible materials either and there is no widely accepted fire exposure for timber structures. As such, a standard fire curve was chosen instead since this is the more typical benchmark and there is some testing data available for timber systems. Ultimately, while the fire type will have some influence on the results, this study is primarily focused on the associated mechanical response and it is expected that a standard fire exposure will give a reasonable approximation for the thermal boundary conditions.

The thermal properties of materials are also needed to model heat transfer by conduction in structural fire engineering. These temperature-dependent parameters are density, specific heat and thermal conductivity. The values adopted in the simulations were based on the recommendations outlined in BS EN 1993-1-2 (2005) for carbon steel, BS EN 1992-1-2 (2019) for concrete and BS EN 1995-1-2 (2004) for timber. In all cases, the four-noded linear heat transfer quadrilateral (DC2D4) element was used in the thermal simulations and a mesh size of around 5 mm was found to be satisfactory for the three materials, offering both computational efficiency and accuracy. This mesh discretization also closely aligns with the heat transfer simulations carried out by other researchers (Ma, Havula and Heinisuo, 2019; Nguyen *et al.*, 2023a; Nguyen *et al.*, 2023b).

4.3.1.1 Thermal Response of CLT Floor

Fragiacomo *et al.* (2013) experimentally investigated the out-of plane behaviour of CLT floors at both ambient and high temperatures. All test specimens were comprised of five layers with a width of 600 mm and a thickness of 150 mm, arranged in a lamella structure of 42-19-28-19-42 mm. One of the tests, involving a CLT specimen with its underside fully exposed to a standard fire, was simulated to capture the thermal response of timber in fire. Figure 4.4 illustrates the comparison of the temperature distribution between the heat transfer model and the measurements recorded by thermocouples at different depths within the specimen. The simulated temperature profiles are also consistent with the numerical results obtained by other researchers (Fragiacomo *et al.*, 2013; Thi *et al.*, 2017; Chen *et al.*, 2022).

In general, it can be observed that the numerical results are in good agreement with the experimental data except for the temperature increase towards the end of the test. This is due to a change from one-dimensional to two-dimensional heat flux experienced by the highly deflected specimen on its sides as it approached failure. However, this response was not simulated because in a steel-timber hybrid beam with the CLT panels forming a continuous envelope, the heating can be assumed to be one-dimensional.

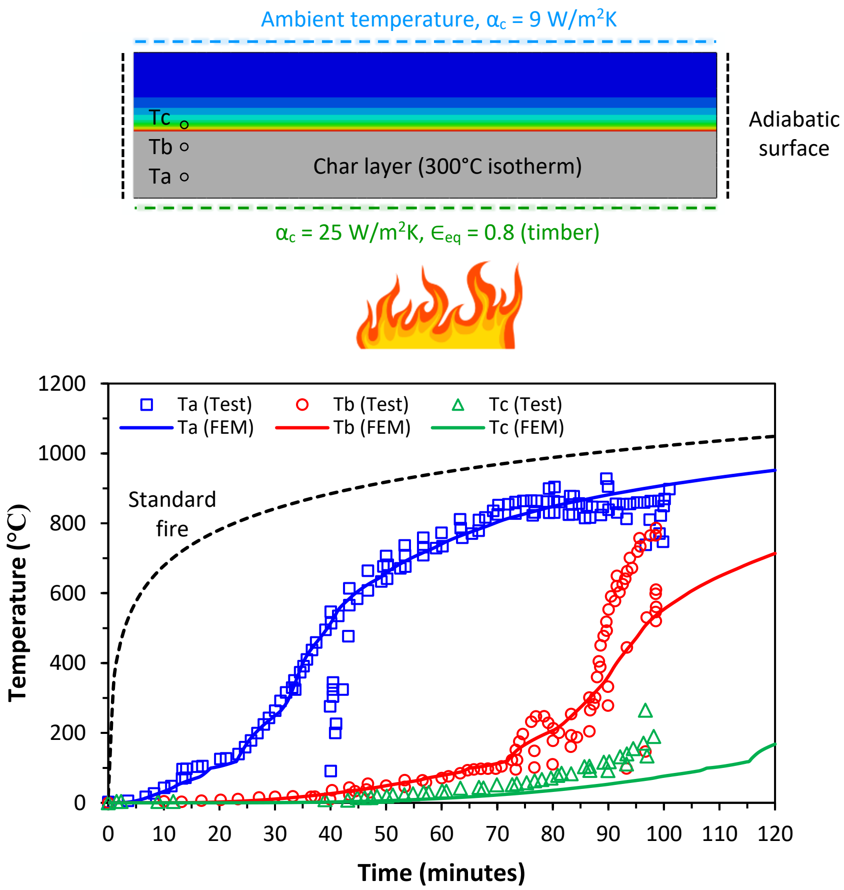

Figure 4.4: Comparison of temperature between experiment and numerical model (FEM) for CLT floor under standard fire conditions

4.3.1.2 Thermal Response of Steel-Concrete Beam

Zhang *et al.* (2019) investigated the restrained behaviour of steel beams in steel-concrete composite systems exposed to increasing temperature in fire. In one of the specimens, the concrete slab, with a width of 1565 mm and a thickness of 120 mm, was connected to a downstand unprotected steel beam HN 250×125×6×9 using shear studs. The test was simulated to capture the thermal response of the specimen with its underside fully exposed to a standard fire. The equivalent emissivity of the steel beam was varied to consider radiative shadowing until the numerical results were consistent with the experimental fire test. The bottom flange and its sides were assigned a value of 0.7 whereas the remaining surfaces of the steel section were given a value of 0.4 to account for reduced radiation.

Figure 4.5 illustrates the comparison of the temperature distribution between the heat transfer model and the measurements recorded by thermocouples at different positions and depths in the experiment. For simplification, it is assumed that the temperatures of the bottom flange and the web are identical as any difference is negligible. In general, it can be observed that the numerical predictions are in good agreement with the experimental data. The simulated temperature profiles are also consistent with the numerical results obtained by Ding, Wang and Jiang (2023). Hence, the modelling approach is deemed to be satisfactory to capture the thermal response of a beam supporting a concrete slab in a downstand arrangement.

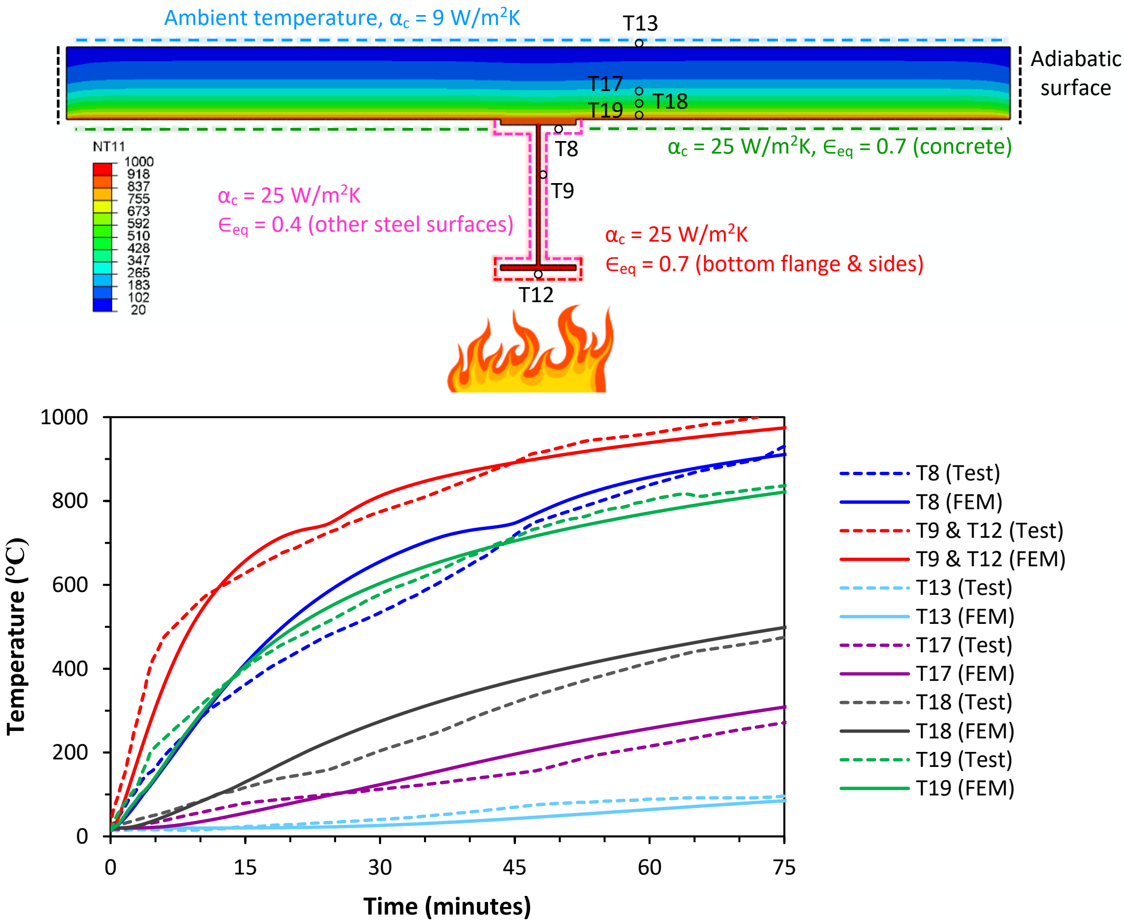

Figure 4.5: Comparison of temperature between experiment and numerical model (FEM) for steel-concrete beam under standard fire conditions

4.3.1.3 Thermal Response of Steel-Timber Beam

The thermal behaviour of a steel-timber beam is inherently more complex due to the combustibility of wood, and is by no means a simple heat transfer problem as seen previously for a steel beam supporting a non-combustible concrete slab. The burning behaviour of timber can be categorised into four important processes: pyrolysis, ignition, flaming combustion, and flame extinction (Bartlett, Hadden and Bisby, 2019). When timber is directly exposed to a fire, it has the potential to alter the fire dynamics of a compartment by adding to the existing fuel load and increasing the temperature or total heat release rate of the enclosure, as evidenced by furnace tests conducted on steel beams with timber encapsulation (Nguyen *et al.*, 2023b) and large-scale mass timber fire tests (Xu *et al.*, 2022; Pope *et al.*, 2023).

In consideration of the above discussion and the lack of experimental test data for a steel-timber downstand beam, the concrete slab mentioned in Section 4.3.1.2 was substituted with timber of density 480 kg/m^3 and 12 % moisture content to simulate the heat transfer. The thermal model assumes that the temperature within the furnace adheres to a standard fire curve, including the energy released by burning of timber. In a furnace test, this is achieved by controlling the rate of fuel supplied to the burner to match the target standard fire curve; a similar approach was adopted in the test on the timber slab detailed in Section 4.3.1.1. This simplification also ensures that the standard fire thermal properties as defined in Eurocode 5 for timber can be used in the heat transfer analysis. In terms of the model boundary conditions, the equivalent emissivity of the steel is assumed to be 0.7 across the entire section as it is expected to receive radiation from the burning timber, thereby lessening the shadow effects. It is acknowledged that the standard fire conditions do not reflect a real fire in a combustible compartment with exposed timber and further research is required to investigate other fire scenarios as well. The likelihood of fire-induced delamination of CLT, which arises from the weakening of the bond line at elevated temperatures, is another phenomenon that can impact both the overall fire severity in a compartment and charring of timber, but not all CLT panels are susceptible to delamination, especially when face bonded using the new generation of adhesives that can maintain glueline integrity under heating (Brandon and Dagenais, 2018; Mindeguia *et al.*, 2020; Hopkin *et al.*, 2022; Arup, 2024). Additionally, the North American standard ANSI/APA PRG 320 requires adhesive certification for CLT panels to ensure that delamination does not cause a secondary flashover. Hence, delamination is not considered within the scope of this study, similar to the approach adopted in investigation (Godoy Dellepiani *et al.*, 2023). However, if delamination is observed during testing, it must be considered in future investigations as more research and fire test data on steel-timber hybrid systems become available. Hence, this study focuses on the use of relatively simple numerical models to simulate the heat absorption in a timber slab without an explicit consideration of factors such as wood combustion and delamination on the influence of the fire dynamics of an enclosure.

Figure 4.6 illustrates the comparison of the simulated temperature distribution between the steel-timber beam and the steel-concrete beam as outlined in Section 4.3.1.2. For simplification, it is assumed that the temperatures of the bottom flange and the web of the downstand steel beam are identical, as any difference is negligible. The temperature profiles in both slabs exhibit trends that are comparable to the in-depth temperature measurements recorded during the Epernon Fire Test Programme on combustible and non-combustible slabs (Bartlett *et al.*, 2020). Furthermore, the temperatures of the unprotected steel beam are also in good agreement with the thermal simulations performed by other researchers for steel-timber hybrid structures in a downstand configuration (Barber, Roy-Poirier and Wingo, 2021; Godoy Dellepiani *et al.*, 2023). Likewise, the results indicate that the top flange of the steel beam is cooler in a steel-concrete beam, indicating that concrete performs as more of a heat sink than timber under the assumed conditions in the heat transfer analysis. Consequently, concrete appears to offer better thermal protection to the steel beam during the fire exposure, reducing the rate of temperature rise in the steel section.

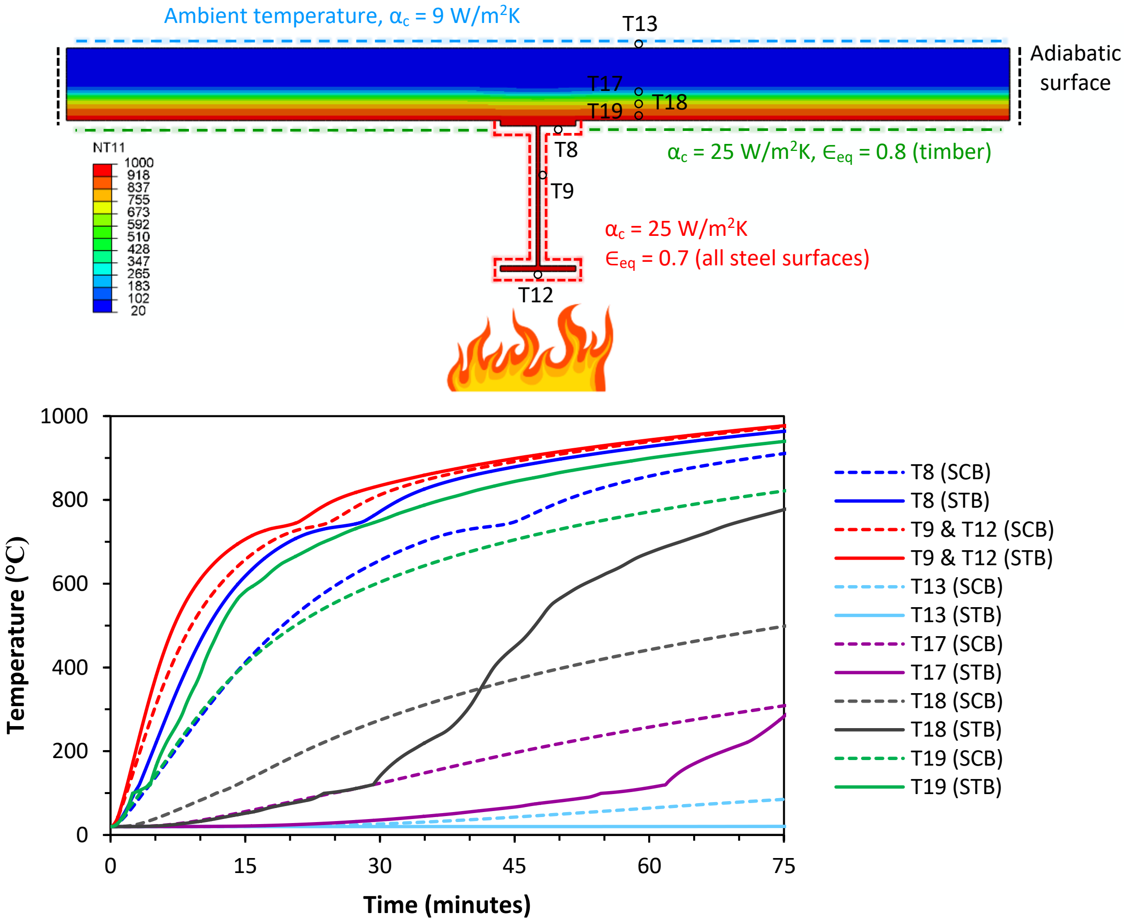

Figure 4.6: Comparison of simulated temperatures between steel-concrete beam (SCB) and steel-timber beam (STB) under standard fire conditions

4.3.2 Development and Validation of High Temperature Mechanical Model

If the temperature history from a heat transfer analysis or experiments is available, it is possible to simulate the mechanical response of a steel beam under fire conditions. This section presents the development of finite element models in *Abaqus* which are able to replicate the lateral-torsional buckling and axially restrained behaviour of heated steel beams. These models are then validated against experimental results found in the literature.

In the numerical simulations, the four-noded quadrilateral (S4R) shell element with reduced integration was adopted for meshing. The high-temperature material properties of carbon steel in terms of non-linear engineering stress-strain relationship and thermal expansion were in accordance with BS EN 1993-1-2 (2005). Two distinct types of end boundary conditions, as schematically depicted in Figure 4.7, were utilised. In Type 1, rigid body constraints connect all nodes of the web to a reference point, whilst the flanges have independent boundary conditions. This method can be used to model a simply supported member with ideal fork support conditions (prevent lateral and vertical translations including torsional rotation but allow warping of the flanges) at the ends. In Type 2, all nodes of the cross-section are constrained to a reference point. This method can be used to model a member with axially and/or rotationally restrained conditions. The restraints to the steel beam were simulated using connector elements, which can define a connection between a node and a rigid body. The validation of the numerical models was performed through a comparison of the predictions with two sets of experimental data under fire conditions, one pertaining to the lateral-torsional buckling of an axially and laterally unrestrained beam (Mesquita *et al.*, 2005), and the other to an axially and laterally restrained beam (Li and Guo, 2008).

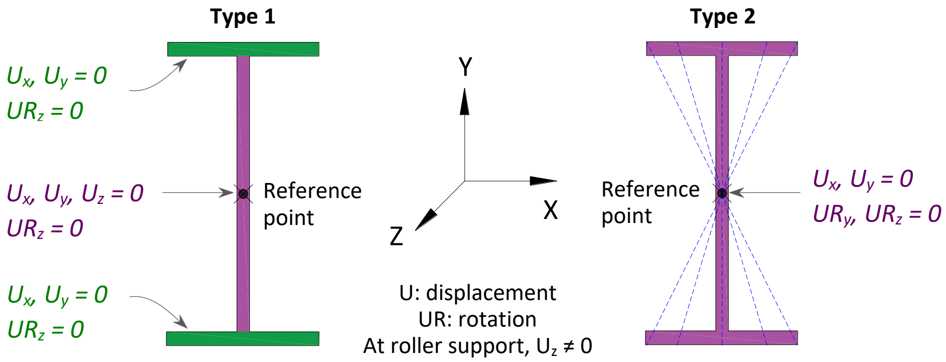

Figure 4.7: Beam end boundary conditions Type 1 and 2

The high-temperature mechanical analysis consisted of two steps: an ambient-temperature loading step during which the load and a geometric imperfection were applied, followed by a heating step in which the temperature of the steel was increased according to a predefined temperature profile while maintaining the applied load. The geometric imperfection was included in the analysis by scaling an eigenmode of a linear buckling analysis on a perfectly straight beam. The static general solver including geometric nonlinearity was used in both steps. To ensure convergence during the thermal loading step, automatic stabilisation using dissipated energy fraction/damping factor and adaptive stabilisation were utilised in *Abaqus* to stabilise the unstable quasi-static problem, i.e. lateral-torsional buckling. Adaptive stabilisation was activated to control the ratio of viscous damping energy to the internal energy (ALLSD/ALLIE ≤ 5%) and to avoid inaccurate results. 5% is the default value in *Abaqus* for many situations because it is generally small enough not to significantly affect results, and was therefore retained to avoid introducing too many variables in the simulations.

4.3.2.1 Mechanical Response of Unrestrained Steel Beam

Mesquita *et al.* (2005) investigated the lateral-torsional buckling behaviour of several fork supported IPE 100 beams at high temperatures. The span of the beams varied from 1.5 m to 4.5 m and three tests were carried out for each beam length. The beams were initially loaded and then uniformly heated at a constant rate of 800 °C/h until failure by lateral-torsional buckling. The beams were made with steel having an average yield strength of 293.2 MPa. Figure 4.8 compares the numerical results obtained in this study, using Type 1 boundary conditions and a half-sine wave geometric imperfection, with the experimental data for the beam of 3.5 m span, as well as the predictions made by Kucukler (2020). Given the small size of the specimen, a mesh size of 5 mm was adopted in the numerical model and an imperfection with a maximum amplitude of span/4000 was defined based on the measurements obtained from the tests. It can be observed that the numerical results are in good agreement with the measured path of the midspan deflection; the differences are imperceptible until 621 °C. The results also align well with the predictions made by other researchers (Martins *et al.*, 2022; Song *et al.*, 2022). This indicates that the simulation strategy adopted is able to mimic the lateral-torsional buckling response of steel beams in fire.

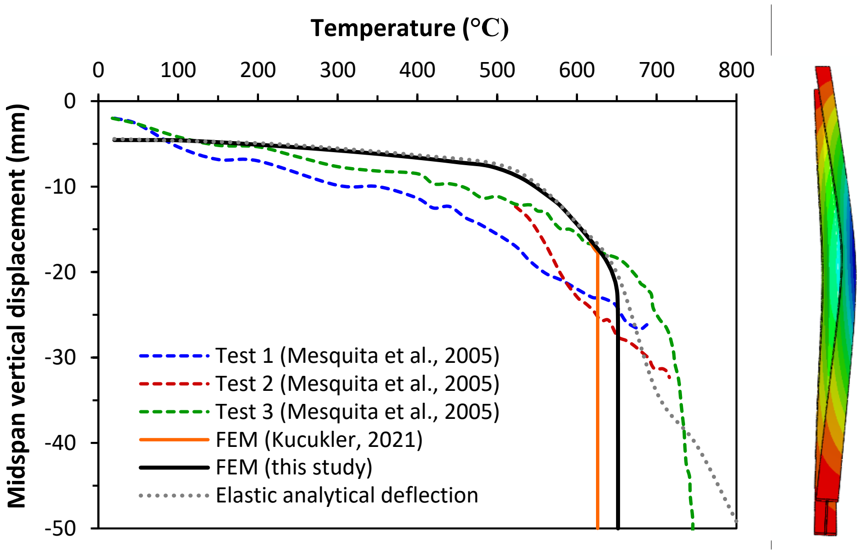

Figure 4.8: Comparison of displacement-temperature curves between experiment and numerical models (FEM)

4.3.2.2 Mechanical Response of Axially Restrained Steel Beam

Li and Guo (2008) investigated the fire performance of two restrained steel beams of H 250×250 ×8×12 section under non-uniform heating conditions. The beams were 4.5 m and loaded with two point loads of 130 kN each. The average yield strength of the steel was 271 MPa. In one of the specimens, the axial (K_a) and end-rotational (K_r) stiffness of the beam were 39.5 kN/mm and 1.09×10^8 Nm/rad, respectively (Zhang, Li and Usmani, 2013; Nguyen and Park, 2022). This test was simulated using Type 2 boundary conditions and a mesh size of 20 mm was found to be satisfactory. A larger mesh was used in this case, in contrast to the 5 mm mesh used in the simulation outlined in Section 4.3.2.1, due to the greater steel cross-section and longer span of the specimen. Figure 4.9 shows the comparison between the numerical results obtained in this study and the experimental data in terms of the axial force and midspan vertical deflection. The predictions made by Dwaikat and Kodur (2011) and Zhang, Li and Usmani (2013) are also illustrated. Overall, it can be inferred that the simulation strategy adopted is able to mimic the restrained behaviour of steel beams in fire using both axial and rotational restraint. The discrepancies between the test results and current predictions are mainly due to the simplified boundary conditions assumed in modelling the supports of the test.

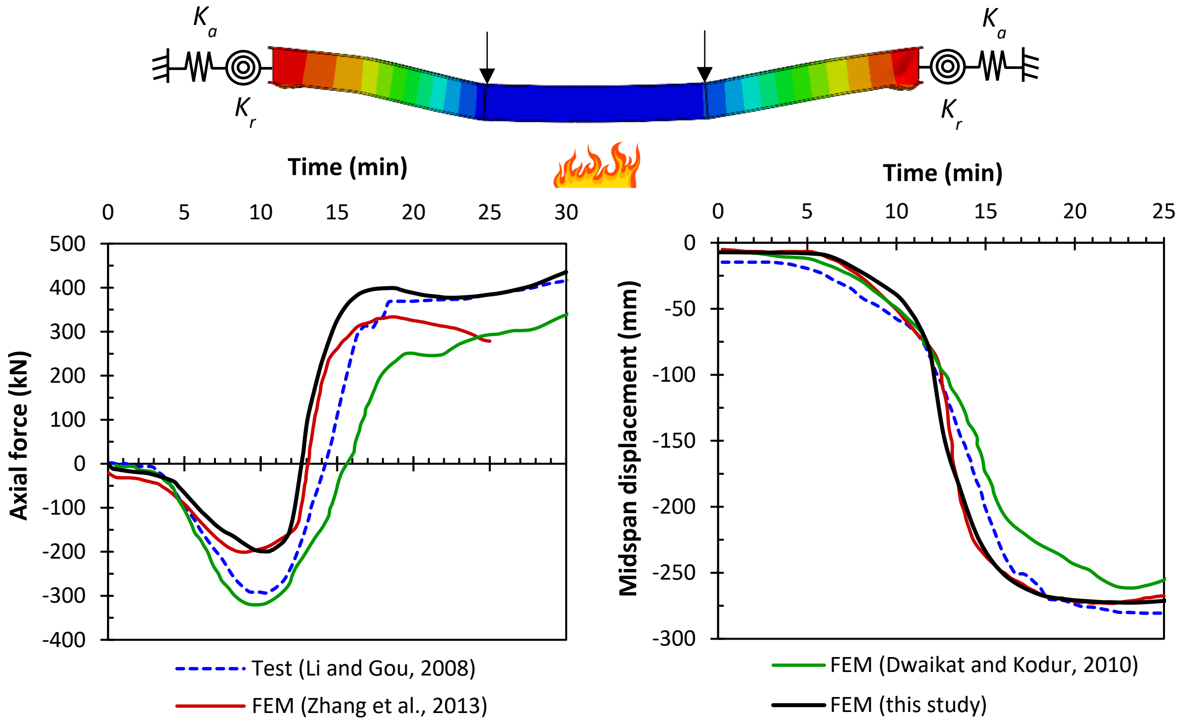

Figure 4.9: Comparison of axial force and displacement between experiment and numerical models

4.4 Parametric Study

The validated numerical models were used to investigate the influence of some key parameters on the thermo-mechanical response of unprotected steel beams in steel-timber hybrid structures. As explained earlier in Section 1, the CLT slab is not incorporated in the mechanical models. However, this modelling assumption adheres to a conservative approach that is in line with current design practice and helps to develop new insights on the structural response of steel-timber hybrid structures in fire. The parameters considered are: (i) the degree of lateral restraint provided by the fasteners, (ii) the axial restraint of the end connections, and (iii) the beam temperature distribution under both uniform and non-uniform heating scenarios. Following the description given in Section 4.3.2, the high-temperature mechanical analysis consisted of two steps: an ambient-temperature loading step followed by a heating step in which the temperature of the steel was increased accordingly while maintaining the applied load.

A hot-rolled steel beam of section UB 457×152×74, grade S355 and 9m span was chosen for the investigation. The 9 m span, giving a span-to-depth ratio of 19.5, was selected to reflect a central secondary beam in a typical steel framing scheme with 9 m × 9 m column grids for a conventional commercial office floor. In terms of applied loading, the dead load is assumed to be 3.0 kN/m^2 (including self-weight of slab, finishes, and services) and the live load is taken as 5.0 kN/m^2. Hence, the top flange of the beam is assumed to be loaded with a line load of 24.75 kN/m at the fire limit state from a tributary width of 4.5 m of the slab, giving a load ratio of 0.44 if the beam is assumed to be fully laterally restrained at ambient temperature. The load ratio is defined as the ratio of the applied moment at the fire limit state to the plastic moment capacity of the member at ambient temperature (load level in BS EN 1994-1-2 (2005)). This study considers only one load ratio, but future work should explore a wider range to more accurately reflect the broader load conditions present in real steel-timber hybrid structures.

4.4.1 Lateral and Axial Restraint

From the experimental investigations described in Section 4.2 to quantify the longitudinal shear behaviour of steel-to-timber connections, the range of lateral stiffness K_{ser} was found to vary approximately between 1500 N/mm to 3500 N/mm for the tested screws. At the fire limit state, K_{fi} can be assumed to vary between 200 N/mm to 467 N/mm in accordance with Eurocode 5 guidance. Hence, a range of lateral restraint K_{fi} was selected for the parametric study: 10 N/mm, 25 N/mm, 100 N/mm, 200 N/mm, 500 N/mm, and ∞ (full lateral restraint). Low values of K_{fi} were also included to investigate the sensitivity of the beam to the effect of low lateral restraint.

Experimental investigations on screws of equal diameter in steel-to-timber connections have demonstrated a range of failure modes, from brittle to typically ductile responses (Merryday, Sener and Roueche, 2023). Therefore, modelling the screw connections as linear elastic-perfectly brittle was adopted as a conservative worst-case design scenario. Additionally, Eurocode 5 specifies a single slip modulus value K_{fi} for screws in fire, which is intended to be both practical and conservative. As such, a sensitivity analysis using alternative models (e.g. bilinear or including temperature-dependent degradation) was not conducted, since reliable experimental data across a sufficient temperature range for this connection type is unavailable, and the intent is to establish a conservative baseline rather than to explore a broader range of screw behaviours. In all cases, it is assumed that the screws are: (i) linear elastic but fail in a brittle manner with a shear deformation capacity of 15 mm, and (ii) staggered at equal spacing of 250 mm on the top flange of the beam. BS EN 26891 (1991) recommends that push-out tests may be stopped when the ultimate load is reached, or when the slip is 15 mm, whichever occurs first. Hence, an ultimate slip of 15 mm was adopted for the parametric study in the absence of connection test data in fire and also due to the fact that some of the screws tested in Merryday, Sener and Roueche (2023) experienced slippage of at least 15 mm along with brittle failure at ambient temperature.

The influence of varying degrees of axial restraint provided by the end connections was also investigated. Seven levels of axial restraint were considered: $0.05K_a$, $0.15K_a$, $0.30K_a$, $0.50K_a$, $1.00K_a$, and ∞ (full axial restraint), where K_a is the axial stiffness of the beam at ambient temperature and is found to be 221 kN/mm. The axial restraint is assumed to be linear and unaffected by temperature. The effect of lateral and axial restraint is simulated using connector elements, following the similar approach adopted in Section 4.3.2. Figure 4.10 illustrates the location of lateral and axial restraint for the beam as part of the parametric study.

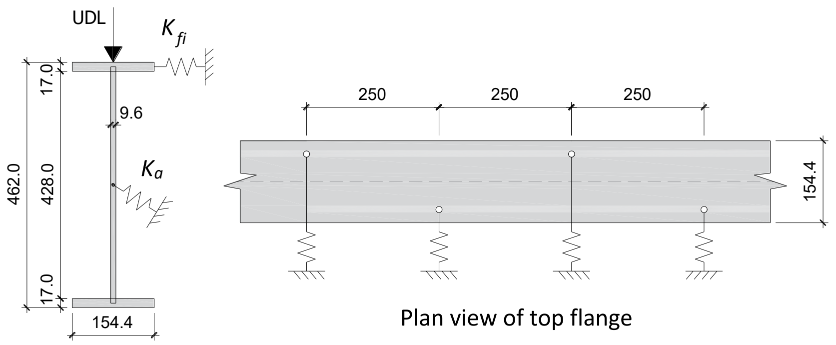

Figure 4.10: Position of lateral (K_{fi}) and axial (K_a) restraint for parametric study

4.4.2 Temperature Distribution

In line with the simulation procedure explained in Section 4.3.1, the thermal response was obtained for the beam supporting a typical 160 mm CLT slab with a density of 480 kg/m^3 and a moisture content of 12%. The width of the slab is assumed to be 1000 mm in the numerical model for computational efficiency (modelling the whole span length does not affect the heat transfer analysis) and thermal boundary conditions are as explained previously. The underside of the CLT is assumed to be fully exposed to a standard fire without any encapsulation. In a real building fire with a decay phase, the actual heating rates will be different, but the adopted temperature regimes in this study will help to obtain an understanding of the structural response of the beam leading to failure, although to a different timescale.

Figure 4.11 illustrates the simulated non-uniform temperature distribution of the steel-timber beam in which the web and bottom flange are assumed to have the same temperature while the top flange is cooler due to the heat sink effect of the timber slab. Given the lack of experimental data for such hybrid systems in fire, it is also assumed that the temperature distribution in the beam is uniform, in which the whole section is taken to be at the temperature of the web. This is a more conservative assumption with a hotter compression flange for the design of steel-timber hybrid structures. It is important to reiterate that this study focuses on relatively simple heat transfer analysis and there is a clear need for complementary experimental work to understand the thermal response of steel-timber beams in fire with coupled interaction between the structural elements and resulting fire dynamics.

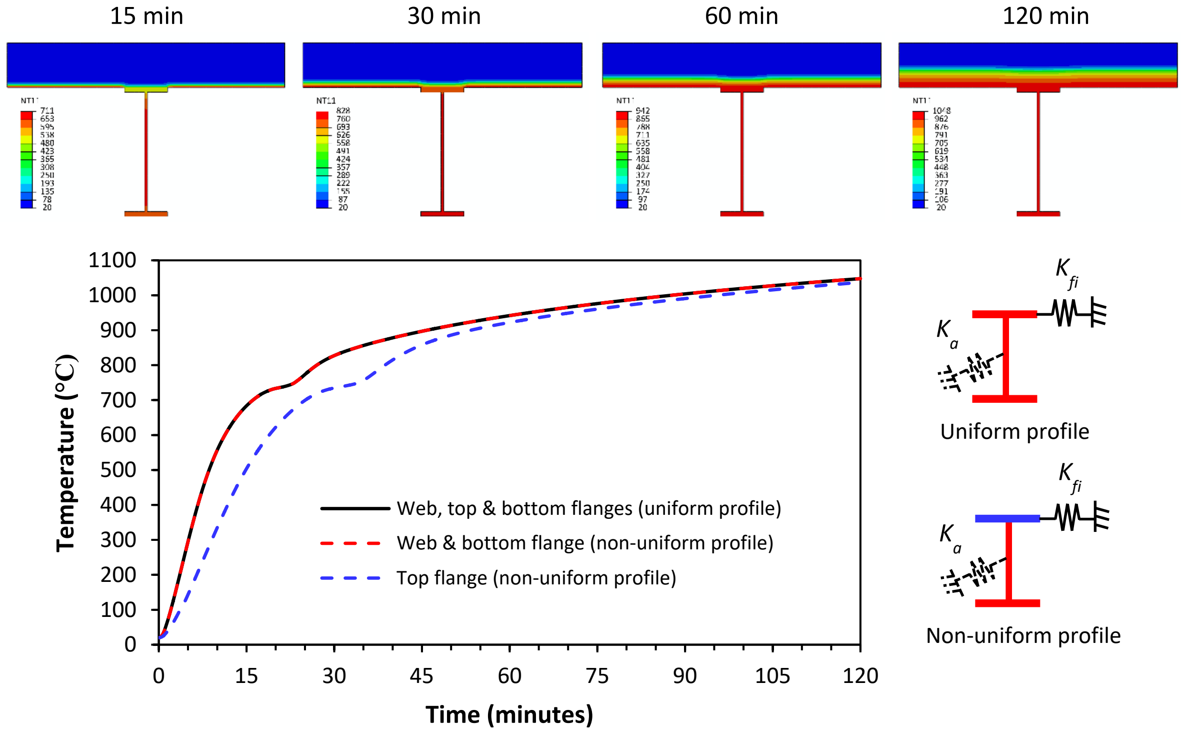

Figure 4.11: Temperature profiles adopted for parametric study

4.4.3 Mesh Sensitivity Analysis

To further complement the validation studies presented in Section 4.3.2, a comparison was made between the critical elastic buckling moment of the beam with lateral restraint for various eigenmodes in *Abaqus* and *LTBeamN* (CTICM, 2023), which is commonly used for linear buckling analysis. This was done to verify the numerical results from the two softwares in the absence of high temperature test data of steel-timber downstand beams. A mesh sensitivity analysis was conducted in two steps to ascertain the optimal mesh size for the parametric study: (i) linear buckling analysis, and (ii) non-linear thermo-mechanical analysis. A finer mesh typically results in a more accurate solution but the simulation becomes more computationally expensive.

4.4.3.1 Linear Buckling Analysis

In the linear buckling analysis, mesh sizes ranging from 40 mm to 5 mm were used to verify the elastic buckling moments of the steel beam with elastic lateral restraint of 200 N/mm (without brittle failure) at 250 mm spacing. The results obtained are summarised in Table 4.1. It can be observed that the results from *Abaqus* are slightly lower than those given by *LTBeamN*. This is largely due to the fact that the fillet radius of the steel beam was not explicitly modelled in *Abaqus* to reduce the complexity of the model, and that reduced integration was also considered in the shell elements. Nevertheless, a mesh size of 20 mm gives an error of less than 2.5% for the first eigenmode. Figure 4.12 illustrates the first three buckling modes of the beam under both unrestrained conditions and partially restrained conditions with closely-spaced top flange lateral restraint. The first eigenmodes were also used to perform an imperfection sensitivity analysis, as elaborated later in Section 4.4.4

Table 4.1: Critical buckling moment in Abaqus and LTBeamN with K_{fi} = 200 N/mm

Eigenmode	**Critical buckling moment (kNm)**					
	LTBeamN	**Abaqus with different mesh sizes (mm)**				
		40	**30**	**20**	**10**	**5**
1	1035	1004	1005	1012	1014	1017
2	1116	1087	1088	1089	1090	1092
3	1822	1688	1689	1694	1693	1695

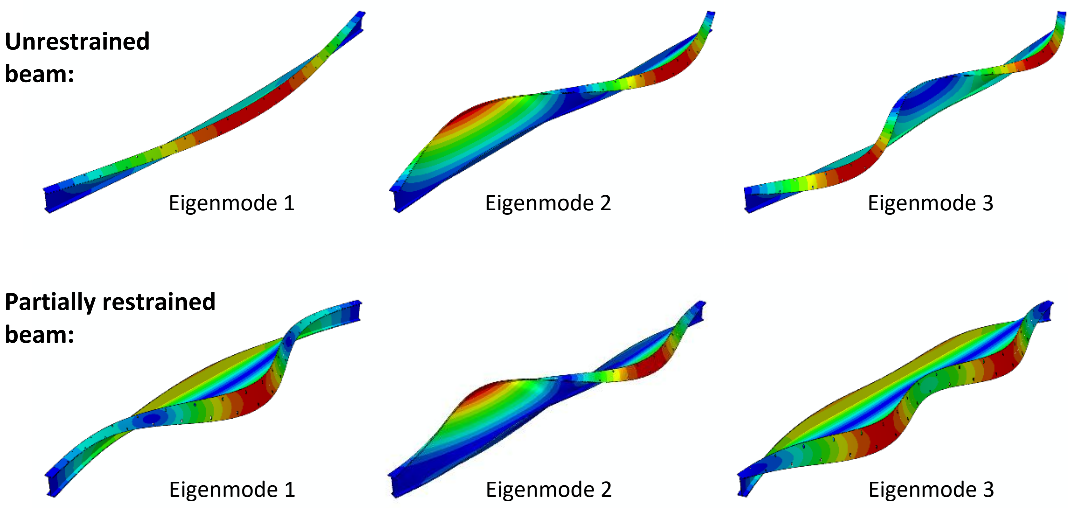

Figure 4.12: Typical buckling modes for unrestrained and partially restrained beams

4.4.3.2 Non-Linear Thermo-Mechanical Analysis

In the non-linear thermo-mechanical analysis, mesh sizes ranging from 40 mm to 10 mm were selected for a further mesh sensitivity analysis (the 5 mm mesh was omitted as it proved to be too computationally expensive). The steel beam was loaded with a line load of 24.75 kN/m and subjected to a uniform increase in temperature as described in Section 4.4.2. The geometric imperfection was initially considered using the conventional half-sine wave of an unrestrained beam. A constant elastic lateral stiffness of 200 N/mm without the 15 mm fracture limit was adopted to avoid convergence issues at this stage of the analysis. The failure temperature is taken as the temperature at which the vertical deflection reaches span/20 irrespective of the magnitude of the lateral deflection. The results of this analysis are summarised in Table 4.2. Considering the minimal variability between the failure temperatures, a mesh size of 20 mm was ultimately selected for the parametric study, which also adequately simulated the test beam in Section 4.3.2.2.

Table 4.2: Failure temperature for different mesh sizes with K_{fi} = 200 N/mm

Mesh size (mm)	**40**	**30**	**20**	**10**
Number of elements	9,622	11,514	19,321	69,644
Failure temperature (°C)	573.7	574.6	574.3	574.2

4.4.4 Imperfection Sensitivity Analysis

Material and geometric imperfections can influence the stability of structural members. Residual stresses, which are generated from the manufacturing process, have been neglected in this investigation as this form of material imperfection decreases with higher temperature levels in a fire. In addition, Vila Real *et al.* (2004) and Kucukler (2020) have demonstrated that the buckling resistance of beams is less sensitive to residual stresses with increasing temperature. Residual stresses have also been omitted in other high temperature numerical simulations including restrained conditions (Yin and Wang, 2003; Yin and Wang, 2004; Santiago *et al.*, 2008). While this assumption holds at lower load levels due to the negligible influence of residual stresses, their inclusion is recommended at load ratios around 0.65 of the load-bearing capacity at ambient temperature, where their effects become significant in numerical analyses (Couto and Vila Real, 2021). In the parametric study, the applied load ratio is 0.44, which is sufficiently low to justify the exclusion of residual stresses from the analysis.

Geometric imperfection, due to manufacturing, transportation or handling processes, were incorporated in the analysis by performing a prior linear buckling analysis and scaling the buckling eigenmode as necessary. A lateral geometric imperfection based on the first lateral-torsional buckling mode of the beam was considered with a maximum amplitude of 1/1000 of the beam length. This value was adopted based on previous numerical studies (Yin and Wang, 2003; Yin and Wang, 2004; Mesquita *et al.*, 2005; Santiago *et al.*, 2008; Couto and Vila Real, 2019; Kucukler, 2020). It was found that the failure temperature was sensitive to the type of imperfection applied, thus a sensitivity analysis was performed to seek the suitable imperfection type. Similarly, Couto and Vila Real (2019) also demonstrated that the shape of the imperfection affects the lateral-torsional buckling resistance of a steel beam. The following imperfections were considered:

- **Imperfection 1**: first eigenmode of a laterally unrestrained beam (half-sine wave);
- **Imperfection 2**: first eigenmode of a partially laterally restrained beam based on K_{fi}.

Table 4.3 illustrates the effect of the imperfection type on the failure temperatures of the beam for the practical range of K_{fi} from 200 N/mm to 500 N/mm. It is typical to assume full lateral restraint at ambient-temperature for the beam due to the high lateral stiffness values of K_{ser} and test observations (Merryday *et al.*, 2023). However, small lateral movements might occur in the simulations which could affect the shape and magnitude of the imperfection. Hence, the use of the full lateral restraint conditions at the ambient-temperature loading step was also considered. This differs from the simulation outlined in Section 4.4.3.2, where K_{fi} rather than the full lateral restraint was applied at ambient temperature, which resulted in a subsequent distortion of the imperfection for the mechanical analysis in fire. Imperfection 2 was eventually selected for the parametric study as it results in the lowest failure temperatures.

Table 4.3: Effect of imperfection type on predicted failure temperature

K_{fi} (N/mm)	Failure temperature (°C)	
	Imperfection 1	**Imperfection 2**
200	580	568
500	593	574

4.5 Results and Discussion

This section presents the numerical results of the parametric study under the influence of various parameters. Also, the simulations now take into consideration the 15 mm fracture limit of the lateral restraint. This was intentionally omitted in the previous models described in Section 4.4 to avoid convergence issues during the analysis.

4.5.1 Influence of Lateral Restraint on Axially Unrestrained Steel Beams (K_a = 0)

Secondary steel beams are generally designed as simply supported members at ambient temperature. This section explores the influence of lateral restraint on the lateral-torsional buckling behaviour of simply supported beams in fire. In the numerical simulations, a Type 1 boundary condition was adopted to ensure that the beam is axially unrestrained and can expand freely during the heating phase.

Figure 4.13 compares the midspan vertical deflections of the chosen beam for various levels of lateral stiffness K_{fi} of the screw connections and considering both the uniform and non-uniform temperature profiles. The deflection-temperature results are also compared to the fully laterally restrained case, as well as to the hand calculated elastic deflection of the beam under uniform heating. The failure line corresponding to the midspan vertical deflection of span/20 is also presented.

It can be observed that the beam is sensitive to low levels of lateral restraint. For both the uniform and non-uniform heating cases, the low lateral restraint (10 N/mm) leads to a much lower runaway deflection temperature than all the other cases. All the other partial lateral restraint levels (equal to or above 100 N/mm) result in similar runaway deflection temperatures. In uniformly heated cases, lateral-torsional buckling leads to runaway deflection at an earlier stage than it does in non-uniformly heated cases, in which the response is closer to the fully laterally restrained beam as the cooler compression flange provides enhanced structural performance in fire but this behaviour is expected to vary across various assumed temperature scenarios. The effect of thermal bowing can also be observed due to the uneven temperature distribution. However, the simply supported behaviour does not accurately reflect the actual thermo-mechanical response under fire conditions as it fails to account for the axial restraint provided by adjacent structures.

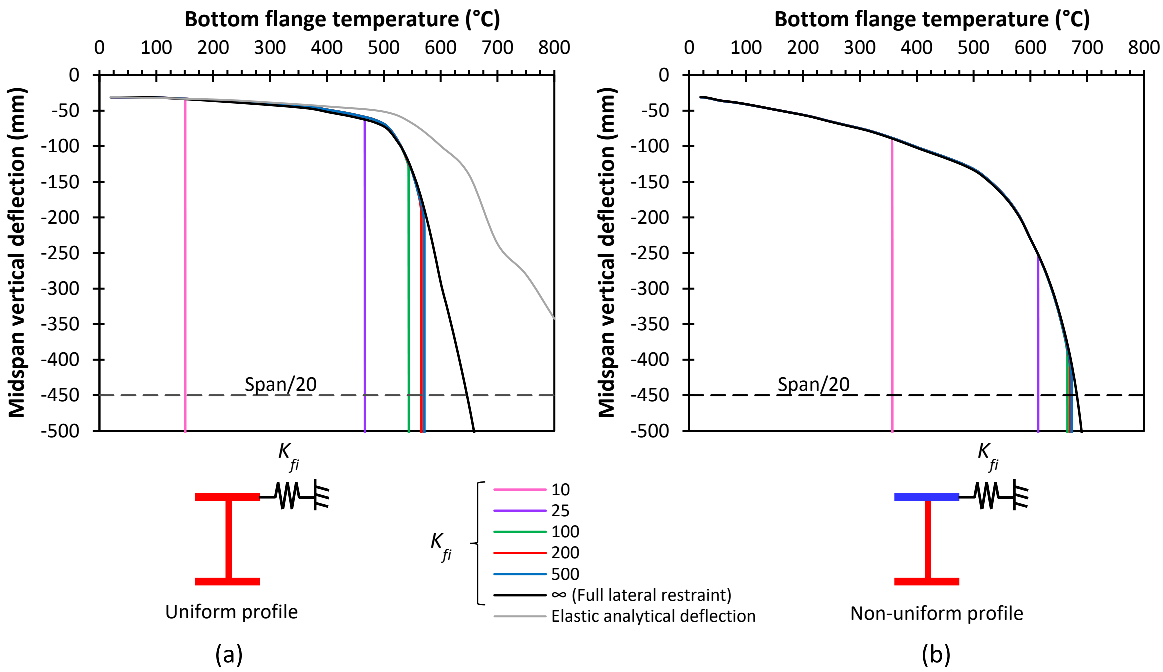

Figure 4.13: Vertical deflection-temperature relationships under varying lateral stiffness K_{fi} for (a) uniform temperature profile and (b) non-uniform temperature profile

4.5.2 Influence of Lateral Restraint on Axially Restrained Steel Beams ($K_a \neq 0$)

In real structures, it is well-established that the surrounding connections generally restrict thermal expansion and induce axial compression force followed by tensile force in a fully laterally restrained steel beam exposed to fire (Yin and Wang, 2004; Wang *et al.*, 2012). The introduction of catenary forces in a fully laterally restrained beam provide an additional mechanism to resist the external loading at high temperature as material degradation occurs and bending resistance decreases.

In this section, the influence of varying degrees of axial restraint provided by the end connections under both uniform and non-uniform heating is investigated for a K_{fi} value of 200 N/mm. Seven levels of axial restraint are considered: 0.05K_a, 0.15K_a, 0.30K_a, 0.50K_a, 1.00K_a, and ∞, where K_a is the axial stiffness of the beam at ambient temperature and is found to be 221 kN/mm. The axial restraint is assumed to be linear and unaffected by temperature. Figure 4.14 (a) to (f) illustrate the evolution of the midspan vertical deflection of the bottom flange and midspan lateral deflection of the top flange along with the axial force development for various axial restraint and temperature distributions. The vertical deflection-temperature and axial force-temperature relationships are also compared to a fully laterally restrained beam ($K_{fi} = \infty$) for the corresponding axial restraint. In some cases, the full thermo-mechanical response could not be captured due to convergence difficulties encountered in the large-displacement analysis.

In general, it can be observed that in the presence of axial restraint, a partially laterally restrained beam initially follows a similar gradient to the fully laterally restrained beam but subsequently undergoes the classical runaway deflection due to lateral-torsional buckling. This is clearly visible in Figure 4.14 (c) and (d) where there is a sudden increase in lateral deflection in the midspan region. A turning point is then reached when the rate of runaway deflection is attenuated due to the development of tensile force in the member, where it starts to behave as a cable. Additionally, the axial-temperature relationships illustrated in Figure 4.14 (e) and (f) indicate that the curves follow similar gradients to the fully laterally restrained beam until a maximum compression force is attained.

As expected the imposition of higher levels of axial restraint reduces the failure temperature at which the beam undergoes instability by lateral-torsional buckling. It is also evident that it is unsafe to assume fully laterally restrained conditions in fire. In general, the thermo-mechanical response of partially laterally restrained beams with end axial restraint can be described as follows:

- Initially, the beam follows the behaviour of a fully laterally restrained beam until a maximum compressive force is reached when the first screw fails in shear in the midspan region.
- Once the first screw fails, the remaining screws start to fail in succession and the beam undergoes runaway deflection whereby there is a rapid increase in both vertical and lateral deflections along with a very sharp transition from compressive to tensile force in the member.
- The catenary stage is then reached and the tensile force generated provides the mechanism to slow down the rate of runaway midspan deflection. The tensile force remains at a fairly constant magnitude up to a maximum until failure occurs when the tensile capacity of the beam is exceeded.

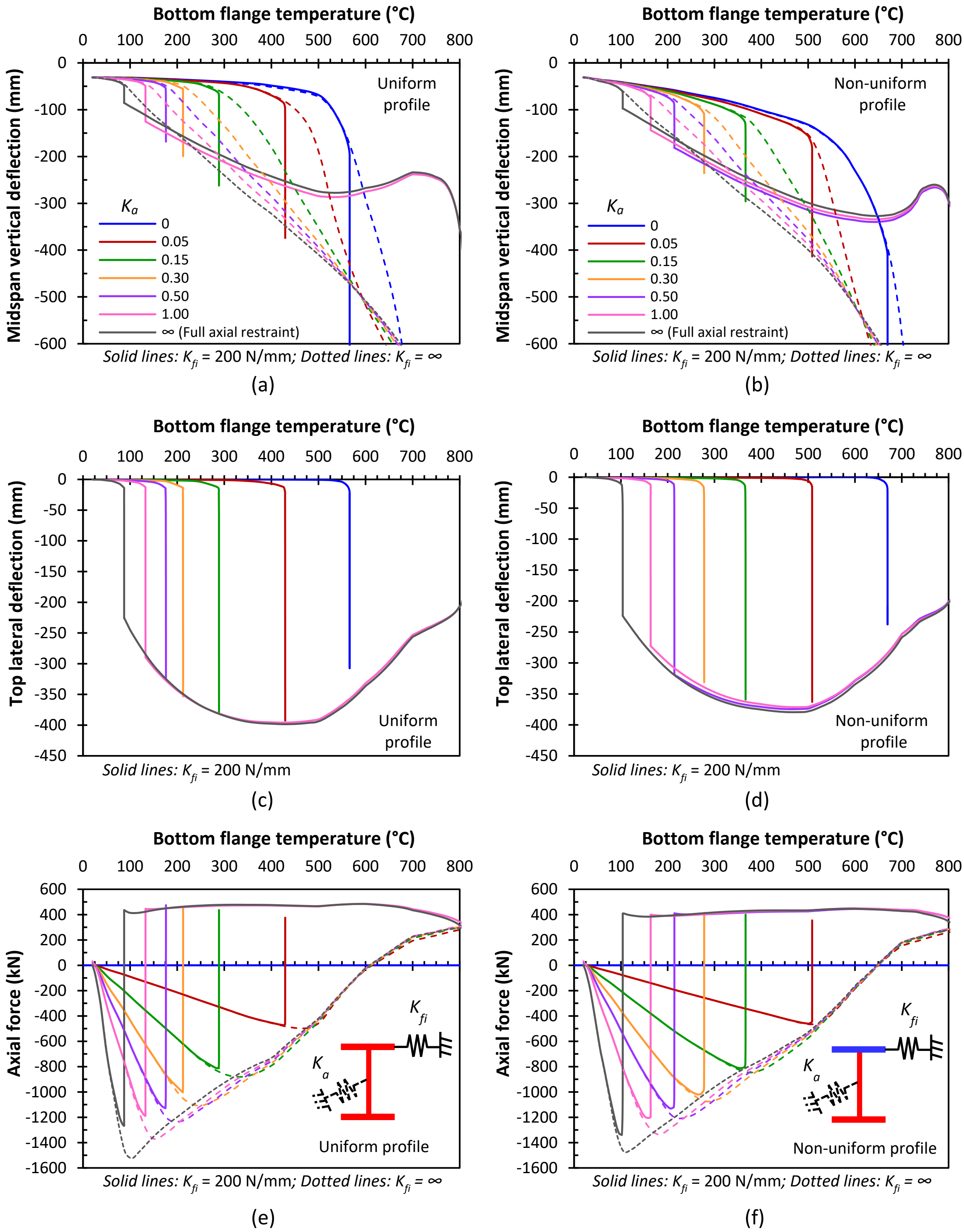

Figure 4.14: Temperature relationships for (a, b) midspan vertical deflection, (c, d) top flange lateral deflection, and (e, f) axial force with varying axial restraint under uniform and non-uniform temperature profiles for K_{fi} = 200 N/mm and $K_{fi} = \infty$

Figure 4.15 shows the variation of the induced axial forces in the beam under different degrees of lateral restraint coupled with uniform and non-uniform temperature distributions. In all cases, the axial restraint level is assumed to be equal to the axial stiffness of the beam at ambient temperature ($1.00K_a$). The trends in the results are remarkably consistent with the axial force development in Figure 4.14 and it can be observed that the imposition of higher levels of lateral restraint increases the failure temperature at which the beam becomes unstable by lateral-torsional buckling. Also, there is no significant difference in the failure temperatures between the uniform and non-uniform heating regimes under the same axial restraint level.

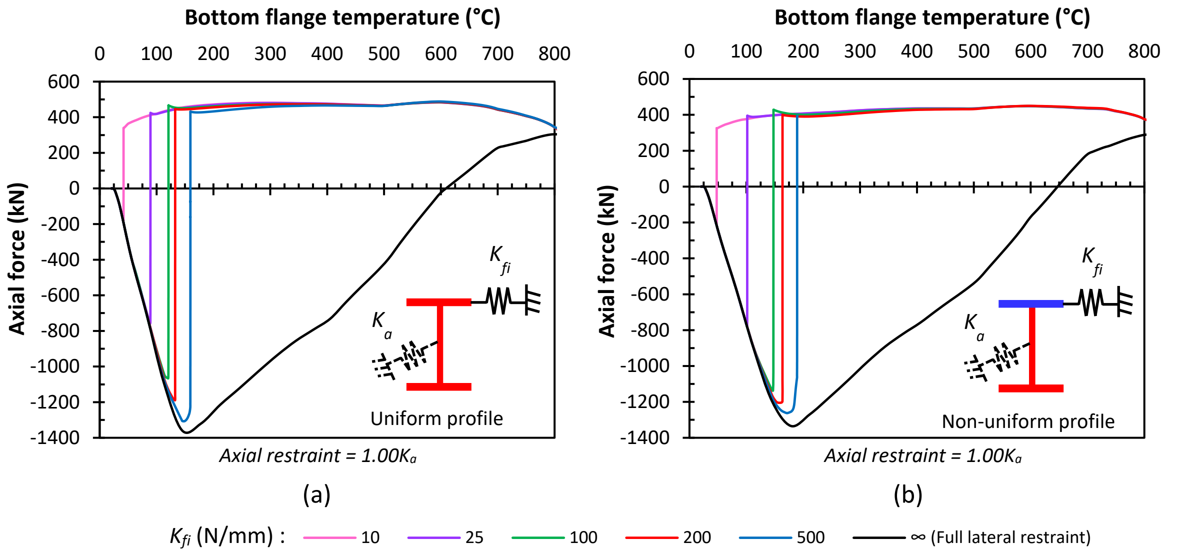

Figure 4.15: Axial force-temperature relationships under varying lateral stiffness K_{fi} and constant axial restraint of $1.00K_a$ for (a) uniform temperature profile and (b) non-uniform temperature profile

4.5.3 Comparison of Failure Temperatures

According to guidance documents (BS EN 1991-1-2, 2002; STA, 2023), construction elements must provide one or more of the performance criteria during a specified fire exposure, namely: (a) load resistance or stability, (b) thermal insulation, and (c) integrity. Allied to this, steel-timber hybrid structures must sustain mechanical loads without exceeding large deflections and disproportionate collapse, limit the temperature rise on the unexposed side of the CLT slab and prevent the passage of flames and hot gases through cracks or gaps in the timber floor structure. The CLT slabs must demonstrate compliance with (a), (b) and (c) whereas the steel beams are only required to satisfy the load bearing capacity criterion. For this study, the failure temperature of the steel beam is therefore taken as either of the following, whichever is exceeded first:

- vertical deflection of span/20 in accordance with BS 476-20 (1987); or
- the temperature at which runaway deflection starts leading to large lateral displacements.

Figure 4.16 illustrates the failure temperatures of the beam with various axial restraint under the heating regimes described in Section 4.4.2 as well as a new case in which the top flange is assumed to be hotter by 10% than the web and bottom flange. This is intended to represent a situation where the burning CLT slab can potentially result in a higher temperature of the compression flange. It can be observed that the failure temperature for this particular scenario is marginally lower than the correspondingly uniformly heated case. As the axial restraint increases, the failure temperature decreases due to increase in axial compression caused by restrained thermal expansion. Hence, the use of steel frame connections that provides sufficient axial ductility to accommodate thermal expansion should be favoured in steel-timber hybrid structures.

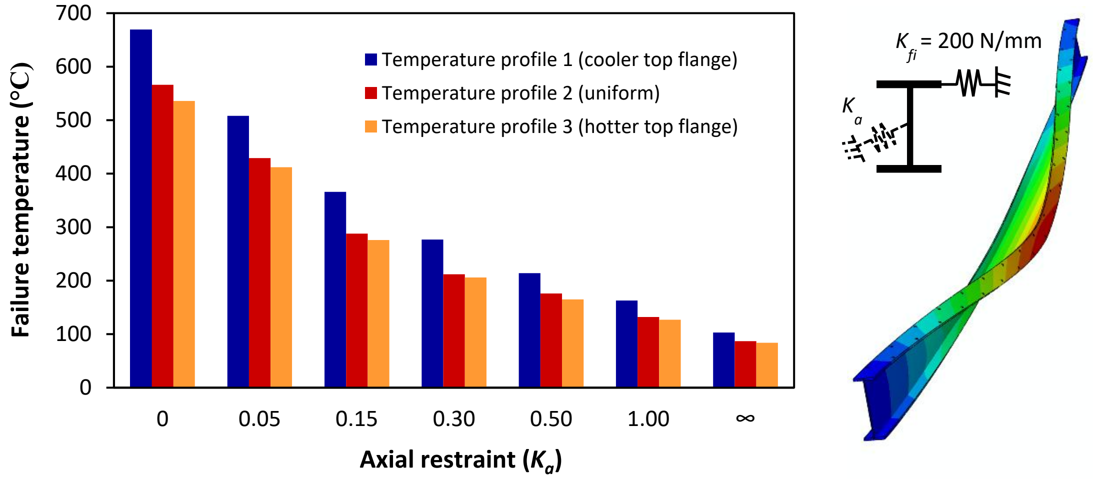

Figure 4.16: Failure temperature with varying axial restraint and temperature profiles under constant lateral restraint K_{fi} = 200 N/mm

4.6 Conclusions

This paper presents results illustrating the influence of lateral and axial restraint on the lateral-torsional buckling behaviour of secondary steel beams in steel-timber hybrid structures at high temperature, considering different heating regimes and mechanical behaviour of the steel-to-timber fixing screws. Based on the results of this investigation, the following conclusions can be drawn:

- In the simply supported condition (no axial restraint), all the partially laterally restrained beams with lateral restraint equal to or above 100 N/mm experience failure temperatures close to those of the fully laterally restrained cases. This level of lateral stiffness is easily achieved by any practical arrangement of 12 mm diameter fixing screws.
- A partially laterally restrained beam (i.e. restraint stiffness of 10 to 500 N/mm) with axial restraint initially behaves similarly to a corresponding fully laterally restrained beam until failure of the first screw occurs in the midspan region. The beam subsequently undergoes runaway deflection due to lateral-torsional buckling until there is an abrupt transition from compression to tension; the development of the catenary action attenuates the runaway deflection until failure occurs when the tensile capacity of the beam is reached.
- Restrained thermal expansion further decreases the failure temperature of a partially laterally restrained beam. It is recommended to adopt steel frame connections with adequate axial ductility and low axial stiffness to accommodate the thermal expansion in steel-timber hybrid structures.
- The results indicate that designing beams in steel-timber hybrid structures as laterally unrestrained in fire is conservative. On the other hand, it is not realistic to assume fully laterally restrained conditions in fire pursuant to the Eurocode 5-based screw characteristics.
- Screws play a crucial role in the fire safety of steel-timber hybrid structures and further testing is required to fully characterise their behaviour in burning timber.
- Further research is required to expand the range of parameters considered. Such work should first be supported by experimental data, especially given the current limited understanding of the local behaviour of screws and the overall performance of steel-

timber hybrid systems in fire. Studies to investigate the effect of realistic fire scenarios (heat sink effect and/or radiation of the CLT and its effects on the local temperature distribution in the steel profile), load ratios, and slenderness ratios are required both experimentally and numerically.

5

Composite Behaviour of Steel-Timber Hybrid Structures in Fire

Summary

This chapter addresses Objective 3 of the research by characterising the evolution of composite action in a typical steel-CLT hybrid assembly during fire exposure. Finite element modelling, validated at the component level against thermal and mechanical benchmark tests, was used to simulate a 9 m unprotected steel-CLT composite beam under ambient and elevated temperatures. The validated CLT floor and restrained steel beam models from Chapter 4 are also used herein, along with newly developed steel-timber connection and steel-CLT composite beam models. The analysis evaluates the influence of varying degrees of composite action, heating regimes, material degradation, and thermal expansion on the global structural response. The results show that while composite action enhances stiffness at ambient conditions, its contribution reduces significantly at elevated temperatures. In fire, different interface conditions (full, partial, and zero composite action) exhibit similar failure temperatures for the case study, all exceeding that of the bare steel beam. The system response is strongly influenced by restrained steel thermal expansion and timber degradation at the steel-timber interface. While Chapters 3 and 4 focus primarily on the influence of restraint on steel beam stability, this chapter extends the investigation to the composite interaction between the steel beam and CLT slab, providing new insight into the fire performance of steel-timber hybrid systems.

Keywords: Steel-timber hybrid structures; Cross-laminated timber; Composite action; Finite element modelling; Fire performance

5.1 Introduction

As the world advances towards sustainable construction, steel-timber hybrid structures are emerging as an innovative solution for the built environment, replacing the poured-in-situ or precast concrete conventionally used in composite construction. This development capitalises on the strength of structural steel while incorporating the carbon-sequestering properties of timber, creating environmentally sustainable structures that respond to the challenges of the climate emergency. A common form of this construction method involves cross-laminated timber (CLT) slabs supported on the top flanges of steel beams. These systems take advantage of the complementary properties of both materials, with steel providing structural capacity and long spans, while timber offers lightweight construction, reduced embodied carbon across the superstructure and substructure, and enhanced aesthetic appeal. As research and development in this field continue to advance, steel-timber hybrid structures are increasingly seen as a viable pathway towards more sustainable and resilient building design (AISC, 2022; SCI, 2024).

In hybrid systems, the CLT slab and steel beam can be connected using various methods depending on the performance requirements. For instance, self-tapping screws, widely used in mass timber projects, offer construction speed and flexibility (AISC, 2022; Merryday, Sener and Roueche, 2025); bolted connections facilitate demountability (Romero and Odenbreit, 2024), which is advantageous in designs prioritising end-of-life disassembly; and shear studs in grouted pockets or slots provide a high degree of composite action (Hicks, Woodward and Hamad, 2025). These represent the key advantages of each method and are among the more practical connection types, although other options may also be considered depending on project requirements (Pimentel, Simões and Silva, 2024).

However, the incorporation of combustible timber elements in hybrid systems lies beyond the scope of current structural design guidance for the fire limit state, introducing additional fire safety challenges and affecting structural performance at elevated temperatures. While fire engineering strategies are critical for addressing combustibility and ensuring life safety in timber buildings, this study focuses on structural fire performance rather than these measures. Critical structural design considerations include complex connection degradation, composite behaviour, and lateral-torsional buckling of beams. While numerous studies have investigated the shear connection performance (Hassanieh, Valipour and Bradford, 2017a; Zhao *et al.*, 2022; Böhm, Vogelsberg and Kühn, 2023; Merryday, Sener and Roueche, 2023; Bompa, Chira and Zwicky, 2024; Romero and Odenbreit, 2024; Hicks, Woodward and Hamad, 2025; Merryday, Sener and Roueche, 2025) and composite behaviour (Hassanieh, Valipour and Bradford, 2017b; Merryday *et al.*, 2023; Böhm, Vogelsberg and Kühn, 2024) of steel-timber systems under ambient conditions, their fire performance remains underexplored (AISC, 2022; SCI, 2024). This represents a critical knowledge gap in fire design, particularly for screwed connections, which are inherently more susceptible to thermal degradation than larger bolts or grout-embedded headed studs. This lack of knowledge is clearly demonstrated in BS EN 1995-1-2 (2004), which reduces the slip modulus to 20% of the ambient value for screws at the fire limit state, in contrast to 67% for bolts. This is a limitation as it does not capture progressive temperature-dependent stiffness degradation.

Hence, this study aims to investigate the composite behaviour of unprotected downstand steel beams supporting CLT floor slabs under fire conditions, with the objective of developing finite element models capable of accurately capturing the steel-CLT interaction and assessing composite action under both ambient and elevated temperatures. Downstand beams are commonly used in multi-storey construction and provide a representative configuration for investigating composite action – while alternative arrangements such as slim-floor or upstand systems exhibit different thermal exposure and structural mechanisms. This research can provide important new insights into the design of steel-timber hybrid structures under fire exposure, enhancing understanding of how composite action influences both structural performance and safety.

It is important to emphasise that this study assumes that the top flange of the steel beam is laterally restrained. This modelling assumption enables a focused investigation into the mechanics of composite interaction between steel and CLT, without introducing the added complexity of lateral-torsional buckling (LTB). Although LTB can be relevant in practice, particularly at elevated temperatures (Jeebodh *et al.*, 2026), its consideration is intentionally deferred in order to establish a baseline for composite behaviour in fire. The findings from this work provide a foundation for future research that incorporates both composite action and stability effects.

5.2 Overview of Steel-Timber Connections

Steel-timber connections play a critical role in the structural performance of mass timber hybrid systems by enabling composite action between steel and timber elements. Previous research has investigated steel-timber hybrid connections using experimental push-out tests, employing a variety of fasteners and engineered wood products such as cross-laminated timber (CLT), glued-laminated timber (glulam), and laminated veneer lumber (LVL). Each timber product offers distinct properties and applications. Typical connectors investigated in the literature include self-tapping screws (Böhm, Vogelsberg and Kühn, 2023; Merryday, Sener and Roueche, 2023; Merryday, Sener and Roueche, 2025), coach screws (Hassanieh, Valipour and Bradford, 2017a; Bompa, Chira and Zwicky, 2024), dog screws (Hassanieh, Valipour and Bradford, 2017a), and bolts, sometimes combined with grout (Hassanieh, Valipour and Bradford, 2017a).

Among these, self-tapping screws are generally preferred in the mass timber industry due to their speed of installation and ease of use (AISC, 2022). Recent innovations, such as demountable bolted connections for disassembly and reuse (Romero and Odenbreit, 2024), and headed studs with concrete slot infill and transverse reinforcement (Hicks, Woodward and Hamad, 2025), provide improved structural performance and enable greater composite action and adaptability. Compared with other connector types, screws are already widely used, whereas demountable bolted connections and headed stud systems represent practical emerging solutions with significant potential for broader industry adoption. Figure 5.1 compares the measured load-slip response of these three groups of steel-timber connections. The screws have comparable nominal diameter, length, spacing, and CLT layer orientation, but each is from a different brand, resulting in variations in stiffness, strength and ductility. The innovative bolted and headed stud connections demonstrate superior mechanical performance compared to screws. As the datasets derive from separate experimental programmes with connectors of different sizes and material grades, the comparison is not intended as a direct performance ranking. The results nevertheless highlight how connector type influences the load-slip response, which can be used to calibrate numerical models to investigate shear connection behaviour in steel-timber composite systems.

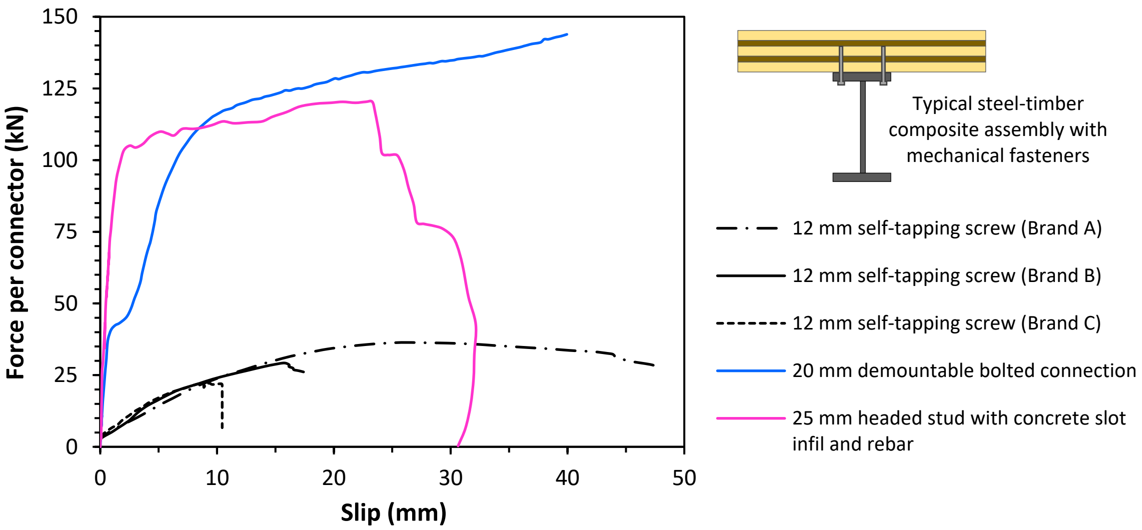

Figure 5.1: Load-slip response of push-out tests of three different screw brands (Merryday, Sener and Roueche, 2023; Merryday, Sener and Roueche, 2025), demountable bolted connection (Romero and Odenbreit, 2024), and headed stud with concrete slot infill and transverse reinforcement (Hicks, Woodward and Hamad, 2025)

Merryday, Sener and Roueche (2023) conducted tests to investigate the influence of screw loading relative to the grain orientation of the outer CLT lamination. The results indicate that the ultimate strength of the self-tapping screws was largely unaffected by grain direction. Nonetheless, connections with screws loaded perpendicular to the outer grain exhibited a reduced initial stiffness compared to those oriented parallel to the outer grain. A similar observation was also made by Hassanieh, Valipour and Bradford (2017a) using coach screws. Figure 5.2 illustrates the effect of CLT grain direction on the load-slip response of 12 mm self-tapping screws. While ambient-temperature studies have established robust load-slip models and shear capacities for various connection types, research on the fire performance of steel-timber connections of steel beams supporting CLT panels on the top flange remains very limited (Barber, Roy-Poirier and Wingo, 2021).

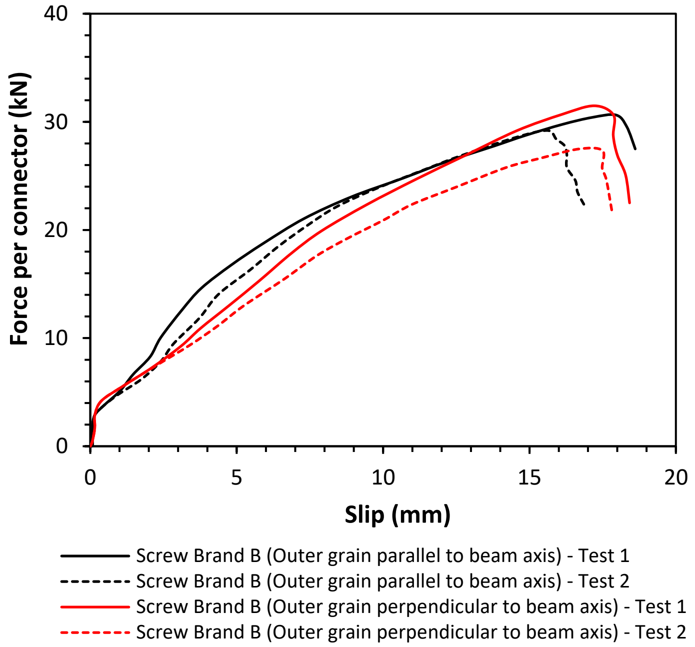

Figure 5.2: Effect of outer grain direction on load-slip response of 12 mm self-tapping screws (Merryday, Sener and Roueche, 2023)

5.3 Composite Behaviour of Steel-Timber Beams

Steel-CLT hybrid systems are still under development, however, several experimental and numerical studies have been undertaken to improve understanding of the composite behaviour of such systems at ambient temperature (Hassanieh, Valipour and Bradford, 2017b; Böhm, Vogelsberg and Kühn, 2024). These studies have consistently demonstrated improvements in structural performance through composite action. By contrast, the fire performance of these systems remains largely unexplored beyond a handful of numerical simulations on downstand configurations (Barber, Roy-Poirier and Wingo, 2021; Godoy Dellepiani *et al.*, 2023), and most available research focuses on slim-floor configurations (Malaska *et al.*, 2023; Dumler *et al.*, 2025).

5.3.1 Ambient Temperature

At ambient temperature, experimental studies on steel-CLT composite systems have demonstrated enhanced stiffness and load-carrying capacity when adequate shear connection is provided. Hassanieh, Valipour and Bradford (2017b) reported flexural stiffness enhancements of 52 to 102 percent and ultimate load capacity increases of 46 to 88 percent across seven full-scale specimens, while Böhm, Vogelsberg and Kühn (2024) demonstrated similar stiffness gains in longer span configurations using inclined screws and grouted studs. Performance gains were also observed in less favourable configurations, such as when the outer CLT layer was oriented perpendicular to the beam axis. While Hassanieh, Valipour and Bradford (2017b) reflected typical industry designs with dominant steel sections and thinner CLT slabs, Böhm, Vogelsberg and Kühn (2024) explored configurations in which the steel beam and CLT slab had comparable depths.

Together, these studies confirm that composite action can be reliably mobilised under ambient conditions, provided appropriate shear connection is achieved. However, while ambient performance is relatively well understood, the mechanisms governing composite action are fundamentally altered under fire exposure, meaning that ambient behaviour provides limited insight into elevated temperature performance, particularly where material degradation and thermal effects influence interface behaviour.

5.3.2 High Temperature

The fire performance of steel-CLT composite systems is of critical concern due to the combustible nature of timber and the susceptibility of shear connections to thermal degradation. Despite growing interest, full-scale experimental research on structural behaviour in fire is virtually non-existent, with only limited numerical studies (Barber, Roy-Poirier and Wingo, 2021; Godoy Dellepiani *et al.*, 2023) addressing downstand configurations. Barber, Roy-Poirier and Wingo (2021) investigated screw resistance under elevated temperatures, while Godoy Dellepiani *et al.* (2023) studied composite behaviour in fire for full and zero composite cases. This highlights that a detailed understanding of the mechanisms governing composite action in steel-timber assemblies under fire conditions, including the degradation of screw stiffness and its influence on structural response, is still lacking. This is particularly important as localised heating above the top flange can initiate degradation of the timber and potentially affect longitudinal shear transfer for composite action. Differential thermal expansion, driven by the rapid heating of the steel relative to the timber, can further contribute to interfacial slip.

Godoy Dellepiani *et al.* (2023) reported limited sensitivity of midspan deflection in steel-CLT composite floors to interface condition after 30 minutes of fire exposure. However, their simulations assumed steel beams fixed at both ends, outer CLT grains parallel to the beam axis, and a severe heating regime close to a hydrocarbon fire curve. Moreover, the underlying mechanisms governing the observed response in fire remain unclear, particularly under structural and thermal conditions representative of multi-storey construction. These limitations highlight the need for further investigation into how interface conditions and heating scenarios influence the evolution of composite action and structural performance in fire. The present study addresses this gap through a numerical case study framework that considers varying levels of composite action to capture the range of structural response under different heating scenarios.

5.4 Finite Element Modelling

In the absence of experimental data for steel beams supporting CLT slabs in fire, finite element (FE) analysis provides a powerful tool to investigate their thermo-mechanical behaviour. To this end, a staged modelling framework comprising sequential heat transfer and high temperature mechanical analyses was developed in *Abaqus* (Abaqus, 2021), with validation performed at the component level.

Thermal models were developed to simulate the temperature evolution within a steel-timber connection and a CLT slab under a standard fire exposure, providing detailed insight into the temperature field that governs structural response. These validation cases were selected to assess the accuracy of heat transfer modelling in timber and at the steel-timber interface. The models consider solid-phase heat transfer only, with timber charring represented implicitly through temperature-dependent material properties, while combustion and delamination are not explicitly modelled. The validated models serve as a baseline for extending the heat transfer analysis to steel-timber hybrid systems under fire conditions.

Mechanical models were subsequently developed to simulate the response of a composite beam at ambient temperature and a heated restrained steel beam, capturing the effects of thermal expansion and progressive material degradation. These cases were chosen to validate the representation of composite action at ambient temperature and the thermo-mechanical response of steel members at elevated temperatures. This sequential validation strategy ensures that the key aspects of the modelling framework (i.e. heat transfer, shear interaction, material degradation, thermal expansion) are accurately represented, providing a solid foundation for investigating the composite behaviour of practical steel-CLT hybrid assemblies in fire.

5.4.1 Development and Validation of Heat Transfer Model

A clear understanding of heat transfer analysis is essential for characterising the thermal response of hybrid structures under fire conditions. In accordance with Eurocode 1 (BS EN 1991-1-2, 2002), the thermal action on a surface exposed to fire can be represented by a net heat flux $\dot{h}_{net}$, which is defined by the sum of convective $\dot{h}_{net,c}$ and radiative $\dot{h}_{net,r}$. The net convective heat flux component is determined using the following equation:

$$\dot{h}_{net,c} = \alpha_c(\theta_g - \theta_m) \tag{5.1}$$

where α_c is the coefficient of heat transfer by convection, θ_g is the gas temperature, and θ_m is the surface temperature of the member. In a heat transfer model, the code recommends that α_c is taken as 25 W/m^{2}K on the fire-exposed surface to a standard fire and 9 W/m^{2}K on the unexposed side.

The net radiative heat flux component per unit surface area is given by:

$$\dot{h}_{net,r} = \epsilon_{eq} \cdot \sigma\left[(\theta_r + 273)^4 - (\theta_m + 273)^4\right] \tag{5.2}$$

with

$$\epsilon_{eq} = \phi \cdot \varepsilon_m \cdot \varepsilon_f \tag{5.3}$$

Where ϕ is the configuration factor, ε_m is the surface emissivity of the material, ε_f is the emissivity of the fire, σ is the Stefan-Boltzmann constant (5.67×10^{-8} W/m^{2}K^4), θ_r is the radiation temperature of the fire environment taken as equal to θ_g in the case of members fully engulfed in fire, and θ_m is the surface temperature of the member. The configuration factor ϕ is normally taken as 1.0 but a lower value can be used to take into consideration shadow effects. Emissivity values are typically $\varepsilon_m = 0.7$ for the surface of steel (BS EN 1993-1-2, 2005) and $\varepsilon_m = 0.8$ for the surface of timber (BS EN 1995-1-2, 2004). The emissivity of the fire is in general taken as $\varepsilon_f = 1.0$. In numerical simulations, the thermal boundary conditions of the surfaces of members exposed to convection and radiation must be realistically represented to obtain accurate temperature distributions.

Temperature-dependent thermal parameters such as density, specific heat and thermal conductivity adopted in the heat transfer simulations were based on the recommendations outlined in BS EN 1993-1-2 (2005) for carbon steel and BS EN 1995-1-2 (2004) for timber. Eight-node linear heat transfer brick (DC3D8) or four-noded linear heat transfer quadrilateral (DC2D4) elements were employed in the simulations. In all cases, an element size of roughly 5 mm was found to be satisfactory for all the materials, with local mesh refinement applied in critical regions. The mesh discretisation is also consistent with heat transfer simulations reported in previous studies (Ma, Havula and Heinisuo, 2019; Nguyen *et al.*, 2023a; Nguyen *et al.*, 2023b). All thermal models were created or assembled as a single part, assuming perfect thermal contact between interfaces, and no explicit thermal contact was used.

5.4.1.1 Thermal Response of Steel-Timber Connection

A thermal model was developed to simulate the temperature evolution within a steel-timber connection exposed to standard fire conditions, with thermal boundary conditions defined using direct measurements from the furnace test. The model was validated against the experimental study conducted by Peng *et al.* (2012), who investigated the fire performance of a bolted steel-wood-steel connection. The connection assembly consisted of a 130 mm × 190 mm timber member sandwiched between two 9.5 mm thick steel plates and fastened with 19.1 mm diameter bolts.

Figure 5.3 compares the temperature distribution predicted by the heat transfer model with thermocouple measurements at various locations within the specimen. Overall, the numerical results show good agreement with the experimental data, with some deviations observed during the early heating stages before the temperatures gradually converge. The simulated temperature profiles in this study also align well with the numerical results reported by Peng *et al.* (2012). The validation results indicate that the model reliably captures the heat transfer through steel-timber mechanical connections, supporting its application for analysing steel-timber assemblies.

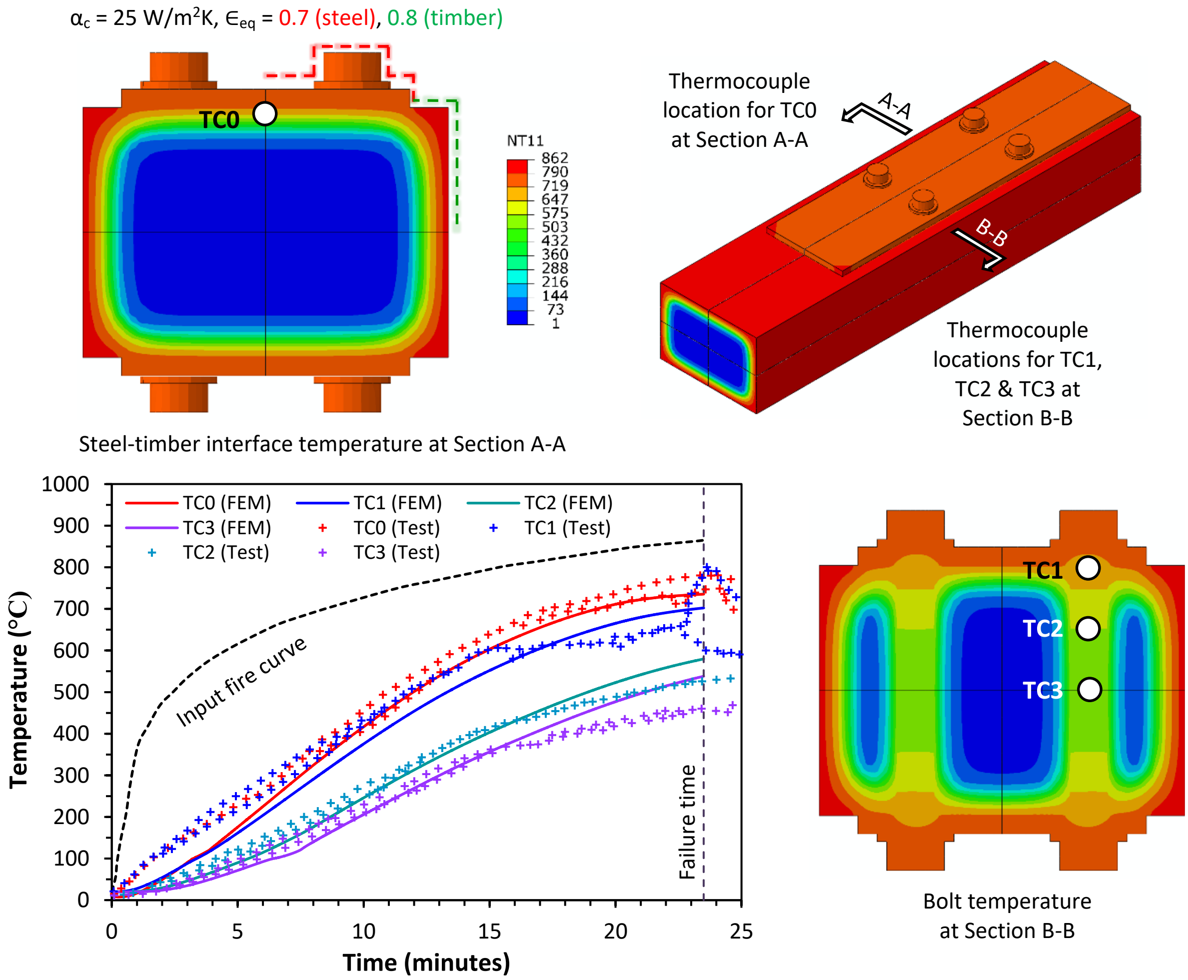

Figure 5.3: Comparison of temperatures between experiment and current work numerical model (FEM) for bolted connection assembly

5.4.1.2 Thermal Response of CLT Floor

The thermal response of a CLT floor exposed to standard fire conditions from the underside was simulated using the proposed transient heat transfer model. The model was configured to replicate a CLT assembly reported by Fragiacomo *et al.* (2013). The specimen was 150 mm thick and 600 mm wide, with a lamellae configuration of 42/19/28/19/42 mm.

Figure 5.4 compares the predicted temperature distribution at different locations with thermocouple measurements. The simulated temperature profiles in this study are also consistent with the numerical results obtained by other researchers (Fragiacomo *et al.*, 2013; Thi *et al.*, 2017; Chen *et al.*, 2022). In general, the numerical model capture the measured temperature profiles reasonably well, except for the temperature increase towards the end of the test. This is due to a change from one-dimensional to two-dimensional heat flux experienced by the highly deflected specimen on its sides as it approached failure. However, this response is not simulated because in a steel-timber hybrid beam with CLT panels forming a continuous envelope, the heating can be assumed to be one-dimensional.

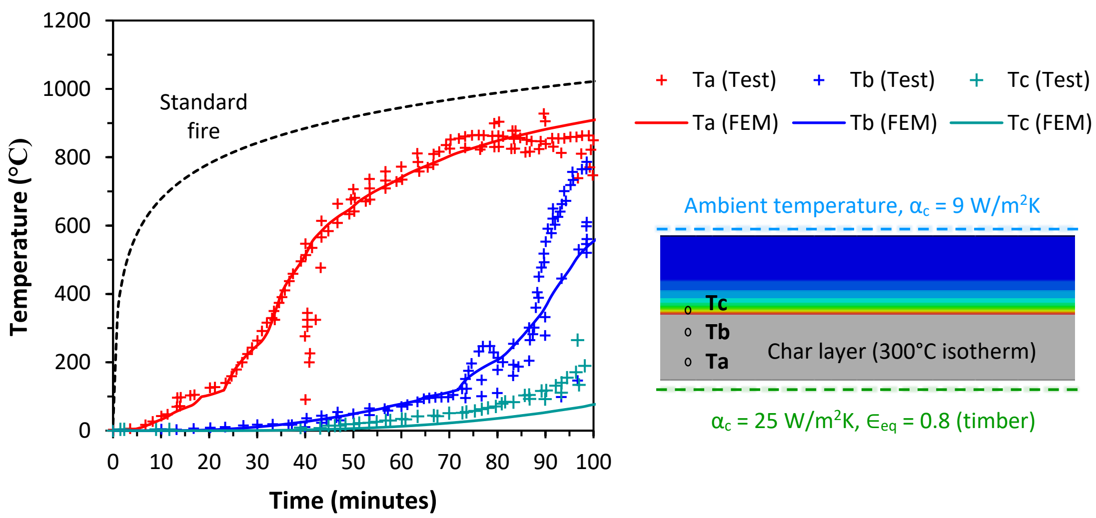

Figure 5.4: Comparison of temperature between experiment (Fragiacomo *et al.*, 2013) and current work numerical model (FEM) for CLT floor

5.4.2 Development and Validation of Mechanical Model

Structural fire modelling for traditional non-combustible materials typically adopts the simplification that the thermal and mechanical analyses can be decoupled (Torero, Law and Maluk, 2017). This is based on the concept that the characteristic timescales of the gas and solid phase are very different (Torero *et al.*, 2014) and there is not significant interaction between them. For timber, the decoupling is more complex since there is additional fuel load, and a feedback loop between charring, cracking, delamination and the fire dynamics in the gas phase (Law, 2017) creating a two-way coupling. To isolate the structural mechanics at elevated temperatures, the common assumption of one-way coupling is adopted here (Welch *et al.*, 2008; Tondini *et al.*, 2016). This enables investigation of the structural behaviour under a given thermal load without detailed understanding of the complex fire dynamics.

This section details the development of numerical models capable of reproducing the behaviour of a steel-CLT composite beam at ambient and elevated temperatures. The high temperature material properties of carbon steel, including its non-linear engineering stress-strain relationship and thermal expansion, were adopted in accordance with BS EN 1993-1-2 (2005).

5.4.2.1 Mechanical Response of Composite Beam at Ambient Temperature

Hassanieh, Valipour and Bradford (2017b) conducted four-point bending tests on steel-CLT composite beams to investigate composite behaviour, alongside numerical modelling. In the present study, a non-linear FE model was developed to simulate one of the test specimens, which featured 16 mm screw connections at 250 mm spacing. The specimen consisted of a 310UB32.0 steel beam supporting segmented CLT panels 120 mm thick and 800 mm wide, with a lamellae structure of 20/20/40/20/20 mm.

The steel beam was modelled using S4R shell elements with a 20 mm mesh, a yield strength of 320 MPa, and an ultimate strength of 440 MPa. The CLT panels were modelled using SC8R continuum shell elements with a mesh size of 40 mm. The 120 mm panel thickness was discretised into twelve 10 mm layers to provide sufficient through-thickness resolution. Layer-wise material orientations were assigned to represent the alternating grain directions of the lamellae. Timber was idealised as an orthotropic material with identical properties in the radial and tangential directions perpendicular to the grain. The material properties were calibrated using the 2D Hashin damage model available in the *Abaqus* library to reproduce the experimental behaviour of the CLT panels. Figure 5.5 illustrates the stress-strain relationship of timber adopted in the Hashin damage model, together with the associated damage initiation and failure parameters. A similar approach is used for the shear behaviour. The corresponding material properties for timber are summarised in Table 5.1

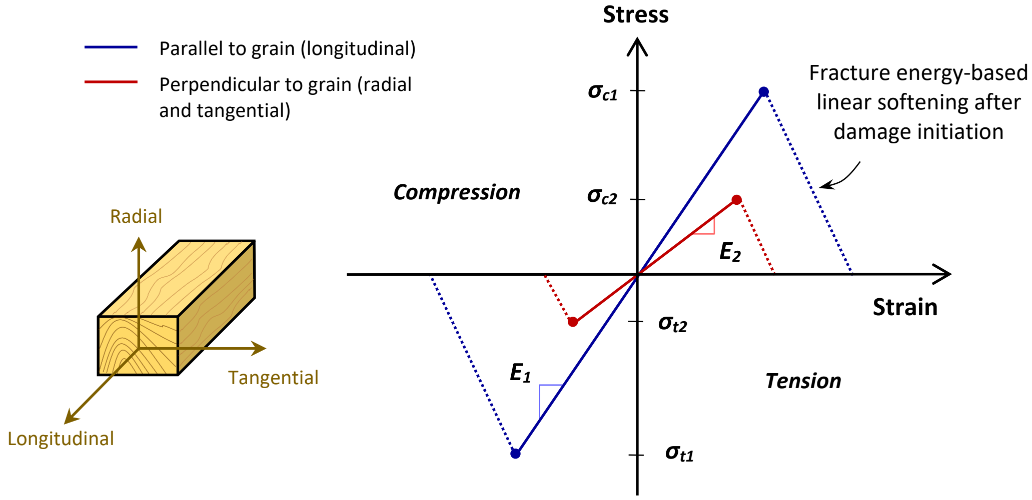

Figure 5.5: Stress-strain relationship for timber based on Hashin damage model

Table 5.1: Material properties of timber for numerical simulations (Hassanieh, Valipour and Bradford, 2017b; Hassanieh et al., 2017; Hassanieh, Valipour and Bradford, 2018)

Orthotropic elastic properties of timber								
Elastic modulus (MPa)			Shear Modulus (MPa)			Poisson's ratio		
E_1	E_2	E_3	G_{12}	G_{13}	G_{23}	ν_{12}	ν_{13}	ν_{23}
11000	370	370	690	690	50	0.48	0.48	0.22

Hashin damage parameters					
Compressive strength (MPa)		Tensile strength (MPa)		Shear strength (MPa)	
σ_{c1}	σ_{c2}	σ_{t1}	σ_{t2}	f_v	$f_{v,roll}$
36	4.3	24	0.7	6.9	0.5

Fracture energy (N/mm)			
Compression		Tension	
$G_{f,c1}$	$G_{f,c2}$	$G_{f,t1}$	$G_{f,t2}$
6.0	0.5	6.0	0.5

Note: Direction 1 is parallel to grain, and Directions 2 and 3 are orthogonal

Zero-length springs were modelled at the semi-rigid steel-CLT interface using SPRING2 elements to capture partial composite action, with the load-slip behaviour derived from push-out tests (Hassanieh, Valipour and Bradford, 2017b). Full- and non-composite actions were also modelled, along with a bare steel beam without CLT panels. For the composite cases, the interface was defined using normal hard contact, with a rough surface for full composite action and a friction coefficient of 0.45 (Hassanieh, Valipour and Bradford, 2017b) for nominally zero composite action in *Abaqus*. The rough contact formulation prevents relative slip between the steel beam and CLT panels, whereas a friction coefficient of 0.45 represents the natural timber-steel interface without shear connectors, permitting slip and approximating non-composite behaviour.

All modelling assumptions, including material properties, follow the simulations by Hassanieh, Valipour and Bradford (2017b), except that this study uses a 3D model with half-symmetry. The adopted mesh sizes provide the required accuracy while maintaining acceptable computational efficiency. Figure 5.6 illustrates the load-deflection response for different interface conditions and constitutive timber models. The inelastic response represents timber modelled using the Hashin damage formulation. It can be seen that the numerical model accurately reproduces the experimental load-deflection response of the tested specimen, demonstrating its reliability in capturing the bending stiffness and peak load-carrying capacity, with only minor discrepancies in the post-peak response. This validation confirms that the model can be applied for further analysis of steel-timber composite beams.

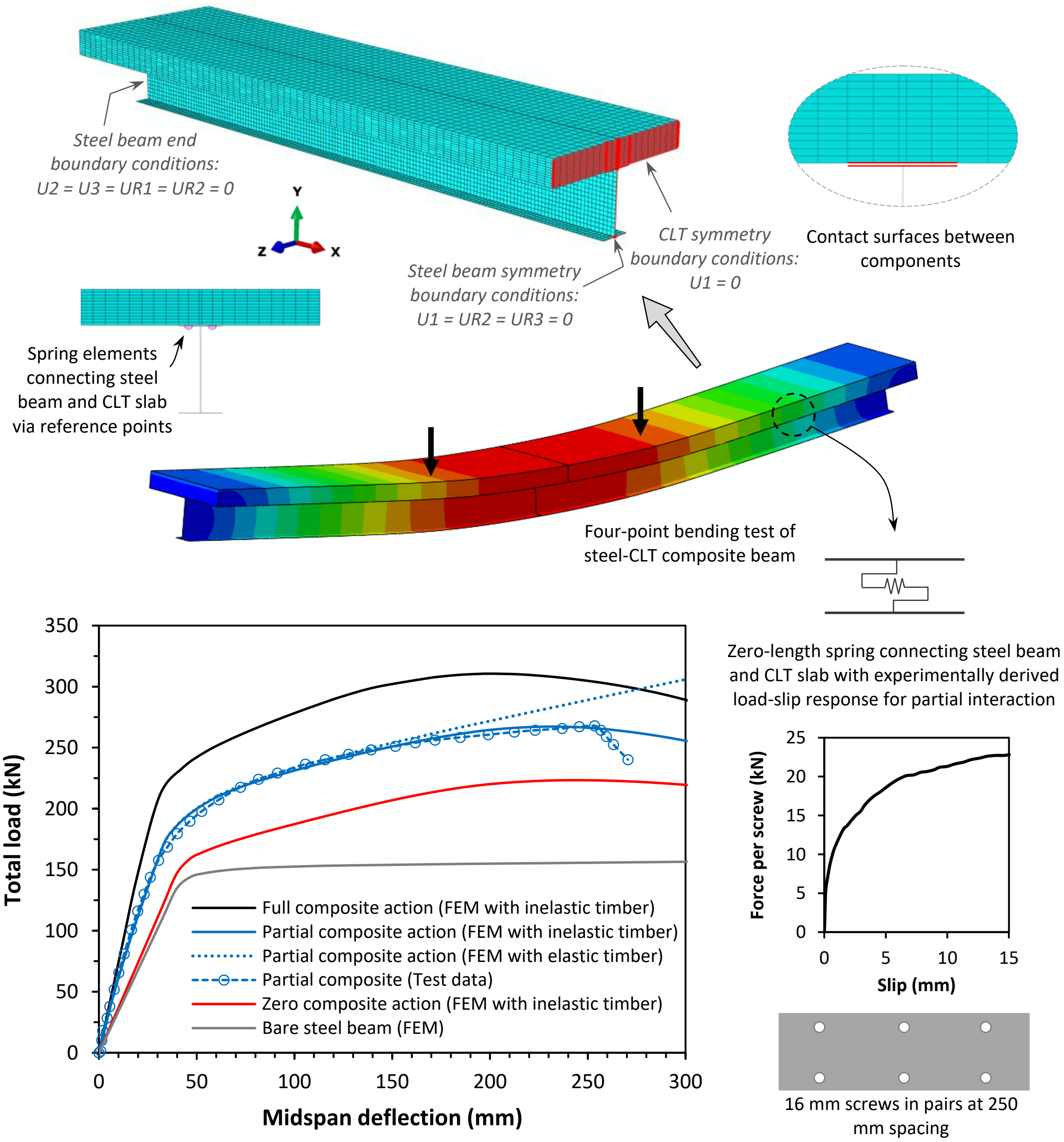

Figure 5.6: Comparison of test data (Hassanieh, Valipour and Bradford, 2017b) with numerical model (FEM) for partial composite action, including full and zero composite action and bare steel beam (not tested)

5.4.2.2 Mechanical Response of Heated Steel Beam

To validate the mechanical model for simulating steel under fire, numerical predictions were compared against the experimental results reported by Li and Guo (2008), in which the web and flanges of the beam experienced different temperatures under fire. Given the complexity of the final model, validation of only the thermo-mechanical behaviour of the steel beam under elevated temperatures is necessary to reduce uncertainty. The specimen consisted of an

H 250×250×8×12 steel beam subjected to axial and rotational end restraints. The beams was 4.5m long and loaded with two point loads of 130 kN each, with an average yield strength of 271 MPa. The axial (K_a) and end-rotational (K_r) stiffness of the beam were 39.5 kN/mm and 1.09×10^8 Nm/rad, respectively (Zhang, Li and Usmani, 2013; Nguyen and Park, 2022).

The beam was simulated using S4R shell elements with a 20 mm mesh and a half-symmetry model. Figure 5.7 compares the numerical results obtained in this study with the experimental measurements, alongside the predictions made by Dwaikat and Kodur (2011) and Zhang, Li and Usmani (2013). The numerical results demonstrate that the simulation approach reasonably captures the response of steel beams under fire. Discrepancies are primarily attributed to simplifications in end boundary conditions and the assumed temperature distribution along the beam.

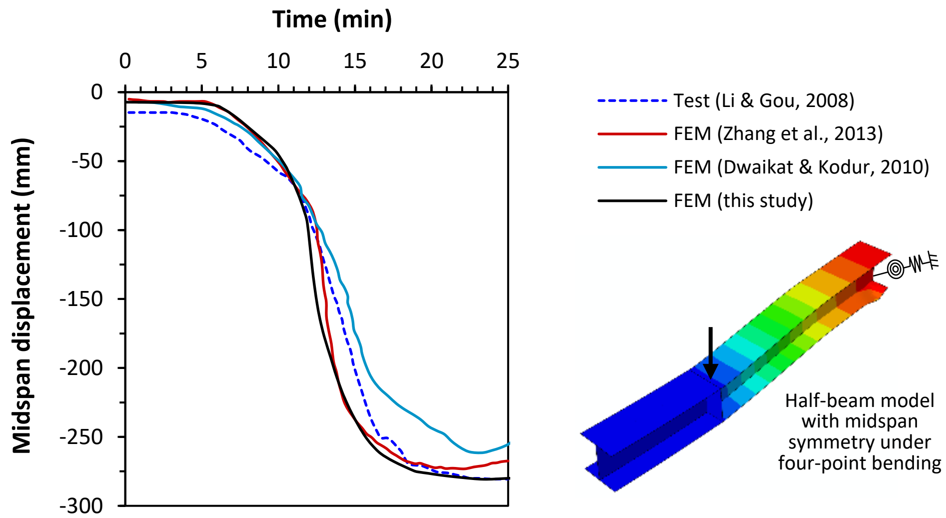

Figure 5.7: Comparison of displacement between experiment (Li and Guo, 2008) and numerical models (FEM) of restrained steel beam

5.5 Case Study of a Typical Steel-Timber Hybrid System

This study focuses on a representative steel-timber hybrid system, consisting of a 9 m simply supported secondary hot-rolled steel beam (UB 457×152×74, grade S355) supporting a 160 mm thick CLT slab with a 40/20/40/20/40 mm layup, arranged in a typical 9 m × 9 m steel framing grid for commercial office use (Figure 5.8). The top flanges of the secondary and primary beams are assumed to be at the same level to support the CLT panels. The outer CLT layer is oriented perpendicular to the secondary beam longitudinal axis and the timber properties are as specified in Section 5.4.2.1. The dead load is assumed to be 3.0 kN/m^2 (including self-weight of the slab, finishes, and services), and the imposed load is taken as 5.0 kN/m^2. Accordingly, the top flange of the beam is subjected to a line load of 51.98 kN/m at the ultimate limit state and 24.75 kN/m at the fire limit state, corresponding to a tributary width of 4.5 m of the slab.

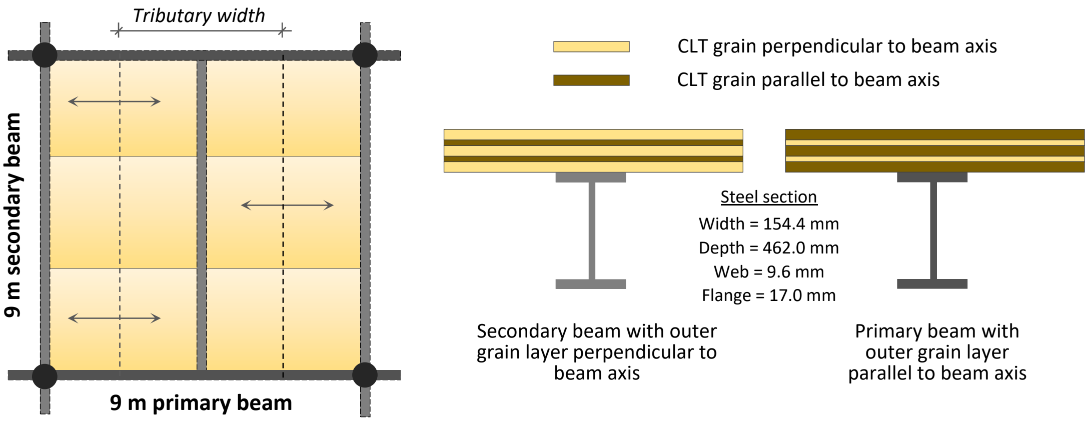

Figure 5.8: Typical office floor with 9m × 9m column grid with beam arrangement and CLT panels orientation

A numerical investigation was undertaken to assess the thermal and structural response of the steel-CLT configuration under both ambient and fire conditions. A thermal analysis was performed to determine the temperature distribution under ISO 834 standard fire exposure. The resulting temperature history was then used as input for a high temperature mechanical analysis, with multiple parameters considered to ensure a realistic representation of the system. For instance, the interface conditions between the steel beam and CLT slab were varied to include full, partial, and zero composite action. In fire, different heating scenarios were investigated, including a cold CLT slab with no thermal degradation and a heated CLT slab, in which charring is represented implicitly through temperature-dependent properties, without modelling pyrolysis gas ignition, char oxidation, or char crushing. The steel beam was subjected to both uniform and non-uniform heating, with a cooler top flange to simulate varying fire exposure. Thermal effects were included by considering the coefficients of thermal expansion (CTE) of both steel and timber, allowing thermal strains to be captured in the structural response. High-temperature thermal and mechanical characteristics of steel and timber were adopted in accordance with BS EN 1993-1-2 (2005) and BS EN 1995-1-2 (2004), respectively. The char layer was treated as mechanically inactive at the 300 °C isotherm.

The secondary beam was modelled as simply supported without restrained thermal expansion. In the study by Godoy Dellepiani *et al.* (2023), the beams investigated were assumed to be fully fixed so this study examines alternative boundary conditions. In the present model, the CLT slab was restrained only at symmetry boundaries and the steel beam response was restricted to vertical bending behaviour only. Lateral-torsional buckling effects were outside the scope of the present study but have previously been investigated in Jeebodh *et al.* (2026). This idealisation was adopted to isolate the key mechanisms governing composite behaviour under fire conditions. Partial composite action models were represented under ambient conditions using: (i) 12 mm screws and (ii) 25 mm headed studs with concrete slot infill and rebar. Figure 5.9 illustrates the load-slip response of the shear connectors assumed in the simulations (see Section 5.2 for details). Under fire conditions, only the screw connection was considered, as it is generally less robust at elevated temperatures and widely used in mass timber projects.

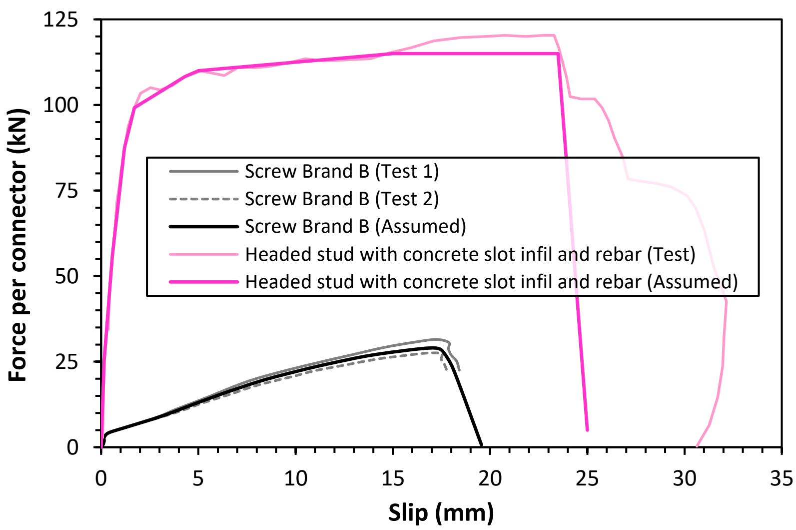

Figure 5.9: Load-slip response of shear connectors assumed in simulations

Due to the lack of experimentally validated temperature-dependent degradation models for screw connections in steel-CLT composite systems (Jeebodh *et al.*, 2024), the partial composite response in fire was modelled assuming brittle failure of the screws and a temperature-dependent degradation law derived from beam-on-elastic-foundation theory. Further details of this approach are provided in Section 5.6.4.3. The full and zero composite action scenarios define the upper- and lower-bound responses within which the actual structural behaviour is expected to lie. Within this multi-faceted framework, the effects of varying degrees of composite action (full to zero), heating scenarios (uniform and non-uniform steel heating), material degradation of steel and timber, and thermal expansion on the global response of the steel-CLT composite system can be systematically assessed under a range of thermo-mechanical conditions.

5.6 Investigation of Composite Behaviour

This section presents the thermal and structural performance of the steel-timber composite beam described in the case study. Both ambient and fire responses are analysed to illustrate the effects of composite action on overall performance under serviceability, ultimate, and fire limit states. The results presented herein also highlight the key design implications for steel-timber composite beams.

5.6.1 Thermal Response of Steel-Timber Beam

In line with the simulation procedure explained in Section 5.4.1, the thermal response of the steel-timber beam was determined for a CLT slab with a density of 480 kg/m^3 and a moisture content of 12%. For computational efficiency, the slab width was taken as 1.0 m in the thermal model. Although this simplification did not affect the heat transfer analysis, the full 4.5 m width was retained for the mechanical analysis. The thermal boundary conditions were as explained in Section 5.4.1 and the underside of the CLT was assumed to be fully exposed to an ISO 834 standard fire without any encapsulation.

Figure 5.10(a) illustrates the simulated temperature profiles for the steel beam. Figure 5.10(b) shows those of the CLT slab at a location away from the steel top flange, where the steel-timber interface does not affect the temperature distribution. The temperatures are also in good agreement with the thermal simulations performed by other researchers for steel-timber hybrid structures in a downstand configuration (Barber, Roy-Poirier and Wingo, 2021; Godoy Dellepiani *et al.*, 2023). For simplification, it is assumed that the temperatures of the bottom flange and the web of the downstand steel beam are identical, as any difference is negligible. For the high temperature mechanical analysis, the steel-timber beam is assigned a non-uniform temperature, characterised by a cooler top flange. In the absence of experimental data for hybrid steel-timber systems in fire, an additional case with a uniform section temperature equal to the web is considered to examine the sensitivity of the structural response to different thermal actions. Figure 5.10(c) illustrates the predicted char depth development in the CLT above the steel top flange and at a location away from it, highlighting spatial variation in charring behaviour alongside the Eurocode 5 charring rate.

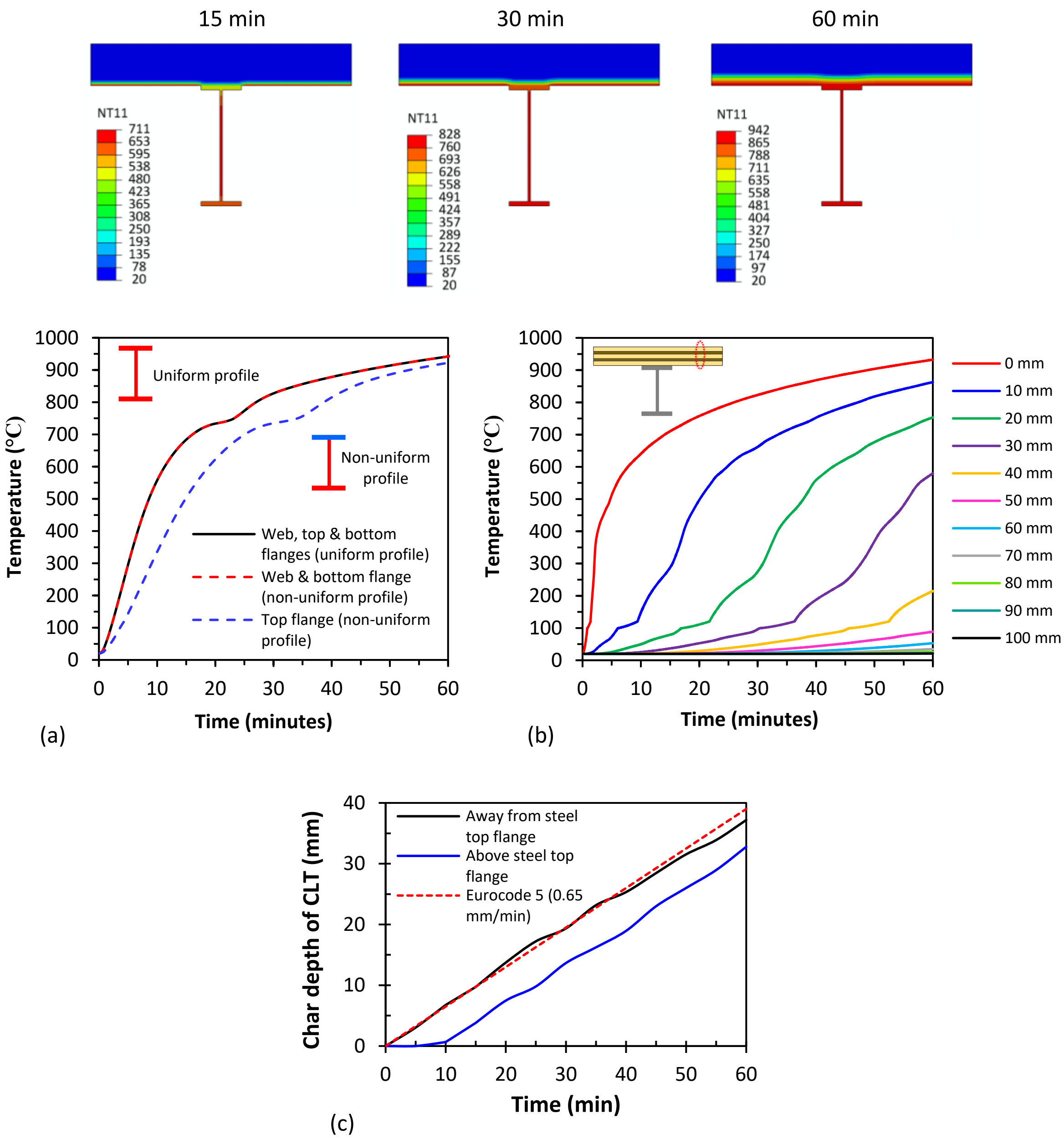

Figure 5.10: Simulated temperature profiles for (a) steel beam and (b) CLT slab at a location away from steel top flange, and (c) char development in CLT over time

5.6.2 Bare Steel Beam at Ambient Conditions

Prior to considering composite action, the steel beam was analysed as a bare section, assuming that it carried the full loading. This assessment provides an evaluation of the load levels relative to the bending capacity of the beam and reflects a common design practice in which composite action in steel-CLT beams is often neglected. The steel was modelled using S4R shell elements with a mesh size of 20mm. Figure 5.11 shows deflection response of the steel beam under various load combinations at ambient temperature. The results indicate that the beam remains within the elastic range under all considered load combinations, including the ultimate limit state. This implies that the steel beam alone is sufficient for ultimate bending resistance, while composite action is expected to enhance bending stiffness and serviceability.

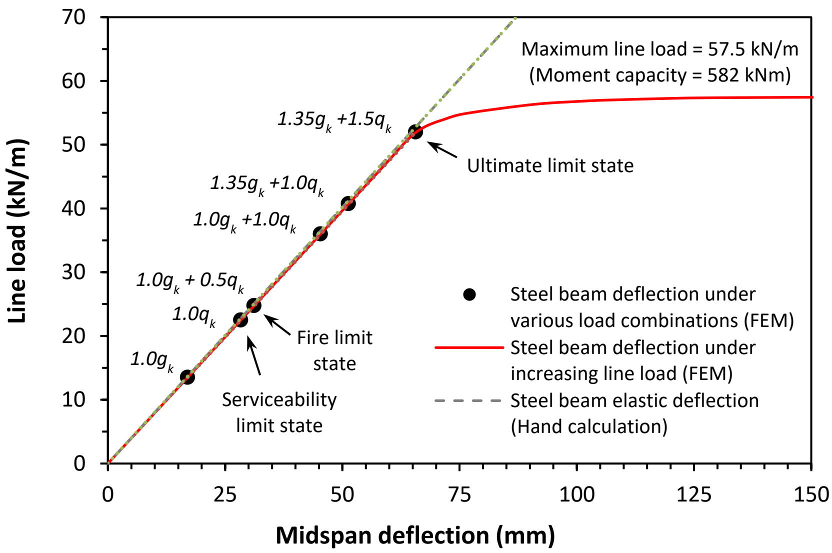

Figure 5.11: Deflection response of bare steel beam under various load combinations at ambient temperature

5.6.3 Composite Behaviour at Ambient Conditions

This analysis examines the behaviour of the steel-timber composite beam in the case study in comparison with the bare steel beam carrying the full applied loading. The steel was modelled using S4R shell elements(20 mm mesh), and the timber was modelled using SC8R continuum shell elements (40 mm mesh) with Hashin damage criteria and material properties as described in Section 5.4.2.1. The 160 mm panel thickness was discretised into sixteen 10 mm layers to provide sufficient through-thickness resolution. Figure 5.12 compares the deflection response of the system under various load combinations and interface conditions. The results demonstrate that zero composite action offers negligible benefit relative to the behaviour of the bare steel beam whereas partial composite action, achieved through screws or headed studs with concrete slot infill and rebar, increases bending stiffness, with more robust connectors and closer spacing offering greater structural benefit.

A structure must be designed to meet all relevant serviceability criteria, which are project-specific and should be agreed with the client and building control authorities. For this case study, the limiting deflection is taken as span/360 under imposed load only, in line with common UK design practice to prevent damage to brittle finishes after permanent loads are in place. At the serviceability limit state under imposed load, the bare steel beam and non-composite arrangement exceed the span/360 deflection limit, whereas both full and partial composite arrangements satisfy the criterion. The full composite action, though generally idealised and requiring a fully bonded interface (Hassanieh, Valipour and Bradford, 2017b) or very densely spaced robust connectors, reduces deflection by approximately 46% compared to the bare steel beam. Among the cases analysed, the partial composite arrangements achieve deflection reductions ranging from 14% to 36%, depending on connector type and spacing. Neglecting composite action entirely offers negligible benefit, with only a 4% reduction in deflection relative to the bare steel beam. Table 5.2 compares the composite efficiency (Hassanieh, Valipour and Bradford, 2017b) of the hybrid beam for different load combinations and connector types. As expected, the highest composite efficiency is achieved with studs compared to screws at the same spacing. Overall, the results demonstrate that partial composite action enhances stiffness and serviceability at ambient temperature design, whereas the bare steel beam alone would exceed the deflection limit. The full composite action represents the upper-bound of structural performance. These ambient-condition results provide a baseline against which the subsequent composite behaviour of the system in fire can be interpreted.

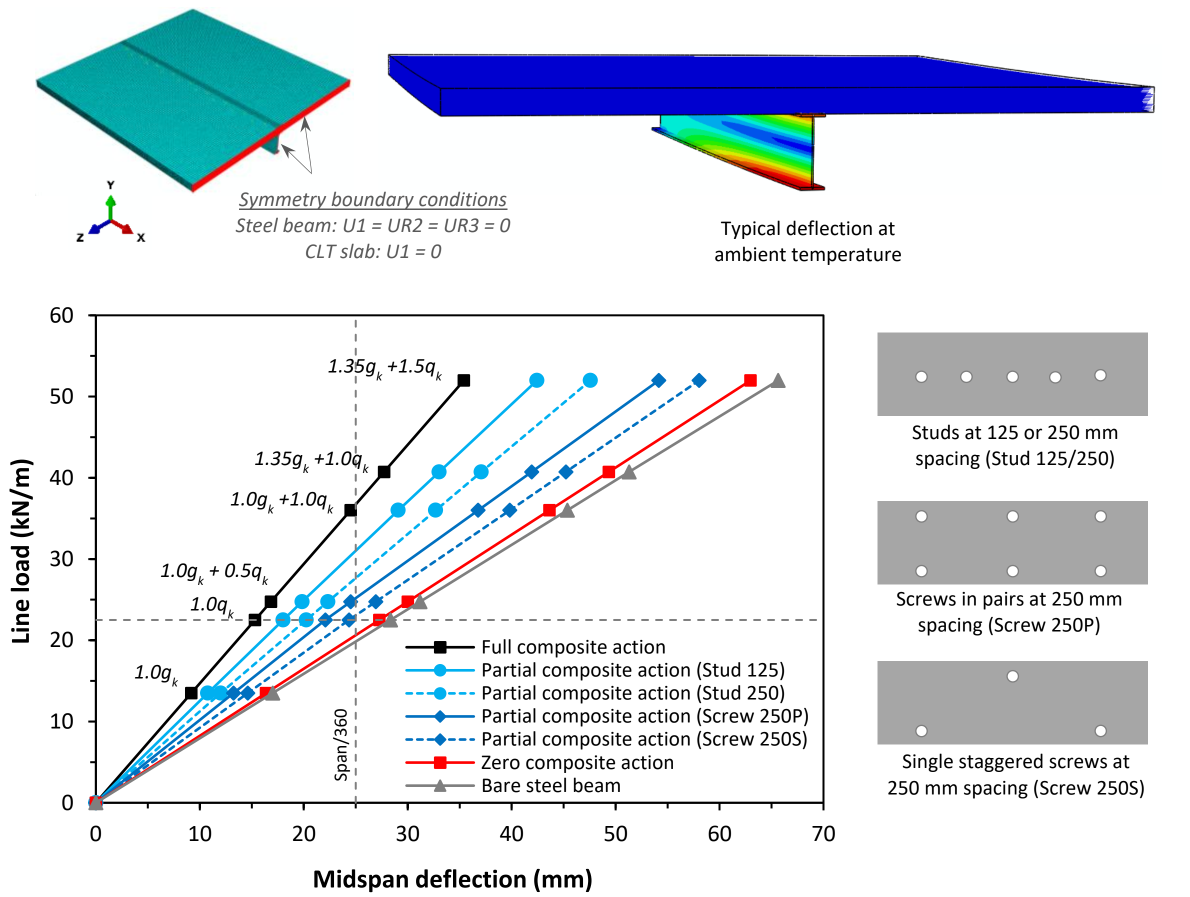

Figure 5.12: Deflection response of composite beam under various load combinations and interface conditions at ambient temperature

Table 5.2: Composite efficiency for different load combinations and connector configurations

Load combination	Composite efficiency (%)			
	Screw 250S	Screw 250P	Stud 250	Stud 125
$1.35g_k + 1.5q_k$	32	18	56	74
$1.35g_k + 1.0q_k$	34	19	57	75
$1.0g_k + 1.0q_k$	36	20	57	76
$1.0g_k + 0.5q_k$	42	23	58	77
$1.0q_k$	43	24	59	77
$1.0g_k$	43	24	61	78

$$\textit{Composite efficiency}\ (\%) = \frac{\delta_{partial} - \delta_{zero}}{\delta_{full} - \delta_{zero}} \times 100 \quad (\delta = \textit{midspan deflection})$$

5.6.4 Composite Behaviour under Fire Conditions

This analysis examines the response of steel-CLT composite beams to fire under two heating regimes: (i) heating of the steel section alone and (ii) heating of both steel and timber components. The steel is exposed to uniform or non-uniform temperature distributions, as outlined in Section 5.6.1. CLT temperatures were prescribed manually throughout its thickness, with all nodes at the same depth assigned the same temperature, and the local heat-sink effect above the steel beam was not included.

In previous ambient-temperature analysis (Section 5.6.3), the timber was modelled using SC8R continuum shell elements with Hashin damage criteria to assess composite action. As the timber exhibited elastic behaviour in ambient conditions, modelling intra-layer failure was unnecessary. However, for fire simulations, these shell elements are limited in their ability to represent through-thickness temperature gradients accurately. To address this, the CLT was modelled using eight-node linear brick elements with reduced integration (C3D8R), which allow direct assignment of temperature fields. Although solid elements do not support Hashin damage, this approach (Godoy Dellepiani *et al.*, 2023) improves numerical convergence under fire-induced large deflections and provides a physically consistent thermal and elastic representation of the CLT. Similar deflections were also observed at the end of the ambient analysis prior to the heating step when using solid elements compared with shell elements.

For fire simulations, the model was further reduced from half- to quarter-symmetry to improve computational efficiency, given the significantly longer computation times associated with high temperature analyses. The partial composite action model was represented using single staggered screws at 250 mm spacing (Screw 250S in Figure 5.12). The temperature-dependent response of the connectors was defined using the Case 2 degradation law presented in Section 5.6.4.3. Spring elements were replaced by translation-type connector elements, which include temperature dependency. The partial composite beam was heated, while the screws were assumed to maintain the ambient-temperature load-slip relationship to allow comparison of the two formulations. The difference in response was less than 3% and was therefore considered negligible for further analysis. For the elevated temperature case, the temperature distribution of the steel top flange was assigned to the reference points connecting the beam and CLT slab to control screw degradation.

5.6.4.1 Heated Steel Beam and Unheated CLT Slab

The steel-CLT composite beam is analysed assuming the slab is insulated via encapsulation or other fire-resistant protection, so that only the steel beam is exposed to elevated temperatures. This idealised configuration isolates the effects of steel heating while keeping the timber slab effectively unheated, although some heat transfer at the interfaces and localised timber heating would certainly occur in practice. This analysis specifically investigates the structural response of the composite system under these conditions.

The deflection-temperature response of the composite beam under steel-only heating is presented in Figure 5.13, showing (a) non-uniform and (b) uniform temperature profiles. The results highlight the influence of varying interface conditions (full, partial, and zero composite action) and the effect of the steel coefficient of thermal expansion (CTE) on fire performance. Cases with zero thermal expansion for full and zero composite action, as well as the bare steel beam, are included to illustrate the effect of thermal expansion on the deflection behaviour, although these conditions are not physically realistic.

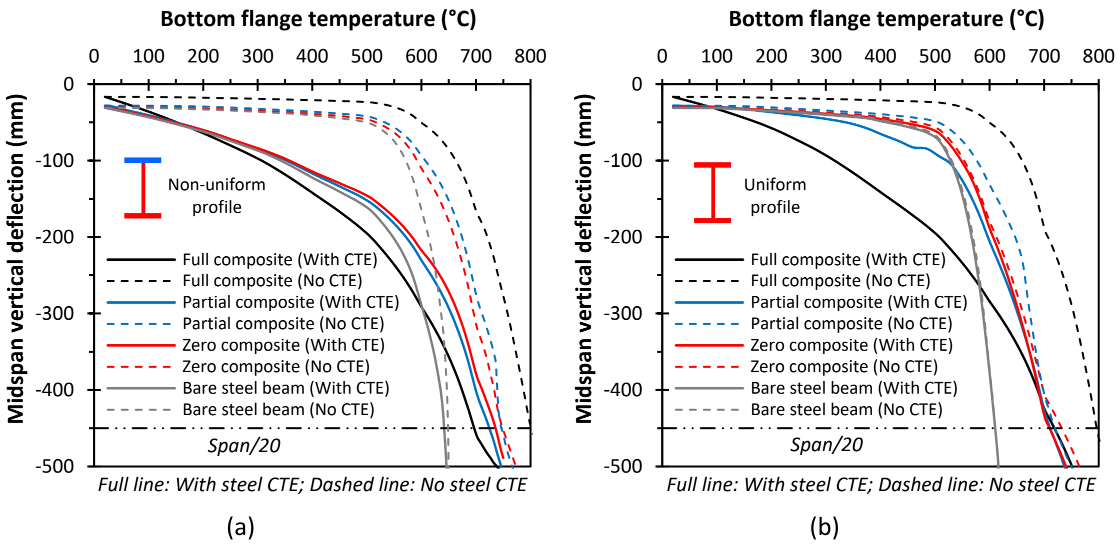

Figure 5.13: Deflection-temperature response of steel-CLT composite beams under steel-only heating for (a) non-uniform and (b) uniform profiles, incorporating varying interface conditions and steel thermal expansion (CTE)

In general, the effect of thermal bowing due to differential expansion across the steel section depth can be observed in the non-uniform heating case. The thermal curvature effect disappears when thermal expansion is not modelled; deflection results only from material degradation and the response is significantly underestimated. Under both non-uniform and uniform heating, the fully composite beam typically exhibits greater midspan deflection than the zero-composite system, except for a slight increase near span/20 in the uniform case. This behaviour may result from the heated steel top flange attempting to expand freely but being restrained by the mechanically connected cold CLT slab. The restraint limits free thermal expansion of the steel, inducing additional stresses that increase beam curvature and deflection, analogous to the behaviour of a bimetallic strip. A similar effect is observed under partial composite action. Furthermore, thermal degradation of the screws reduces the mechanical restraint between the steel beam and the CLT slab, causing the structural response to approach that of a zero composite action system. The fully and zero composite systems thus represent the upper- and lower-bound responses, with the partial composite case expected to lie between them.

Both the full and zero composite cases reach a midspan deflection of span/20 at comparable critical temperatures, higher than that of the bare steel beam. This indicates that composite action enhances the fire resistance of the system. However, despite the CLT slab remaining cold in all analyses, pronounced early-stage thermal curvature is observed only when composite action is present (full or partial connection), confirming that the additional deflection arises solely from mechanical restraint imposed by the cold timber slab on the expanding steel beam. These results demonstrate that, with ideal fire protection of the CLT, composite action improves overall fire resistance (assuming failure at span/20) despite the accompanying increase in early thermal curvature under both non-uniform and uniform heating scenarios.

5.6.4.2 Heated Steel Beam and Heated CLT Slab

Following the previous cold-slab assumption, the composite beam is now analysed with both the steel and the CLT exposed to elevated temperatures, representing a more realistic fire condition within a compartment. This allows the model to capture the degradation of the timber in fire. In this scenario, the thermal expansion of the CLT is also included using constant CTE values from 20 °C to 200 °C, with longitudinal expansion along the grain taken as 4×10^{-6}/°C and transverse expansion perpendicular to the grain as 25×10^{-6}/°C (Goli *et al.*, 2019). Above 300 °C, thermal expansion is set to zero to represent the collapse of the cellular structure within the char layer (Adibaskoro *et al.*, 2021). Nevertheless, sensitivity checks show that including CLT thermal expansion has virtually no effect on the modelled structural response.

The deflection-temperature response of the composite beam under heating of both the steel and CLT components is presented in Figure 5.14, showing (a) non-uniform and (b) uniform temperature profiles. The results highlight the influence of varying interface conditions and compare the effect of the cold CLT slab on fire performance. In the advanced heating phase (beyond 300 °C), the deflection responses of full, partial, and zero composite action are very similar for both non-uniform and uniform steel heating, despite the overall trends differing between the two heating regimes due to temperature gradients in the non-uniform case.

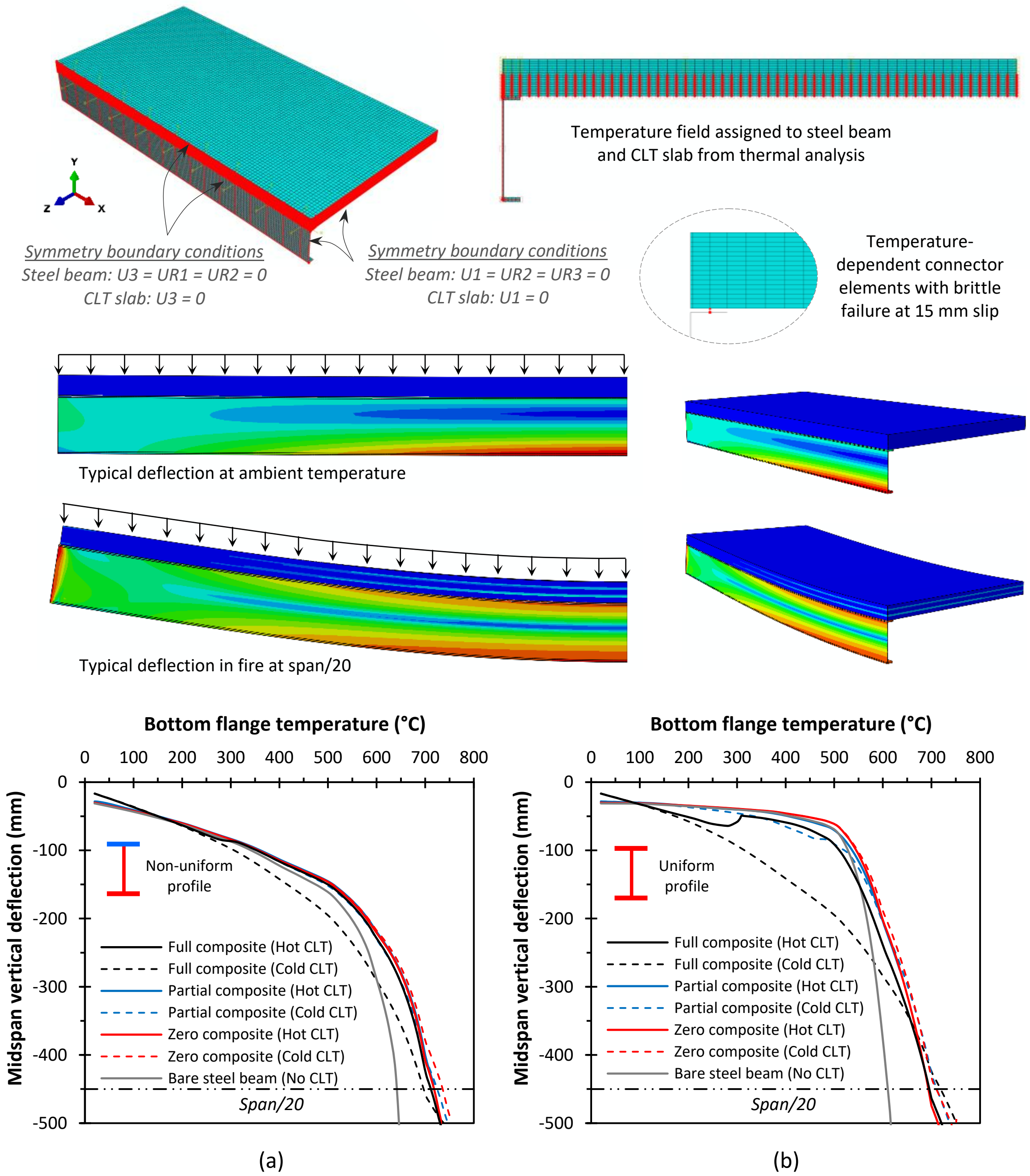

Figure 5.14: Deflection-temperature response of steel-CLT composite beams under steel and CLT heating for (a) non-uniform and (b) uniform profiles, incorporating varying interface conditions

As noted in Section 5.6.4.1, when the CLT is cold while the steel heats up, it restrains the thermal expansion of the steel top flange, leading to an increase in early midspan deflection. However, for full and partial composite action with a heated CLT, there is a deviation or sudden drop in deflection response around a bottom flange temperature of 300 °C compared to the composite beam with cold CLT, after which the response aligns with the zero composite trend. This drop is barely noticeable in the non-uniform heating case, as the thermal gradient along the beam tends to mask or reduce the sudden change.

From a structural mechanics perspective, the CLT provides mechanical resistance, while the shear connectors enable the transfer of forces between the CLT and the steel. Mechanical restraint to thermal expansion is only mobilised when the CLT is present and engaged through the connectors. In the absence of shear connectors, the CLT does not provide mechanical restraint to the steel, although it can still affect the system response. As the CLT heats and its stiffness decreases, the mobilised restraint progressively weakens, allowing the steel beam to expand more freely. The resulting sudden drop in deflection can thus be attributed to the progressive degradation of the CLT. Consequently, as the bottom CLT layer softens and chars and the shear interface begins to degrade, both full and partial composite cases converge towards the zero composite behaviour at approximately 300 °C bottom flange temperature. This highlights the critical role of the bottom CLT layer and shear interface integrity in sustaining composite action at elevated temperatures.

This response can also be interpreted using Figure 5.15, which illustrates the variation of longitudinal stress distribution in the CLT at midspan under ambient conditions and during fire when the deflection reaches span/20, for different interface conditions and heating profiles. For the fully composite steel-CLT beam, the stress distribution under ambient conditions is dominated by full compression. However, when the deflection reaches span/20 during fire, the bottom of CLT layers experience tension while the top remain in compression, resembling the behaviour of a non-composite beam with an unconnected slab. As also observed by Godoy Dellepiani *et al.* (2023), fire induces a redistribution of stresses in a fully composite beam, with the slab transitioning from a fully compressed state at ambient temperature to a state exhibiting both compressive and tensile stresses after charring.

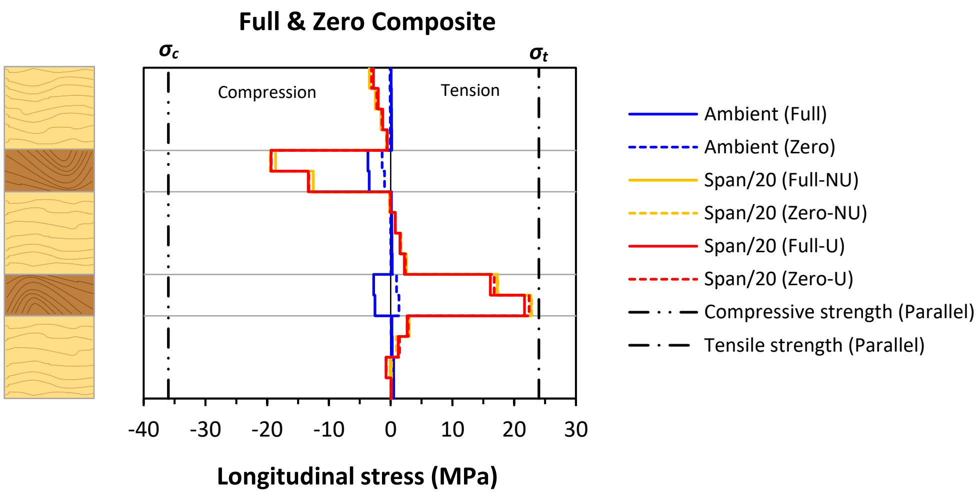

Figure 5.15: Longitudinal stress distribution in the CLT at midspan under ambient conditions and during fire at span/20, for various interface conditions and heating profiles (non-uniform, NU; and uniform, U)

Figure 5.16 presents the longitudinal stress distribution in the steel section at midspan under three representative conditions: ambient temperature, a bottom flange temperature of 550 °C, and failure corresponding to a deflection of span/20. The comparison across heating profiles and interface conditions highlights the sensitivity of the stress field to fire exposure and to variations in composite action, ranging from full interaction to zero interaction and the bare steel case. At failure under fire conditions, steel stresses in both the fully composite and zero composite cases remain lower than those observed in the bare steel beam. Moreover, the fully connected and unconnected slab cases exhibit very similar stress fields at failure in fire within each heating scenario. In the non-uniform temperature case, the thermal gradient shifts the neutral axis noticeably upward at failure, whereas under uniform heating, the neutral axis for zero composite action beam remains close to the mid-depth of the steel section.

Despite differences in stress distribution, full, partial, and zero composite action exhibit similar failure temperatures for a given heating scenario. Early-stage thermal deflection is higher in composite configurations, particularly in the fully composite case under uniform heating, due to restrained thermal expansion of the steel beam by the relatively cooler CLT slab, while subsequent degradation of the timber and interface reduces this restraint as temperatures increase. Overall, the results confirm that treating the beam as a bare steel section provides a conservative baseline for fire design, even though composite action can increase the failure temperature across the heating and interface conditions considered.

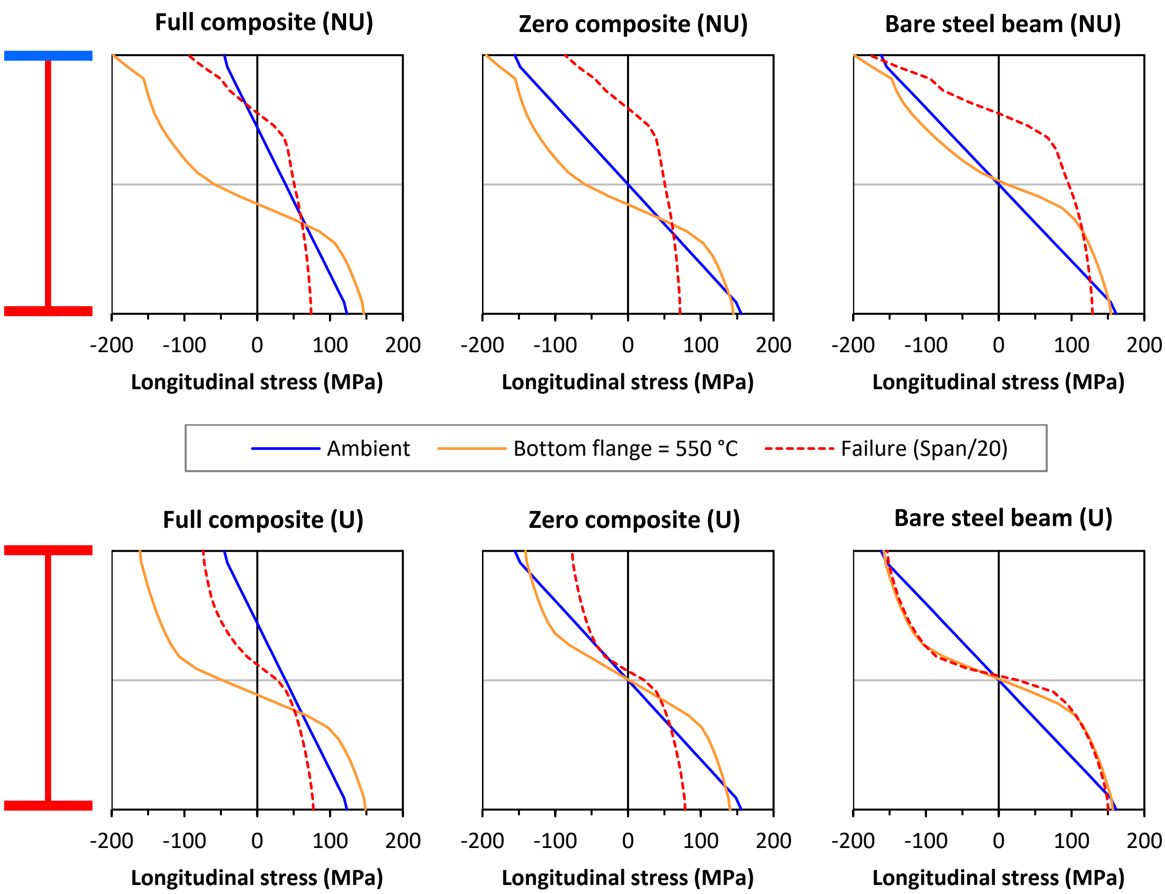

Figure 5.16: Longitudinal stress distribution in the steel section at midspan under ambient conditions, at a bottom flange temperature of 550 °C, and at failure at span/20, for various interface conditions and heating profiles (non-uniform, NU; and uniform, U)

5.6.4.3 Analysis of screw degradation in fire using beam-on-elastic-foundation theory

The results presented in Sections 5.6.4.1 and 5.6.4.2 highlight the influence of composite action on the structural response. To analyse the potential impact of elevated temperatures, a beam-on-elastic-foundation (BoEF) model was used to represent screw degradation in fire for the partial composite case. The elevated temperature connector degradation model was theoretically derived and calibrated using ambient temperature test results. However, it has not been validated against fire tests of steel-CLT screw connections because such data are not currently available in the literature. The unheated CLT slab case (Section 5.6.4.1) was selected as it showed the greatest sensitivity between partial and zero composite action. In the heated CLT slab scenario (Section 5.6.4.2), the envelope between the full and zero composite action responses is considerably narrower, indicating negligible influence of screw degradation.

The stiffness behaviour of a screw in a steel-timber connection can be represented as a finite beam of length L on an elastic foundation with stiffness k, subjected to a concentrated shear load P at the free end, as illustrated in Figure 5.17(a). The deflection y at the load application point is given by the Hetényi solution (Hetényi, 1946):

$$y = \frac{2P\lambda}{k} \frac{\sinh \lambda L \cosh \lambda L - \sin \lambda L \cos \lambda L}{\sinh^2 \lambda L - \sin^2 \lambda L} \tag{5.4}$$

with $$\lambda = \sqrt[4]{\frac{k}{EI}} \tag{5.5}$$

In expressions (5.4) and (5.5), λ is a dimensionless foundation parameter, E is the elastic modulus of the screw, and I is the second moment of area of the screw. The foundation stiffness per unit area k (N/mm^2) is determined as the product of the foundation modulus of timber k_0 (N/mm^3) and the projected screw beam width in contact with the elastic foundation b (mm).

To account for the effect of charring in fire, the screw can be idealised as a beam with a gap representing an unsupported charred portion of length a, while the foundation is active over the remaining supported length c, as illustrated in Figure 5.17(b). Following the approach of Kanninen (1973), the deflection at the load application point can be modified to consider this partially supported condition. The deflection y' at the load application point is given by:

$$y' = \frac{2P\lambda}{3k} \left[\begin{array}{l} 2\lambda^3 a^3 + 6\lambda^2 a^2 \left(\dfrac{\sinh \lambda c \cosh \lambda c + \sin \lambda c \cos \lambda c}{\sinh^2 \lambda c - \sin^2 \lambda c} \right) + \\ 6\lambda a \left(\dfrac{\sinh^2 \lambda c + \sin^2 \lambda c}{\sinh^2 \lambda c - \sin^2 \lambda c} \right) + 3 \left(\dfrac{\sinh \lambda c \cosh \lambda c - \sin \lambda c \cos \lambda c}{\sinh^2 \lambda c - \sin^2 \lambda c} \right) \end{array} \right] \tag{5.6}$$

This solution captures the increased slip due to loss of embedment support from charring. As the char layer forms, the effective embedment length is reduced from L to c, resulting in lower connection stiffness. Equation (5.6) reduces to Equation (5.4) when the parameter a is set to zero.

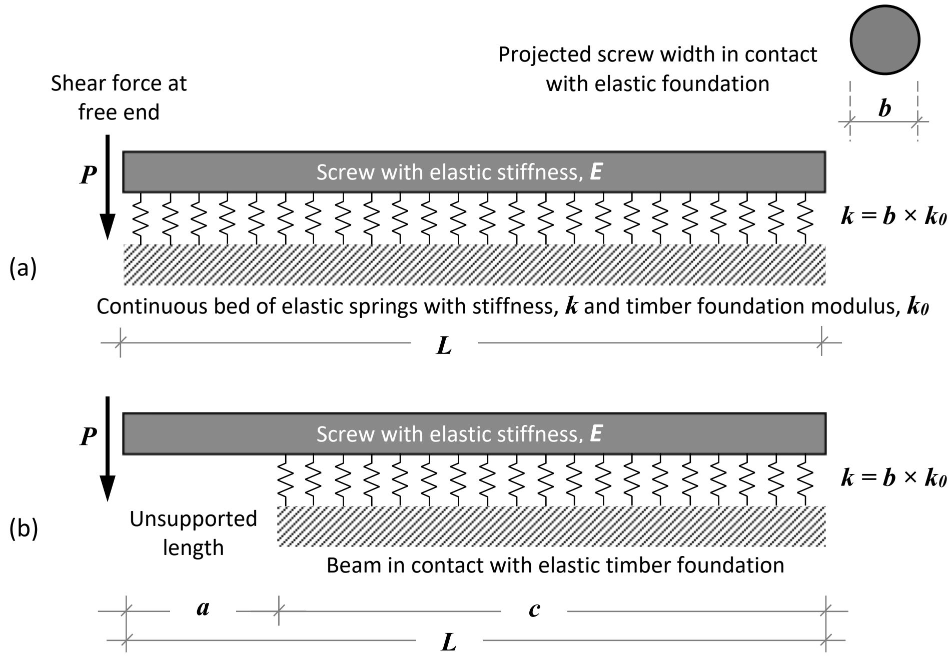

Figure 5.17: Screw on elastic timber foundation (a) fully supported, and (b) partially supported

In accordance with BS EN 26891 (1991), the serviceability slip modulus of the screw connection shown in Figure 5.9 was determined to be approximately 2160 N/mm. Further details of the calculation procedure can be found in Jeebodh *et al.* (2024). The slip modulus was also predicted using the BoEF model and found to be 2215 N/mm. The parameters adopted include a screw shank diameter of 8.1 mm, an effective screw length of 143 mm, and a foundation modulus of 16 N/mm^3 (Gikonyo, Schweigler and Bader, 2024). The results are illustrated in Figure 5.18(a), with brittle failure assumed to occur at a slip of 15 mm.

To account for heating effects, three cases were considered. Case 1 assumes full foundation support (k_0 = 16 N/mm^3) with screw steel stiffness degradation in accordance with BS EN 1993-1-2 (2005). Case 2 incorporates charring while maintaining k_0 = 16 N/mm^3. The foundation response is expected to be non-linear in practice but is modelled herein as linear elastic for simplicity. Case 3 follows Case 2 but reduces the foundation modulus by 50% to assess its influence on the response. The results are illustrated in Figure 5.18(b) together with the Eurocode 5 approach, which assumes a single degraded stiffness throughout the fire scenario.

Figure 5.18(c) and (d) show the influence of different degradation laws (Case 2 and 3) on the partial composite action. It can be observed that as the connector degrades, the response approaches that of zero composite action. Case 2 was used in the results presented in Sections 5.6.4.1 and 5.6.4.2. Figure 5.18(c) shows negligible influence while Figure 5.18(d) indicates a minor impact, implying that thermal degradation of the connectors is not a governing mechanism. These suggest that the results presented in Sections 5.6.4.1 and 5.6.4.2 are robust, and that thermal degradation of the screw is likely to vary from negligible (Section 5.6.4.2 and Figure 5.18(c)) to having little impact (Figure 5.18(d)). Given the theoretical nature of the present BoEF model and the lack of test data, this degradation requires validation using high-temperature push-out tests. The validity of the analytical model must also be investigated for different screw lengths and diameters.

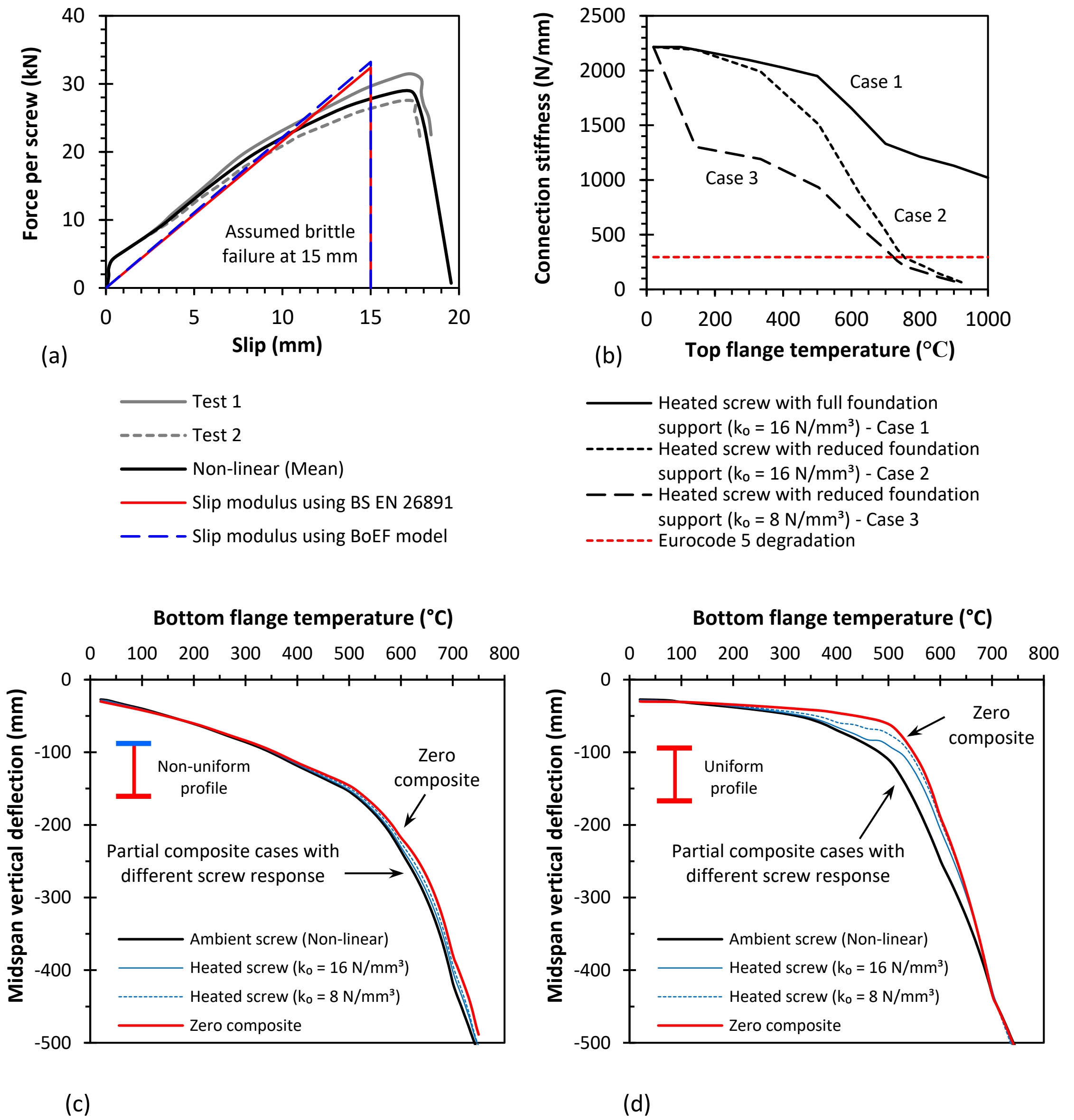

Figure 5.18: (a) Ambient load-slip relationship of screw connection and its prediction using the BoEF model; (b) predicted connection stiffness at different temperatures using BoEF model; and deflection-temperature response of composite beams under steel-only heating for (c) non-uniform and (d) uniform temperature profiles, considering different screw degradation laws and reduced foundation support due to charring

5.6.5 Design Implications for Composite Action

In ambient conditions, the design of steel-timber hybrid systems is generally governed by the serviceability limit state rather than the ultimate limit state. For the case study, relying on a bare steel beam to resist the full applied loading is insufficient to satisfy the deflection limit, which can vary depending on project-specific criteria and client expectations. Introducing partial composite action with the CLT slab provides a notable increase in stiffness and serviceability, with the level of deflection reduction influenced by the type and spacing of shear connectors.

The other key serviceability consideration is floor vibration, as excessive vibration can affect user comfort or sensitive equipment. While vibration control must be ensured in steel-timber hybrid systems, the present study does not address this aspect due to the limited validation of existing formulations available for the dynamic performance of such systems (Aloisio *et al.*, 2024) and because the anticipated office occupancy category for the case study may not impose particularly stringent vibration requirements. Nonetheless, vibration performance remains an essential aspect of the broader design of steel-timber hybrid structures.

In fire conditions, heating of the lower CLT layers and degradation of the shear interface can significantly reduce composite action between the steel beam and CLT slab. Accordingly, fire design should generally not rely on sustained full or partial composite interaction, and non-composite behaviour may be more appropriate for conservative assessment. Even when the CLT slab remains ideally protected, mechanical restraint from the slab can induce early-stage thermal curvature, which may result in greater deflection than in a bare steel beam, and this effect should be considered when evaluating fire performance under such conditions.

Nevertheless, analyses of full, partial, and zero composite cases indicate an overall increase in fire resistance (based on a span/20 deflection failure criterion), with failure temperatures ranging from 695 to 735 °C, compared with 610 to 640 °C for the bare steel beam. Although composite configurations may develop high early-stage deflections due to restrained thermal expansion, the presence of the CLT slab contributes to improved fire resistance at later stages, even when composite action is significantly degraded.

Although the present analysis shows that the steel-CLT composite beam, under all considered interface conditions and heating scenarios, can sustain steel bottom flange temperatures approaching 700 °C, current prescriptive fire design practice is based on a conservative limiting steel temperature of 550 °C. This threshold incorporates inherent safety margins to account for uncertainties in fire exposure, material degradation, and connection behaviour. The results of this study further suggest that performance-based fire design may allow for more efficient structural solutions, including reduced fire protection thickness or higher allowable steel temperatures, provided that relevant performance criteria are satisfied.

5.7 Conclusions

This paper has investigated the composite behaviour of an unprotected downstand steel beam supporting a CLT floor slab under ambient and elevated temperatures, demonstrating the influence of varying degrees of composite action, heating scenarios, material degradation, and thermal expansion on global structural response. The thermal degradation of the connectors was theoretically derived but has only been calibrated using ambient temperature test results. The steel beam was assumed to be laterally restrained to prevent lateral-torsional buckling (Jeebodh *et al.*, 2026). This assumption was adopted to isolate the mechanisms governing composite behaviour in fire. At ambient conditions, the serviceability limit state typically governs the design of steel-timber hybrid systems, with partial composite action improving bending stiffness and reducing deflection depending on shear connector characteristics. The following conclusions can be drawn:

- For the case study and modelling assumptions, full, partial, and zero composite action exhibit similar failure temperatures in fire, all exceeding those of the bare steel beam. However, composite systems develop higher early-stage deflections due to restrained thermal expansion at the steel-timber interface.
- The thermo-mechanical response is strongly influenced by the thermal state of the CLT slab. A comparatively cool slab partially restrains steel thermal expansion, inducing additional early-stage thermal curvature in composite configurations (full and partial).

This restraint reduces with increasing temperature due to degradation of timber and the formation of mechanically ineffective char at the shear interface.

- Fire exposure leads to progressive degradation of the bottom CLT layer and the steel-timber interface, reducing longitudinal shear transfer in composite systems and resulting in a gradual transition towards non-composite behaviour.
- The stiffness benefits of composite action at ambient temperature are largely diminished in fire due to combined effects of restrained thermal expansion and degradation of timber, particularly near the interface.
- The results indicate that composite action cannot be assumed to be maintained in fire. Design of steel-CLT composite beams therefore requires performance-based assessment that accounts for steel heating, the evolving thermal state of the CLT slab, and the integrity of the shear interface.
- Further research should consider a wider range of steel-CLT configurations, including fire protection to steel members, different heating scenarios, and axial restraint, as these factors can substantially alter heat transfer to the CLT slab and affect the development of composite action in fire. The influence of concrete infill or grouted shear connections should also be investigated.
- Notwithstanding the insights provided by numerical studies, dedicated fire testing of shear connector degradation and loaded steel-CLT composite systems remains indispensable for capturing the complex thermo-mechanical interactions that govern fire performance and for establishing robust design guidance for steel-timber hybrid structures.

6

Discussion

This chapter synthesises the findings of the three research studies to develop a comprehensive understanding of steel-timber hybrid structures in fire. It integrates insights from each study to explain the key thermo-mechanical mechanisms governing structural response. By examining lateral-torsional buckling and composite action independently, the underlying mechanics of each phenomenon are identified. The chapter also outlines the implications for structural fire design and identifies critical knowledge gaps requiring experimental validation.

6.1 Key Mechanisms of Steel-Timber Hybrid Beams in Fire

The response of steel-timber hybrid structures in fire is governed by a set of interacting mechanisms. Elevated temperatures reduce the stiffness and strength of steel, while timber chars and loses effective cross-section. Mechanical fasteners connecting the steel beam to the CLT slab deteriorate as steel temperatures rise and the embedding timber degrades. These connectors serve a dual role by providing composite interaction and lateral restraint.

Restrained thermal expansion from adjacent structural frames introduce compressive axial forces that further reduce stability and increase susceptibility to lateral-torsional buckling. The heating scenario additionally influences the structural response, as differing thermal properties of steel and timber create through-section temperature gradients and thermal bowing, thereby altering deformation patterns and the onset of instability.

Overall, the structural performance of steel-timber hybrid systems in fire is controlled by the combined effects of material degradation, connection deterioration, restraint conditions, and thermally induced actions. These mechanisms collectively influence stability, composite action, and the failure modes that develop in hybrid beams. While the study does not attempt a statistical quantification of these effects, the results indicate that certain mechanisms become dominant under specific conditions. For example, the interaction between lateral and axial restraint governs early-stage instability, whereas degradation of the steel-timber interface influences the transition from composite to non-composite behaviour. A conceptual framework summarising the governing mechanisms and structural fire design implications of steel-timber hybrid beams is presented in Figure 6.1, with several aspects explored in greater detail in the subsequent sections.

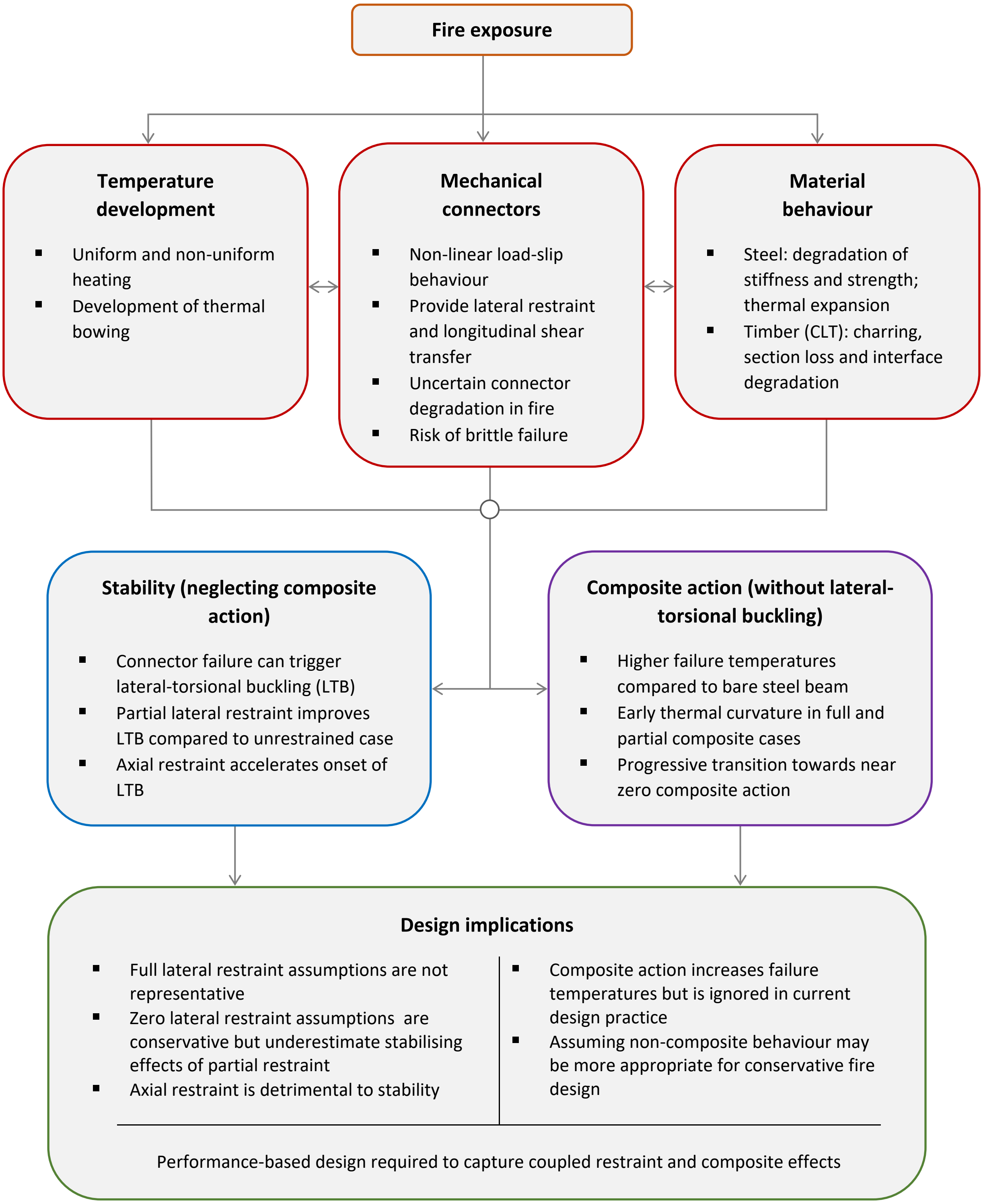

Figure 6.1: Conceptual framework of key mechanisms and structural fire design implications for steel-timber hybrid beams

6.2 Behaviour of Steel-Timber Connections in Fire

The load-slip behaviour of steel-to-CLT connections is inherently complex and exhibits nonlinearity even at ambient temperature. For design purposes, this behaviour is simplified through the use of slip moduli at different limit states. At ambient conditions, the serviceability slip modulus is determined experimentally or through established empirical relationships, while the ultimate slip modulus is typically taken as two-thirds of the serviceability slip modulus. However, existing empirical equations for steel-to-timber connections may not be directly applicable to steel-to-CLT connections with self-tapping screws. Given the limited experimental data, the equation proposed by Ehlbeck and Larsen (1993) in Section 3.3 was modified using a correction factor of 0.5. Although this represents a crude approximation, this modification provides a reasonable lower-bound estimate of stiffness based on the test results (Figure 3.5) reported by Merryday, Sener and Roueche (2023) and Merryday, Sener and Roueche (2025). More recent empirical equations for connections with self-tapping screws can be found in Deeves and Woods (2025).

In fire design, Eurocode 5 adopts a simplified approach in which the slip modulus of mechanical connections is reduced to a constant value. This corresponds to an 80% reduction in the ultimate slip modulus for screws and 33% for bolts, irrespective of temperature or fire exposure duration. As a result, progressive connector degradation at elevated temperatures is not explicitly represented, and a single degraded stiffness is assumed throughout the fire scenario (Figure 6.2). No temperature-dependent strength reduction model is provided for connection capacity. In addition, self-tapping screws may fail in a brittle manner at ambient temperature and this limited ductility may persist in fire. In this study, brittle behaviour of the screws was assumed to investigate lateral-torsional bucking, while a temperature-dependent degradation model was theoretically derived using beam-on-elastic-foundation theory to examine partial composite action.

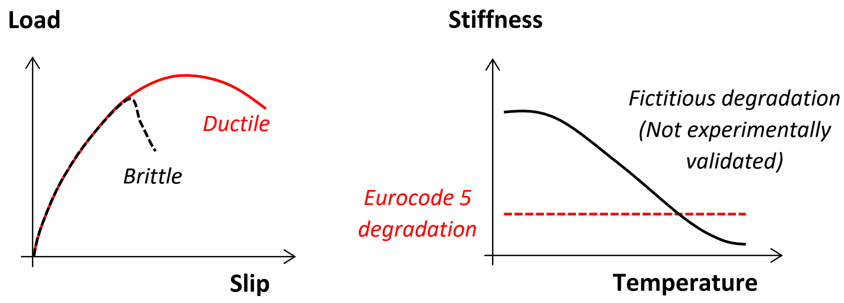

Figure 6.2: Illustrative load-slip curve for steel-timber screw connection and assumed (fictitious) degradation, compared with Eurocode 5 guidance

The degradation of connectors has two important implications for structural response. First, reduced longitudinal shear transfer at the interface alters load sharing between the steel and timber components, thereby affecting the degree of composite action during heating. The results show that connector degradation has negligible to little impact on composite action. Second, the deterioration of connector stiffness reduces the lateral restraint provided by the slab to the steel beam, potentially compromising global stability in fire. Even relatively low levels of lateral restraint were found to improve the lateral-torsional buckling behaviour of steel beams, although screw failure and the resulting loss of restraint can trigger instability. Assuming a constant reduced stiffness (80% for screws and 33% for bolts) implies reduced lateral restraint from the onset of fire exposure. A temperature-dependent degradation model could alter the timing of screw failure and the subsequent loss of lateral restraint, which should be investigated in future work.

This simplification highlights a key limitation in current design provisions. The lack of experimentally validated degradation models for steel-to-CLT connections in fire underscores the need for further research to characterise the temperature-dependent evolution of connector stiffness and strength, and to support the development of performance-based design approaches for hybrid structures.

6.3 Interaction between Lateral and Axial Restraint on Stability

The stability of steel beams, particularly secondary beams, in hybrid structures is a critical design consideration in fire. At ambient temperature, lateral restraint provided by the CLT slab through the stiffness of the mechanical connectors improves resistance to lateral-torsional buckling. However, as the connectors degrade and the surrounding timber chars, the effectiveness of this restraint progressively diminishes, alongside reduction in steel stiffness and strength at elevated temperatures.

The analytical and numerical investigations in this study indicate that designing beams as fully laterally restrained, as commonly assumed in steel-concrete composite systems, is not representative of steel-timber hybrid behaviour in fire. In contrast, although assuming no lateral restraint is conservative, it underestimates the beneficial contribution of partial lateral restraint. Importantly, even relatively low levels of lateral restraint can provide meaningful stabilising effects, particularly in the later stages of heating when steel has significantly degraded. This is demonstrated in Figure 6.3, with the analytical results showing a normalised relationship between the partially restrained, unrestrained and fully restrained cases, while the numerical results demonstrate the effect of both lateral and axial restraint under uniform and non-uniform temperature profiles. These findings are consistent with the parametric studies in Chapters 3 and 4, which showed that realistic screw stiffness values do not justify full restraint assumptions, yet still provide substantial improvements over the unrestrained case. It is also noted that higher-stiffness connection systems (e.g. shear studs with concrete infill) are expected to reduce susceptibility to lateral-torsional buckling compared to self-tapping screws commonly used in mass timber construction.

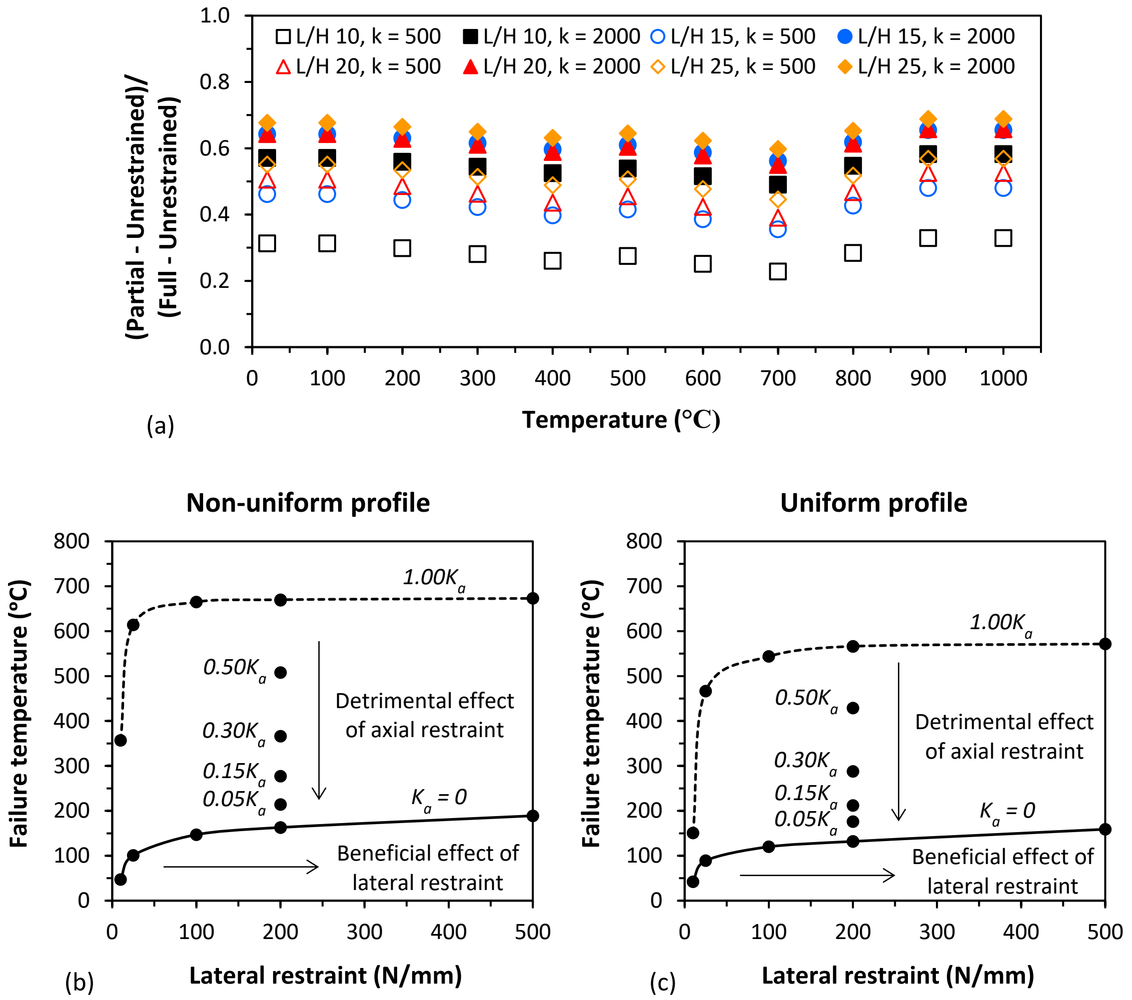

Figure 6.3: (a) Normalised relationship of partially restrained case with practical range of continuous lateral restraint *k* (kN/m/m) relative to unrestrained and fully restrained cases from analytical investigation, and (b, c) effect of lateral and axial restraint from numerical investigation for non-uniform and uniform temperature profiles.

The findings demonstrate that lateral restraint has a stabilising influence on beam response, whereas axial restraint has a destabilising effect, reducing failure temperature due to compressive forces generated by restrained thermal expansion. Figure 6.3(b) and (c) illustrate the effect of varying axial restraint on the failure temperature, from no axial restraint to a restraint stiffness equal to the ambient temperature axial stiffness of the beam. As temperature rises and steel degrades, these thermally induced axial forces become increasingly significant, accelerating the onset of lateral-torsional instability even when some degree of lateral restraint is present. For beams connected with brittle self-tapping screws, fastener failure in the midspan region typically occurs near the peak compressive axial force, after which the loss of lateral restraint triggers lateral-torsional buckling (Figure 6.4). This is consistent with the runaway deflection mechanism identified in Chapter 4 and highlights the importance of the connector load-slip behaviour. In this study, the screws were assumed to fail in a brittle manner at a slip of 15 mm, based on the test results shown in Figure 4.2 by Merryday, Sener and Roueche (2023) and the 15 mm slip criterion in BS EN 26891 (1991). Future work could examine the influence of the slip capacity, connector spacing, and connector type on lateral-torsional buckling.

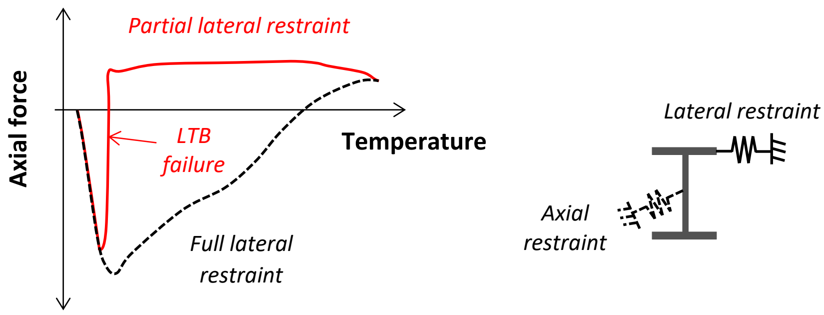

Figure 6.4: Comparison of full and partial lateral restraint in beams under axial restraint

The influence of the heating scenario appears secondary compared to mechanical restraint conditions, with only marginal differences in failure temperature between uniform heating and cases where the top flange is slightly hotter. In contrast, cooler top flange conditions increase failure temperatures and improve stability performance under fire exposure.

Overall, the interaction between lateral and axial restraint governs beam stability in fire and is critical for performance-based design of hybrid beams. This underlines the need for connector-specific fire design guidance, rather than relying on direct analogy with steel-concrete systems or idealised assumptions of full or zero lateral restraint. In particular, axial restraint should be treated as a critical and potentially detrimental factor, especially where end connections cannot accommodate thermal expansion through ductile deformation.

6.4 Composite Action in Fire

Composite action in steel-timber hybrid systems is governed by the ability of the interface to transfer longitudinal shear between the steel beam and the timber slab. This behaviour is controlled by the load-slip characteristics of the fasteners, which exhibit temperature-dependent degradation in stiffness and strength. As a result, the degree of composite action is not constant during fire exposure but evolves with the heating scenario and fastener performance.

At ambient conditions, composite action enhances structural efficiency by increasing flexural stiffness and load-carrying capacity. However, its contribution in fire may diminish, with behaviour increasingly influenced by the connector type, the thermal state of the CLT slab, and the integrity of the steel-timber interface. In the early stages of heating, a relatively cool CLT slab can restrain the thermal expansion of the steel beam, inducing thermal curvature in both full and partial composite configurations. As the slab heats and the interface deteriorates, this restraint reduces and the system may progressively transition towards non-composite behaviour (Figure 6.5). When the temperature distribution of the steel beam is non-uniform (i.e. a cooler top flange), thermal bowing can dominate the overall deflection response.

It must also be noted that timber stiffness degradation was considered in the heated mechanical model, whereas temperature-dependent strength degradation using Hashin damage was not explicitly considered. Therefore, potential crushing or cracking of the CLT and the resulting stress redistribution were not captured. Such damage could reduce the contribution of the CLT to bending, transferring more load to the steel beam and reducing composite action. The numerical models assumed a continuous CLT slab, without segmentation or gaps between adjacent panels. Previous experimental research with adjacent panels placed tightly together found only minor differences in stiffness and strength compared with a continuous slab (Deeves and Woods, 2026). However, larger gaps would need to close before the CLT becomes effective in compression, potentially reducing the initial stiffness. Thus, this modelling assumption is not expected to significantly affect the overall trends observed in this study.

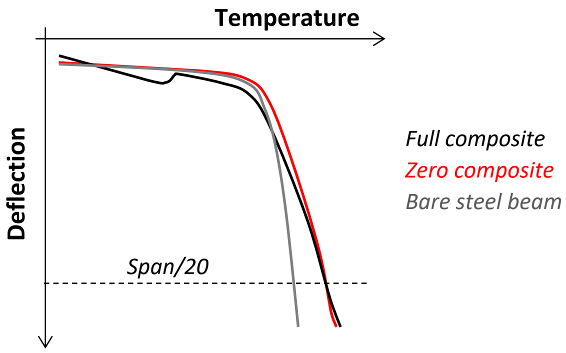

Figure 6.5: Deflection-temperature response of steel-CLT composite beams without thermal bowing

Despite these reductions in composite action, the presence of the CLT slab still provides measurable benefits to fire performance compared to a bare steel beam. Full, partial, and zero composite configurations can achieve higher failure temperatures than a bare steel beam, even under significantly degraded composite action. This indicates a nuanced response in which composite systems may exhibit higher early-stage curvature due to restrained thermal expansion, yet ultimately reach failure temperatures comparable to zero composite configurations.

Godoy Dellepiani *et al.* (2023) also reported limited sensitivity of midspan deflection to interface condition after 30 minutes of fire exposure for fully fixed steel beams with full and zero composite action. However, the influence of axial restraint on composite action and the resulting compressive forces on lateral-torsional buckling during fire require further investigation. In this study, composite action and lateral-torsional buckling were considered separately. Therefore, the higher failure temperatures obtained for the composite configurations do not account for possible instability triggered by the degradation of lateral restraint. Future work should investigate these mechanisms simultaneously to establish how composite action, connector degradation and lateral-torsional buckling interact during fire.

From a design perspective, neglecting composite action in fire is conservative. Prescriptive limiting temperatures, such as the commonly adopted 550 °C threshold, are based primarily on isolated steel members. These limits may be overly conservative for hybrid systems, as this study indicates higher steel temperatures at the deflection-based failure criterion. This suggests that current prescriptive approaches do not fully capture the structural behaviour of hybrid systems in fire, highlighting the need for more performance-based design methods.

6.5 Influence of Heating Scenarios on Stability and Composite Action

The fire dynamics within a compartment play an important role in the thermal response of steel-timber hybrid structures. The steel-CLT heat transfer is inherently complex and temperature distributions across the steel section directly affect the structural behaviour. The CLT slab alters the thermal exposure of the steel beam, typically shielding the top flange but also potentially leading to localised heating. Hence, this study considers both a non-uniform heating case with a cooler top flange and an idealised uniform-heating scenario. However, the resulting temperature distribution depends strongly on compartment conditions, ventilation, and the extent of exposed timber, and remains an area of ongoing research

Non-uniform temperature distributions generate thermal gradients across the steel section, leading to thermal bowing through differential thermal expansion between the flanges, while the compression flange temperature strongly influences the development of lateral-torsional buckling. Consequently, the structural response is highly sensitive to these thermal gradients and accurate prediction of the top flange temperature is essential for assessing both instability and composite action. For lateral-torsional buckling, a cooler top flange scenario can lead to higher failure temperatures due to reduced steel degradation of the compression flange (Figure 6.6).

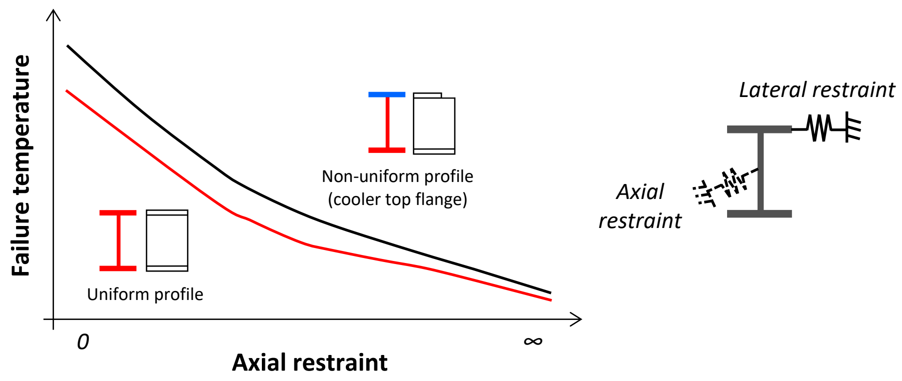

Figure 6.6: Failure temperatures with varying axial restraint and temperature profiles under constant lateral restraint

In composite systems, the thermal state of the CLT slab influences the expansion of the steel beam and contributes to early-stage thermal curvature. As the timber heats and char develops at the steel-timber interface, the restraint provided by the slab progressively decreases. Although a cooler top flange profile generally results in slightly higher failure temperatures than uniform heating, thermal bowing effects remain significant.

Overall, the structural performance of steel-timber hybrid systems in fire cannot be fully represented using a single idealised heating condition. Robust fire design should therefore consider a range of realistic heating scenarios, including thermal shielding effects and cases where the compression flange may experience elevated temperatures earlier than expected. Incorporating thermal gradients into performance-based design is essential for capturing the behaviour of hybrid systems under fire conditions.

6.6 Structural Response and Failure of Hybrid Beams

In fire conditions, the structural response of heated steel beams in hybrid structures typically progresses from an initial elastic behaviour to increasingly non-linear behaviour with increasing temperature. Partially laterally restrained beams may initially behave similarly to fully laterally restrained beams, but if the lateral restraint is insufficient, lateral-torsional buckling may occur before yielding of the steel. The level of restraint depends on the stiffness and integrity of the connectors, and in systems using brittle screws, temperature-induced degradation or sudden failure of the connectors can trigger premature loss of restraint and early instability.

Where axial restraint is present, thermal expansion generates significant compressive axial forces within the beam, and the first screw failure typically occurs prior to the peak compressive force. Failure of a midspan screw can then trigger rapid successive failure of the remaining screws, resulting in loss of lateral restraint and lateral-torsional buckling. While this instability initiates structural failure in terms of load-carrying capacity, the beam subsequently undergoes an abrupt transition from compression-dominated behaviour to tensile catenary action. This catenary response temporarily slows the rate of runaway deflection, although the beam is highly distorted and no longer structurally viable.

The inclusion of composite action increases the failure temperature compared with a bare steel beam, as the CLT slab provides additional resistance. In these analyses, failure is typically taken to occur when the deflection limit of span/20 is reached. While this assumes the beam remains laterally restrained against instability, composite action may alter compression demand in the top flange, with possible implications for lateral-torsional buckling. The findings from Chapter 4 demonstrate that partial lateral restraint improves stability, while axial restraint is detrimental. Chapter 5 shows that composite action increases failure temperature. However, these results cannot be directly superimposed because lateral-torsional buckling and composite action were investigated separately. Nevertheless, it may be hypothesised that connection systems capable of providing sufficiently high lateral restraint in fire could significantly delay the onset of lateral-torsional buckling. In such cases, the composite response may follow the trends observed in the present composite action analyses.

6.7 Limitations of Current Design Guidance and Need for Full-Scale Testing

There is a lack of experimental and numerical data on composite behaviour and connector performance at elevated temperatures. Current structural fire design generally does not assume composite action in fire. However, the numerical findings of this study indicate that composite action can improve structural performance compared to a bare steel beam by increasing failure temperatures. At the same time, degradation or brittle failure of connectors may result in loss of lateral restraint to steel beams, potentially triggering instability failures such as lateral-torsional buckling. The analytical and numerical results demonstrate that assuming full lateral restraint of secondary steel beams, as in steel-concrete composite systems, is unsafe for steel-timber hybrids. If a performance-based fire design permits loss of the timber floor system while maintaining overall stability of the steel framing, the secondary beams should conservatively be assessed without reliance on lateral restraint from the floor system.

Furthermore, current fire design guidance for steel-timber hybrid structures remains limited compared with the well-established guidance available for steel-concrete composite systems. The presence of CLT affects fire dynamics by contributing to the compartment fire load, while thermal feedback from radiating surfaces and potential delamination may sustain combustion and hinder self-extinction. These phenomena are not fully addressed within simplified prescriptive fire design methods and therefore performance-based fire assessment may be required rather than reliance on standard fire curves or assumed charring rates, which do not capture the complex thermal behaviour of mass timber.

These limitations demonstrate the need for full-scale fire testing to better understand the interaction between composite action, restraint effects, connector degradation, and instability-driven failure mechanisms in steel-timber hybrid systems under realistic heating scenarios, including potential CLT delamination. Ultimately, experimental data are essential to validate advanced numerical models and support the development of robust performance-based design approaches for hybrid structures under fire conditions.

6.8 Design Implications

The findings of this study have several implications for the fire design of steel-timber hybrid structures. As discussed in Section 1.2, there is a lack of understanding regarding the stability of steel beams under combined lateral and axial restraint during fire exposure and the composite behaviour of steel-CLT assemblies at elevated temperatures. This study provides further insight into the effects of restraint on beam stability and the mechanics of composite action at elevated temperatures, while also highlighting the lack of temperature-dependent degradation models for connectors that provide both lateral restraint and longitudinal shear transfer. The key implications of these findings for current fire design practice are summarised below:

1. A constant reduced slip modulus in Eurocode 5 may misrepresent the progressive degradation of composite action and lateral restraint in fire, affecting predictions of structural response.
2. Full lateral restraint assumptions are not representative of hybrid beams in fire. Zero lateral restraint assumptions are conservative but underestimate the stabilising effects of partial restraint. Axial restraint is detrimental to stability under fire conditions.
3. Composite action increases failure temperatures but is typically ignored in current design practice. Assuming non-composite behaviour may therefore be more appropriate for conservative fire design.
4. Accurate prediction of the compression-flange temperature is essential for lateral-torsional buckling and the thermal state of the CLT slab affects the response of composite systems. Design must consider a range of realistic heating scenarios.
5. Fire design of hybrid beams should consider the interaction between lateral-torsional buckling and composite action, as connector performance may influence the onset of instability and the ability of composite action to delay failure.
6. Performance-based design and fire testing are required to capture coupled restraint and composite effects in steel-timber hybrid structures.

7

Conclusions and Future Work

7.1 Conclusions

Steel-timber hybrid structures are emerging as low-carbon solutions that combine steel framing with CLT panels, yet their behaviour in fire remains insufficiently understood. As temperatures rise, mechanical connectors lose stiffness and strength, reducing both lateral restraint and composite action in steel beams supporting timber flooring. Consequently, current fire design practice conservatively neglects composite action and provides limited guidance on the level of lateral restraint that can be reliably assumed.

To address these challenges, this thesis investigated the structural fire performance of representative steel-CLT hybrid downstand configurations using analytical and numerical methods. The studies focused on the lateral-torsional buckling behaviour of heated beams under lateral and axial restraint, as well as the contribution of composite action in laterally restrained systems. These phenomena were examined independently to isolate the structural response associated with each mechanism. Uniform and non-uniform heating scenarios, including thermal bowing effects, were considered to assess structural stability and response.

The results demonstrate that the lateral-torsional buckling behaviour of hybrid beams is governed by the interaction between lateral and axial restraint. Even relatively low levels of lateral restraint enhance stability at elevated temperatures compared to a laterally unrestrained beam. Fastener failure in the midspan region typically initiates the loss of lateral restraint and subsequent lateral-torsional buckling. Axial restraint, arising from restrained thermal expansion, introduces thermally induced compressive forces and accelerates the onset of instability. These findings indicate that assumptions of full lateral restraint, commonly adopted in steel-concrete composite design, are not representative of steel-timber hybrid behaviour in fire, whereas assumptions of zero restraint may be overly conservative.

Design approaches assuming uniform steel temperature may be unconservative when higher temperatures develop in the top flange, but conservative in cooler-flange scenarios.

The results further indicate that composite action, while less influential than restraint conditions, still provides a consistent and beneficial contribution to the structural fire performance of hybrid systems. Across full and zero composite configurations, which represent the upper and lower bounds of composite action, hybrid systems achieve higher failure temperatures than a bare steel beam. While composite action enhances flexural stiffness and load-carrying capacity at ambient conditions, its contribution diminishes in fire due to restrained steel thermal expansion against the relatively cool CLT slab and degradation at the steel-timber interface, reducing longitudinal shear transfer. As a result, a fully composite system may exhibit pronounced thermal curvature early in the heating phase but progressively converge towards the behaviour of a zero composite system as timber degrades at the interface. Nevertheless, the presence of the CLT slab consistently improves performance compared to a bare steel beam across all levels of composite action.

Overall, the findings demonstrate that the structural response of steel-timber hybrid beams in fire is governed by the coupled interaction between restraint conditions, connector degradation, thermal exposure, and composite behaviour. Current design assumptions derived from steel-concrete systems do not fully capture these complex interactions and may therefore lead to either unconservative or overly conservative predictions of structural fire performance, highlighting the need for performance-based design approaches.

7.2 Future Work

While the numerical results provide valuable insights, computational modelling alone cannot fully capture the complex fire behaviour of hybrid systems, particularly mechanisms such as temperature-dependent connector degradation, charring and subsequent char crushing, restrained thermal expansion, thermal bowing, and potential delamination. These limitations highlight the need for component-level and full-scale fire testing to investigate a broader range of system configurations, connection types, fire protection strategies, boundary conditions, and heating scenarios, including cooling phases. Ultimately, experimental evidence is essential to validate the numerical findings and provide quantitative data on key mechanisms governing structural response in fire.

Furthermore, experimental data could be used to calibrate and refine the finite element models developed in this study, thereby improving their accuracy in predicting the fire performance of steel-timber hybrid beams. Given the strong influence of connector performance on both lateral-torsional buckling and composite action, future research should establish temperature-dependent constitutive models for screws and quantify connection stiffness, slip behaviour, and degradation laws for different fastener types. In addition, the assessment should be extended from isolated beam analyses to system-level models incorporating primary and secondary beams, floor panels, and columns to better understand load redistribution, restraint development, and global stability under fire conditions.

Finally, future work should explore the development of simplified analytical and design methods that capture the interaction between restraint, composite action, and thermal exposure. These tools would help bridge the gap between detailed numerical simulations and practical fire design. Collectively, these experimental, numerical, and analytical investigations would improve understanding of the complex thermo-mechanical interactions that govern hybrid systems in fire. The resulting knowledge would support the development of robust design guidance and performance-based approaches, helping to realise the full structural potential of steel-timber hybrid systems in the built environment.

References

1. Abaqus (2021) *Abaqus/CAE User's Guide*: Dassault Systèmes.

2. Adibaskoro, T., Makowska, M., Rinta-Paavola, A., Fortino, S. and Hostikka, S. (2021) 'Elastic Modulus, Thermal Expansion, and Pyrolysis Shrinkage of Norway Spruce Under High Temperature', *Fire Technology*, 57(5), pp. 2451-2490. DOI: https://doi.org/10.1007/s10694-021-01123-z.

3. AISC (2022) *Design Guide 37: Hybrid Steel Frames with Wood Floors*, USA: American Institute of Steel Construction.

4. Ali Awadallah, A. A., Hadden, R. M. and Law, A. (2024) 'Meta-analysis of temperature, heat release rate, delamination and auto-extinction of timber compartments', *Fire Safety Journal*, 146, pp. 104164. DOI: https://doi.org/10.1016/j.firesaf.2024.104164.

5. Aloisio, A., Pasca, D. P., Owolabi, D. and Loss, C. (2024) 'Vibration serviceability of hybrid CLT-steel composite floors based on experimental and numerical investigations using random walk models', *Engineering Structures*, 304, pp. 117600. DOI: https://doi.org/10.1016/j.engstruct.2024.117600.

6. Aprisa, D. P., Agrawal, A., Sauca, A., Pope, I., Blondeau-Pâtissier, R., Bisby, L. and McLaggan, M. S. (2026) 'Thermal response of hybrid steel-timber floor cross-sections exposed to standard fire: experimental and numerical investigations', *Fire Safety Journal*, 159, pp. 104593. DOI: https://doi.org/10.1016/j.firesaf.2025.104593.

7. Arup (2024) *Fire Safe Design of Mass Timber Buildings*: Arup.

8. Asiz, A. and Smith, I. (2011) 'Connection system of massive timber elements used in horizontal slabs of hybrid tall buildings', *Journal of Structural Engineering*, 137(11), pp. 1390-1393. DOI: https://doi.org/10.1061/(ASCE)ST.1943-541X.0000363.

9. Bailey, C. (1998) 'Computer modelling of the corner compartment fire test on the large-scale Cardington test frame', *Journal of Constructional Steel Research*, 48(1), pp. 27-45. DOI: https://doi.org/10.1016/S0143-974X(97)00078-3.

10. Bailey, C. G., Burgess, I. W. and Plank, R. J. (1996) 'The lateral-torsional buckling of unrestrained steel beams in fire', *Journal of Constructional Steel Research*, 36(2), pp. 101-119. DOI: https://doi.org/10.1016/0143-974X(95)00014-M.

11. Barber, D., Roy-Poirier, A. and Wingo, L. 'Modelling the fire performance of steel beam to CLT connections for hybrid construction'. *Proceedings of the 12th Asia-Oceania symposium on fire science and technology (AOSFST 2021)*, Brisbane, Australia. DOI: https://doi.org/10.14264/E58A1CA.

12. Bartlett, A. I., Hadden, R. M. and Bisby, L. A. (2019) 'A Review of Factors Affecting the Burning Behaviour of Wood for Application to Tall Timber Construction', *Fire Technology*, 55(1), pp. 1-49. DOI: https://doi.org/10.1007/s10694-018-0787-y.

13. Bartlett, A. I., Hadden, R. M., Hidalgo, J. P., Santamaria, S., Wiesner, F., Bisby, L. A., Deeny, S. and Lane, B. (2017) 'Auto-extinction of engineered timber: Application to compartment fires with exposed timber surfaces', *Fire Safety Journal*, 91, pp. 407-413. DOI: https://doi.org/10.1016/j.firesaf.2017.03.050.

14. Bartlett, A. I., McNamee, R., Robert, F. and Bisby, L. A. (2020) 'Comparative energy analysis from fire resistance tests on combustible versus noncombustible slabs', *Fire and Materials*, 44(3), pp. 301-310. DOI: https://doi.org/10.1002/fam.2760.

15. BCSA (2024) *BCSA Annual Review 2024/25*, London.

16. Becker, I., Anderson, F. and Phillips, A. R. (2023) 'Structural design of hybrid steel-timber buildings for lower production stage embodied carbon emissions', *Journal of Building Engineering*, 76, pp. 107053. DOI: https://doi.org/10.1016/j.jobe.2023.107053.

17. Belaid, T., Ammari, F. and Adman, R. (2018) 'Influence of load position on critical lateral torsional buckling moment of laterally restrained beam at tense flange', *Asian Journal of Civil Engineering*, 19(7), pp. 839-848. DOI: https://doi.org/10.1007/s42107-018-0067-7.

18. Bisby, L., Gales, J. and Maluk, C. (2013) 'A contemporary review of large-scale non-standard structural fire testing', *Fire Science Reviews*, 2(1), pp. 1. DOI: https://doi.org/10.1186/2193-0414-2-1.

19. Bøe, A. S., Friquin, K. L., Brandon, D., Steen-Hansen, A. and Ertesvåg, I. S. (2023) 'Fire spread in a large compartment with exposed cross-laminated timber and open ventilation conditions: #FRIC-02 - Exposed wall and ceiling', *Fire Safety Journal*, 141, pp. 103986. DOI: https://doi.org/10.1016/j.firesaf.2023.103986.

20. Böhm, N., Vogelsberg, A. and Kühn, B. (2023) 'Investigations of the shear connectors and the load-bearing behaviour of steel cross-laminated timber composite beams', *ce/papers*, 6, pp. 78-83. DOI: https://10.1002/cepa.2379.

21. Böhm, N., Vogelsberg, A. and Kühn, B. (2024) 'Bending and Vibration Behaviour of CLT-Steel Composite Beams', *Journal of Sustainable Architecture and Civil Engineering,* 34, pp. 75-88. DOI: https://10.5755/j01.sace.34.1.35467.

22. Bompa, D. V., Chira, A. and Zwicky, D. (2024) 'Constitutive modelling of deformation rate dependent response of steel timber shear connections', *Journal of Building Engineering,* 98, pp. 111159. DOI: https://doi.org/10.1016/j.jobe.2024.111159.

23. Brandner, R., Flatscher, G., Ringhofer, A., Schickhofer, G. and Thiel, A. (2016) 'Cross-Laminated Timber (CLT): Overview and Development', *European Journal of Wood and Wood Products,* 74(3), pp. 331-351. DOI: https://doi.org/10.1007/s00107-015-0999-5.

24. Brandner, R., Tomasi, R., Moosbrugger, T., Serrano, E. and Dietsch, P. (2018) *Properties, Testing and Design of Cross Laminated Timber: A state-of-the-art report by COST Action FP1402 / WG 2.* Germany: Shaker Verlag.

25. Brandon, D. and Dagenais, C. (2018) *Fire Safety Challenges of Tall Wood Buildings – Phase 2: Task 5 – Experimental Study of Delamination of Cross Laminated Timber (CLT) in Fire*: National Fire Protection AssociationFPRF-2018-05).

26. British Steel (1999) *The Behaviour of Multi-storey Steel Framed Buildings in Fire*, United Kingdom: British Steel.

27. Browne, F. L. (1958) *Theories of the Combustion of Wood and Its Control: A Survey of the Literature* (2136.

28. BS 476-20 (1987) *Fire tests on building materials and structures - Part 20: Method for determination of the fire resistance of elements of construction (general principles).* British Standards Institution.

29. BS EN 1363-1 (2020) *Fire resistance tests - General requirements.* British Standards Institution.

30. BS EN 1991-1-2 (2002) *Eurocode 1: Actions on structures - Part 1-2: General actions - Actions on structures exposed to fire.* British Standards Institution.

31. BS EN 1992-1-2 (2019) *Eurocode 2: Design of concrete structures - Part 1-2: General rules - Structural fire design.* British Standards Institution.

32. BS EN 1993-1-1 (2005) *Eurocode 3: Design of steel structures - Part 1-1: General rules and rules for buildings.* British Standards Institution.

33. BS EN 1993-1-2 (2005) *Eurocode 3: Design of steel structures - Part 1-2: General rules - Structural fire design.* British Standards Institution.

34. BS EN 1994-1-2 (2005) *Eurocode 4: Design of composite steel and concrete structures - Part 1-2: General rules - Structural fire design.* British Standards Institution.

35. BS EN 1995-1-1:2004+A2 (2014) *Eurocode 5: Design of Timber Structures - Part 1-1: General - Common Rules and Rules for Buildings.* British Standards Institution.

36. BS EN 1995-1-2 (2004) *Eurocode 5: Design of Timber Structures - Part 1-2: General - Structural Fire Design.* British Standards Institution.

37. BS EN 16351 (2021) *Timber Structures - Cross Laminated Timber - Requirements.* British Standards Institution.

38. BS EN 26891 (1991) *Timber structures. Joints made with mechanical fasteners. General principles for the determination of strength and deformation characteristics.* British Standards Institution.

39. Buchanan, A., Moss, P., Seputro, J. and Welsh, R. (2004) 'The effect of stress–strain relationships on the fire performance of steel beams', *Engineering Structures,* 26(11), pp. 1505-1515. DOI: https://doi.org/10.1016/j.engstruct.2004.05.003.

40. Built by Nature (2026) *UK Roadmap for Fire Safe Mass Timber*.

41. Chen, C., Jiang, L., McLaggan, M. S., Wang, S. and Usmani, A. (2026) 'Modelling Heat Transfer of Timber Sections Subjected to Non-standard Fire Action', *Fire Technology,* 62(1), pp. 5. DOI: https://doi.org/10.1007/s10694-025-01833-8.

42. Chen, C., Jiang, L., Qiu, J., Orabi, M. A., Chan, W. and Usmani, A. (2022) 'OpenSees development for modelling timber structural members subjected to realistic fire impact', *Fire and Materials*. DOI: https://doi.org/10.1002/fam.3115.

43. Chen, Z., Tung, D. and Karacabeyli, E. (2022) *Modelling Guide for Timber Structures.* 1st edn. Pointe Claire, Québec: FPInnovations.

44. Chiniforush, A. A., Akbarnezhad, A., Valipour, H. and Xiao, J. (2018) 'Energy implications of using steel-timber composite (STC) elements in buildings', *Energy and Buildings,* 176, pp. 203-215. DOI: https://doi.org/10.1016/j.enbuild.2018.07.038.

45. Chiniforush, A. A., Valipour, H. R. and Akbarnezhad, A. (2021) 'Long-term coupled analysis of steel-timber composite (STC) beams', *Construction and Building Materials*, 278, pp. 122348. DOI: https://doi.org/10.1016/j.conbuildmat.2021.122348.

46. Chiniforush, A. A., Valipour, H. R., Bradford, M. A. and Akbarnezhad, A. (2019) 'Long-term behaviour of steel-timber composite (STC) shear connections', *Engineering Structures*, 196, pp. 109356. DOI: https://doi.org/10.1016/j.engstruct.2019.109356.

47. Christoforo, A. L., Arroyo, F. N., Dantas De Sousa, A. M., Mascarenhas, F. J. R., Panzera, T. H., Lahr, F. A. R. and Geraldes Dias, A. M. P. (2025) 'Concrete Damaged Plasticity (CDP) adjustment parameters for the application in simulations of timber or wood composite structures', *Structures*, 73, pp. 108334. DOI: https://doi.org/10.1016/j.istruc.2025.108334.

48. Couto, C. and Vila Real, P. (2019) 'Numerical investigation on the influence of imperfections in the lateral-torsional buckling of beams with slender I-shaped welded sections', *Thin-Walled Structures*, 145, pp. 106429. DOI: https://doi.org/10.1016/j.tws.2019.106429.

49. Couto, C. and Vila Real, P. (2021) 'The influence of imperfections in the critical temperature of I-section steel members', *Journal of Constructional Steel Research*, 179, pp. 106540. DOI: https://doi.org/10.1016/j.jcsr.2021.106540.

50. CTICM (2023) 'Logiciel LTBeamN – Déversement élastique de poutres fléchies comprimées'. Available at: https://www.cticm.com/logiciel/ltbeamn/.

51. D'Amico, B., Pomponi, F. and Hart, J. (2021) 'Global potential for material substitution in building construction: The case of cross laminated timber', *Journal of Cleaner Production*, 279, pp. 123487. DOI: https://doi.org/10.1016/j.jclepro.2020.123487.

52. Deeves, B., P. H. and Woods, J., E. (2026) 'Structural Behavior of CLT-Steel Composite Beams with Self-Tapping Screw Shear Connections', *Journal of Structural Engineering*, 152(8), pp. 04026088. DOI: https://doi.org/10.1061/JSENDH.STENG-15889.

53. Deeves, B. P. H. and Woods, J. E. (2025) 'Experimental investigation of steel-timber shear connections with self-tapping screws', *Construction and Building Materials*, 492, pp. 142999. DOI: https://doi.org/10.1016/j.conbuildmat.2025.142999.

54. Ding, F.-X., Wang, W. and Jiang, B. (2023) 'Numerical study on the fire behaviour of restrained steel-concrete composite beams', *Journal of Building Engineering*, 70, pp. 106358. DOI: https://doi.org/10.1016/j.jobe.2023.106358.

55. Ding, J. and Wang, Y. C. (2009) 'Temperatures in unprotected joints between steel beams and concrete-filled tubular columns in fire', *Fire Safety Journal,* 44(1), pp. 16-32. DOI: https://doi.org/10.1016/j.firesaf.2008.02.004.

56. Doyle, N., Emberley, R. and Torero, J. L. (2017) 'Fire Behavior of Cross-Laminated Timber (CLT) Slabs: Two-Way Action', *Fire Science and Technology 2015*, Singapore, 2017: Springer Singapore, 281-288.

57. Dumler, P., Blankenhagen, J., Mensinger, M. and Winter, S. (2025) 'Fire Safe Design of Hybrid Steel-Timber Construction Systems', *14th World Conference on Timber Engineering 2025 (WCTE 2025)*, Brisbane, Australia: World Conference on Timber Engineering 2025, 3665-3673. DOI: https://doi.org/10.52202/080513-0449.

58. Dwaikat, M. and Kodur, V. (2011) 'Engineering Approach for Predicting Fire Response of Restrained Steel Beams', *Journal of Engineering Mechanics,* 137, pp. 447–461. DOI: https://doi.org/10.1061/(ASCE)EM.1943-7889.0000244.

59. Ehlbeck, J. and Larsen, H. J. (1993) 'Eurocode 5 - Design of timber structures: Joints', *International Workshop on Wood Connectors.*, Madison, WI, United States: Forest Products Society. Available at: https://www.cost.eu/uploads/2018/11/Design-of-Connections-in-Timber-Structures.pdf.

60. Fang, D., Kenny, P. and Mueller, C. (2026) 'Material Efficiency as a Key Opportunity to Reduce Embodied Carbon in Structural Systems: Data Insights from 226 Fully Designed Projects', *Journal of Structural Engineering,* 152(2), pp. 04025275. DOI: https://doi.org/10.1061/JSENDH.STENG-14451.

61. Flint, A. R. (1951) *The Influence of Restraints on the Stability of Beams.* The Structural Engineer, p. 235-246.

62. Fragiacomo, M., Menis, A., Clemente, I., Bochicchio, G. and Ceccotti, A. (2013) 'Fire Resistance of Cross-Laminated Timber Panels Loaded Out of Plane', *Journal of Structural Engineering,* 139(12), pp. 04013018. DOI: https://doi.org/10.1061/(ASCE)ST.1943-541X.0000787.

63. Frangi, A., Just, A., Krenn, H., Schmid, J., Werther, N., Hakkarainen, J., Blondeau, R. and Stapf, G. (2025) 'The Second Generation of Eurocode 5 - Fire Design', *14th World Conference on Timber Engineering 2025 (WCTE 2025)*, Brisbane, Australia.: World Conference on Timber Engineering 2025, 11-18. DOI: https://doi.org/10.52202/080513-0002.

64. Franssen, J.-M. and Gernay, T. (2017) 'Modeling structures in fire with SAFIR®: theoretical background and capabilities', *Journal of Structural Fire Engineering,* 8(3), pp. 300-323. DOI: https://doi.org/10.1108/JSFE-07-2016-0010.

65. Franssen, J.-M. and Vila Real, P. (2015) *Fire Design of Steel Structures.* 2nd edition edn. Multicomp Lda, Mem Martins, Portugal: ECCS and Ernst & Sohn.

66. Franssen, J. M., Cooke, G. M. E. and Latham, D. J. (1995) 'Numerical simulation of a full scale fire test on a loaded steel framework', *Journal of Constructional Steel Research,* 35(3), pp. 377-408. DOI: https://doi.org/10.1016/0143-974X(95)00010-S.

67. Gan, V. J. L., Chan, C. M., Tse, K. T., Lo, I. M. C. and Cheng, J. C. P. (2017) 'A comparative analysis of embodied carbon in high-rise buildings regarding different design parameters', *Journal of Cleaner Production,* 161, pp. 663-675. DOI: https://doi.org/10.1016/j.jclepro.2017.05.156.

68. Ganjali, H., Pace, A. and Tannert, T. (2025) 'Structural performance of adhesively bonded and hybrid screw-adhesive CLT panel-to-panel floor joints', *Construction and Building Materials,* 475, pp. 141139. DOI: https://doi.org/10.1016/j.conbuildmat.2025.141139.

69. Gao, T. and Moen, C. D. (2012) 'Predicting rotational restraint provided to wall girts and roof purlins by through-fastened metal panels', *Thin-Walled Structures,* 61, pp. 145-153. DOI: https://doi.org/10.1016/j.tws.2012.06.005.

70. Garcia-Castillo, E., Gernay, T. and Paya-Zaforteza, I. (2023) 'Probabilistic Models for Temperature-Dependent Compressive and Tensile Strengths of Timber', *Journal of Structural Engineering,* 149(2), pp. 04022239. DOI: https://doi.org/10.1061/JSENDH.STENG-11369.

71. Gernay, T. (2024) 'Performance-based design for structures in fire: Advances, challenges, and perspectives', *Fire Safety Journal,* 142, pp. 104036. DOI: https://doi.org/10.1016/j.firesaf.2023.104036.

72. Ghojel, J. I. and Wong, M. B. (2005) 'Heat transfer model for unprotected steel members in a standard compartment fire with participating medium', *Journal of Constructional Steel Research,* 61(6), pp. 825-833. DOI: https://doi.org/10.1016/j.jcsr.2004.11.003.

73. Gikonyo, J. W., Schweigler, M. and Bader, T. K. (2024) 'Beam-on-Foundation modelling of dowel-type single fastener connections in cross laminated timber', *Engineering Structures,* 303, pp. 117519. DOI: https://doi.org/10.1016/j.engstruct.2024.117519.

74. Godoy Dellepiani, M., Roa Munoz, G., Yanez, S. J., Guzmán, C. F., Saavedra Flores, E. I. and Pina, J. C. (2023) 'Numerical study of the thermo-mechanical behavior of steel–timber structures exposed to fire', *Journal of Building Engineering,* 65, pp. 105758. DOI: https://doi.org/10.1016/j.jobe.2022.105758.

75. Goli, G., Becherini, F., Di Tuccio, M. C., Bernardi, A. and Fioravanti, M. (2019) 'Thermal expansion of wood at different equilibrium moisture contents', *Journal of Wood Science*, 65(1), pp. 4. DOI: https://doi.org/10.1186/s10086-019-1781-9.

76. Gupta, V. (2021) *Open-plan compartment fire dynamics.* PhD Thesis, The University of Queensland.

77. Hadden, R. M., Bartlett, A. I., Hidalgo, J. P., Santamaria, S., Wiesner, F., Bisby, L. A., Deeny, S. and Lane, B. (2017) 'Effects of exposed cross laminated timber on compartment fire dynamics', *Fire Safety Journal*, 91, pp. 480-489. DOI: https://doi.org/10.1016/j.firesaf.2017.03.074.

78. Harmathy, T. Z. (1981) 'The fire resistance test and its relation to real-world fires', *Fire and Materials*, 5(3), pp. 112–122.

79. Hassanieh, A., Valipour, H. R. and Bradford, M. A. (2016) 'Load-slip behaviour of steel-cross laminated timber (CLT) composite connections', *Journal of Constructional Steel Research*, 122, pp. 110-121. DOI: https://doi.org/10.1016/j.jcsr.2016.03.008.

80. Hassanieh, A., Valipour, H. R. and Bradford, M. A. (2017a) 'Composite connections between CLT slab and steel beam: Experiments and empirical models', *Journal of Constructional Steel Research*, 138, pp. 823-836. DOI: https://doi.org/10.1016/j.jcsr.2017.09.002.

81. Hassanieh, A., Valipour, H. R. and Bradford, M. A. (2017b) 'Experimental and numerical investigation of short-term behaviour of CLT-steel composite beams', *Engineering Structures*, 144(C), pp. 43-57. DOI: https://doi.org/10.1016/j.engstruct.2017.04.052.

82. Hassanieh, A., Valipour, H. R. and Bradford, M. A. (2018) 'Bolt shear connectors in grout pockets: Finite element modelling and parametric study', *Construction and Building Materials*, 176, pp. 179-192. DOI: https://doi.org/10.1016/j.conbuildmat.2018.05.029.

83. Hassanieh, A., Valipour, H. R., Bradford, M. A. and Sandhaas, C. (2017) 'Modelling of steel-timber composite connections: Validation of finite element model and parametric study', *Engineering Structures*, 138, pp. 35-49. DOI: https://doi.org/10.1016/j.engstruct.2017.02.016.

84. Hetényi, M. (1946) *Beams on Elastic Foundation: Theory with Applications in the Fields of Civil and Mechanical Engineering.* Ann Arbor: University of Michigan Press.

85. Hicks, S. J., Woodward, A. and Hamad, W. (2025) 'Development of an innovative composite steel and cross laminated timber floor system', *IABSE Symposium Tokyo 2025*, Tokyo, Japan: International Association for Bridge and Structural Engineering, 1-3489.

86. HM Government (2019) *The Building Regulations 2010 Approved Document B Volume 2: Buildings other than dwellings*

87. Hopkin, D., Węgrzyński, W., Spearpoint, M., Fu, I., Krenn, H., Sleik, T., Gorska, C. and Stapf, G. (2022) 'Large-Scale Enclosure Fire Experiments Adopting CLT Slabs with Different Types of Polyurethane Adhesives: Genesis and Preliminary Findings', *Fire,* 5(2), pp. 39. Available at: https://www.mdpi.com/2571-6255/5/2/39.

88. Hosseini, A., Shahnewaz, M., Zhou, J. and Tannert, T. (2025) 'Structural performance of CLT moment connections in the minor strength axis', *Engineering Structures,* 328, pp. 119788. DOI: https://doi.org/10.1016/j.engstruct.2025.119788.

89. Huang, Z., Burgess, I. W. and Plank, R. J. (1999) 'The influence of shear connectors on the behaviour of composite steel-framed buildings in fire', *Journal of Constructional Steel Research,* 51(3), pp. 219-237. DOI: https://doi.org/10.1016/S0143-974X(99)00028-0.

90. Ingberg, S. H. (1928) 'Tests of the Severity of Building Fires', pp. 43–61.

91. Iwase, T., Nakayama, Y., Hirashima, T. and Totsuka, M. 'Numerical Study on Fire Performance of Timber-Concrete Composite Beams'. *14th World Conference on Timber Engineering 2025 (WCTE 2025)*, Brisbane, Australia: World Conference on Timber Engineering 2025, 3527-3533. DOI: https://doi.org/10.52202/080513-0432.

92. Jeebodh, A., Davison, B., McLaggan, M. S., Burgess, I., Hopkin, D. and Huang, S.-S. (2024) 'Influence of continuous elastic lateral restraints on beams and beam-columns of steel-timber hybrid structures in fire', *Fire Safety Journal,* 146, pp. 104172. DOI: https://doi.org/10.1016/j.firesaf.2024.104172.

93. Jeebodh, A., Davison, B., McLaggan, M. S., Burgess, I., Hopkin, D. and Huang, S.-S. (2026) 'Behaviour of heated steel beams with lateral and axial restraint in steel-timber hybrid structures', *Engineering Structures,* 349, pp. 121887. DOI: https://doi.org/10.1016/j.engstruct.2025.121887.

94. Jockwer, R., Caprio, D. and Jorissen, A. (2022) 'Evaluation of parameters influencing the load-deformation behaviour of connections with laterally loaded dowel-type fasteners', *Wood Material Science & Engineering,* 17(1), pp. 6-19. DOI: https://doi.org/10.1080/17480272.2021.1955297.

95. Jockwer, R. and Jorissen, A. (2018) *Stiffness and deformation of connections with dowel-type fasteners* Shaker Verlag.

96. Kanninen, M. F. (1973) 'An augmented double cantilever beam model for studying crack propagation and arrest', *International Journal of Fracture,* 9(1), pp. 83-92. DOI: https://doi.org/10.1007/BF00035958.

97. Kinnersley, D., Hull, T. R., Glockling, J. L. D. and Campbell, S. (2026) 'Reduction of Load Capacity of Screw Fixings into a Timber Soffit During and After Fire', *Fire Technology,* 62(1), pp. 20. DOI: https://doi.org/10.1007/s10694-025-01841-8.

98. Kleinhenz, M., Just, A. and Frangi, A. (2021) 'Temperature-dependent thermal properties for cross-laminated timber exposed to standard fire', *INTER - International Network on Timber Engineering Research*: Timber Scientific Publishing. DOI: https://doi.org/10.3929/ethz-b-000515188.

99. KLH (2021) *European Technical Assessment ETA-06/0138*. Available at: https://www.klhuk.com/wp-content/uploads/2019/10/klh-eta-en.pdf.

100. König, J. (2005) 'Structural fire design according to Eurocode 5—design rules and their background', *Fire and Materials,* 29(3), pp. 147-163. DOI: https://doi.org/10.1002/fam.873.

101. König, J. (2006) 'Effective thermal actions and thermal properties of timber members in natural fires', *Fire and Materials,* 30(1), pp. 51-63. DOI: https://doi.org/10.1002/fam.898.

102. Kucukler, M. (2020) 'Lateral instability of steel beams in fire: Behaviour, numerical modelling and design', *Journal of Constructional Steel Research,* 170, pp. 106095. DOI: https://doi.org/10.1016/j.jcsr.2020.106095.

103. LaMalva, K. and Hopkin, D. (2021) *International Handbook of Structural Fire Engineering. The Society of Fire Protection Engineers Series* Switzerland: Springer International Publishing.

104. Lange, D., Sjöström, J., Schmid, J., Brandon, D. and Hidalgo, J. (2020) 'A Comparison of the Conditions in a Fire Resistance Furnace When Testing Combustible and Non-combustible Construction', *Fire Technology,* 56(4), pp. 1621-1654. DOI: https://doi.org/10.1007/s10694-020-00946-6.

105. Law, A. H., Rory (2017) 'Burnout means Burnout', *SFPE*.

106. Létourneau-Gagnon, M., Dagenais, C. and Blanchet, P. (2021) 'Fire Performance of Self-Tapping Screws in Tall Mass-Timber Buildings', *Applied Sciences,* 11(8), pp. 3579. DOI: https://doi.org/10.3390/app11083579.

107. Li, G.-Q. and Guo, S.-X. (2008) 'Experiment on restrained steel beams subjected to heating and cooling', *Journal of Constructional Steel Research*, 64(3), pp. 268-274. DOI: https://doi.org/10.1016/j.jcsr.2007.07.007.

108. Lineham, S. A., Thomson, D., Bartlett, A. I., Bisby, L. A. and Hadden, R. M. (2016) 'Structural response of fire-exposed cross-laminated timber beams under sustained loads', *Fire Safety Journal*, 85, pp. 23-34. DOI: https://doi.org/10.1016/j.firesaf.2016.08.002.

109. Ling, Z., Rong, X. and Xiang, Z. (2021) 'Laterally loaded performance of single dowel-type fastener used for steel plate-to-timber connections', *Structures*, 34, pp. 1985-1997. DOI: https://doi.org/10.1016/j.istruc.2021.08.115.

110. Liu, J. and Fischer, E. C. (2022) 'Review of large-scale CLT compartment fire tests', *Construction and Building Materials*, 318, pp. 126099. DOI: https://doi.org/10.1016/j.conbuildmat.2021.126099.

111. Liu, T. C. H., Fahad, M. K. and Davies, J. M. (2002) 'Experimental investigation of behaviour of axially restrained steel beams in fire', *Journal of Constructional Steel Research*, 58(9), pp. 1211-1230. DOI: https://doi.org/10.1016/S0143-974X(01)00062-1.

112. Loss, C., Piazza, M. and Zandonini, R. (2016) 'Connections for steel-timber hybrid prefabricated buildings. Part I: Experimental tests', *Construction and Building Materials*, 122, pp. 781-795. DOI: https://doi.org/10.1016/j.conbuildmat.2015.12.002.

113. Ma, C., Garcia-Castillo, E., Paya-Zaforteza, I. and Gernay, T. (2025) 'Modeling fire resistance of timber columns: Influence of elevated-temperature material models in finite element analysis', *Structures*, 82, pp. 110629. DOI: https://doi.org/10.1016/j.istruc.2025.110629.

114. Ma, Z., Havula, J. and Heinisuo, M. (2019) 'Structural fire analysis of simple steel structures by using LS-DYNA explicit solver', *Rakenteiden Mekaniikka*, 52, pp. 1-22. DOI: https://doi.org/10.23998/rm.77252.

115. Malaska, M., Alanen, M., Salminen, M., Jokinen, T. and Ranua, R. (2023) 'Fire Performance of Steel-Timber Hybrid Beam Section', *Fire Technology*, 60(4), pp. 2581-2600. DOI: https://doi.org/10.1007/s10694-023-01471-y.

116. Marcolan Júnior, A. C. and Dias de Moraes, P. (2022) 'Probabilistic model for determining the failure time of steel-to-timber connections with multiple dowel-type fasteners exposed to fire', *Fire Safety Journal*, 133, pp. 103646. DOI: https://doi.org/10.1016/j.firesaf.2022.103646.

117. Martins, A. D., Camotim, D., Gonçalves, R., Lopes, N. and Vila Real, P. (2022) 'Transversally loaded stainless steel beams under fire: Local/global behaviour, strength and design', *Journal of Constructional Steel Research*, 189, pp. 107080. DOI: https://doi.org/10.1016/j.jcsr.2021.107080.

118. McCann, F., Gardner, L. and Wadee, M. A. (2013) 'Design of steel beams with discrete lateral restraints', *Journal of Constructional Steel Research*, 80, pp. 82-90. DOI: https://doi.org/10.1016/j.jcsr.2012.09.011.

119. Merryday, H., Potuzak, M., Roueche, D. and Sener, K. (2023) 'Experimental and Numerical Investigations on the Usage of CLT Panels to Form Timber-Steel Composite Floor Systems', *World Conference on Timber Engineering (WCTE 2023)*, Oslo, Norway, 3373-3381. DOI: https://doi.org/10.52202/069179-0439.

120. Merryday, H., Sener, K. and Roueche, D. (2025) 'Structural performance of self-tapping screws for use in steel-CLT composite members', *Engineering Structures*, 340, pp. 120652. DOI: https://doi.org/10.1016/j.engstruct.2025.120652.

121. Merryday, H. C., Sener, K. and Roueche, D. (2023) 'Pushout Tests on Steel-Timber Connections Using Self-Tapping Screws', *Structures Congress 2023*, pp. 312-327. DOI: https://doi.org/10.1061/9780784484777.028.

122. Mesquita, L. M. R., Piloto, P. A. G., Vaz, M. A. P. and Vila Real, P. M. M. (2005) 'Experimental and numerical research on the critical temperature of laterally unrestrained steel I beams', *Journal of Constructional Steel Research*, 61(10), pp. 1435-1446. DOI: https://doi.org/10.1016/j.jcsr.2005.04.003.

123. Mindeguia, J.-C., Mohaine, S., Bisby, L., Robert, F., McNamee, R. and Bartlett, A. (2020) 'Thermo-mechanical behaviour of cross-laminated timber slabs under standard and natural fires', *Fire and Materials*, 45(7), pp. 866-884. DOI: https://doi.org/10.1002/fam.2938.

124. MTC Solutions (2019) *Steel to CLT Lateral Connections*, Surrey, BC, Canada: MyTiCon Timber Connectors. Available at: https://mtcsolutions.com/resources/white-papers/steel-to-clt-lateral-connections/.

125. Nguyen, M. H., Ouldboukhitine, S.-E., Durif, S., Saulnier, V. and Bouchair, A. (2023a) 'Method of measuring the temperature of wood exposed to fire with type K thermocouples', *Fire Safety Journal*, 137, pp. 103752. DOI: https://doi.org/10.1016/j.firesaf.2023.103752.

126. Nguyen, M. H., Ouldboukhitine, S.-E., Durif, S., Saulnier, V. and Bouchair, A. (2023b) 'Passive fire protection of steel profiles using wood', *Engineering Structures*, 275, pp. 115274. DOI: https://doi.org/10.1016/j.engstruct.2022.115274.

127. Nguyen, X. T. and Park, J. S. (2022) 'Design equations for buckling strength of steel I-beam under non-uniform heating condition', *Fire Safety Journal,* 127, pp. 103464. DOI: https://doi.org/10.1016/j.firesaf.2021.103464.

128. Östman, B., Brandon, D. and Frantzich, H. (2017) 'Fire safety engineering in timber buildings', *Fire Safety Journal,* 91, pp. 11-20. DOI: https://doi.org/10.1016/j.firesaf.2017.05.002.

129. Peng, L., Hadjisophocleous, G., Mehaffey, J. and Mohammad, M. (2012) 'Fire Performance of Timber Connections, Part 2: Thermal and Structural Modelling', *Journal of Structural Fire Engineering,* 3(2), pp. 133-154. DOI: https://doi.org/10.1260/2040-2317.3.2.133.

130. Pettersson, O., Magnusson, S. E. and Thor, J. (1976) *Fire Engineering Design of Steel Structures.* Stockholm: Swedish Institute of Steel Construction.

131. Philion, E., Chorlton, B., Gales, J. and Kotsovinos, P. (2022) 'Structural Fire Modeling Strategies for Exposed Mass Timber Compartments and Experimental Gaps for Model Validation', *Journal of Performance of Constructed Facilities,* 36(6), pp. 04022049. DOI: https://doi.org/10.1061/(ASCE)CF.1943-5509.0001761.

132. Pimentel, R., Simões, R. and Silva, L. (2024) 'Hybrid steel frames with mass timber floors: performance, challenges and sustainability benefits', *ce/papers,* 7, pp. 228-239. DOI: https://10.1002/cepa.3040.

133. Pope, I., Gupta, V., Xu, H., Wiesner, F., Lange, D., Torero, J. L. and Hidalgo, J. P. (2023) 'Fully-developed compartment fire dynamics in large-scale mass timber compartments', *Fire Safety Journal,* 141, pp. 104022. DOI: https://doi.org/10.1016/j.firesaf.2023.104022.

134. Quiquero, H., Gales, J., Abu, A. and Al Hamd, R. (2020) 'Finite Element Modelling of Post-tensioned Timber Beams at Ambient and Fire Conditions', *Fire Technology,* 56(2), pp. 737-767. DOI: https://doi.org/10.1007/s10694-019-00901-0.

135. Romero, A. and Odenbreit, C. (2024) 'Experimental investigation on novel shear connections for demountable steel-timber composite (STC) beams and flooring systems', *Engineering Structures,* 304, pp. 117620. DOI: https://doi.org/10.1016/j.engstruct.2024.117620.

136. Sacadura, J. F. (2005) 'Radiative heat transfer in fire safety science', *Journal of Quantitative Spectroscopy and Radiative Transfer,* 93(1), pp. 5-24. DOI: https://doi.org/10.1016/j.jqsrt.2004.08.011.

137. Salgado, R. A. and Guner, S. (2021) 'Characterization of the out-of-plane behavior of CLT panel connections', *Engineering Structures*, 229, pp. 111596. DOI: https://doi.org/10.1016/j.engstruct.2020.111596.

138. Santiago, A., da Silva, L. S., Real, P. V. and Veljkovic, M. (2008) 'Numerical study of a steel sub-frame in fire', *Computers & Structures*, 86(15), pp. 1619-1632. DOI: https://doi.org/10.1016/j.compstruc.2008.01.006.

139. SCI (2011) *Stability of Steel Beams and Columns*, SCI P360: The Steel Construction Institute.

140. SCI (2015) *Minimum Degree of Shear Connection Rules for UK Construction to Eurocode 4. SCI P405*: Steel Construction Institute.

141. SCI (2024) *Best Practice for Designing Low Embodied Carbon Steel Buildings. SCI P449*: Steel Construction Institute.

142. Šejna, J., Průšová, K., Cábová, K., Rušarová, S. and Wald, F. (2025) 'Cracks in the charred layer of timber panels: Fire experiments and probabilistic solution', *Case Studies in Thermal Engineering*, 74, pp. 106788. DOI: https://doi.org/10.1016/j.csite.2025.106788.

143. Senalik, C. A. and Farber, B. (2021) *Chapter 5: Mechanical properties of wood*, Madison, Wisconsin: Forest Products Laboratory, United States Department of Agriculture Forest Service

144. SIA 265 (2012) *Timber Structures*. Zurich, Switzerland: SIA Swiss Society of Engineers and Architects.

145. Smith, A. L., Hicks, S. J. and Devine, P. J. (2009) *Design of Floors for Vibration: A New Approach.* Revised ed edn. Ascot, Berkshire: Steel Construction Institute.

146. Song, T.-Y., Qu, X.-Y., Zhou, H. and Xiang, K. (2022) 'Advanced critical temperature method for steel beams exposed to different fire scenarios', *Structures*, 44, pp. 200-215. DOI: https://doi.org/10.1016/j.istruc.2022.08.019.

147. STA (2023) *Structural timber buildings fire safety in use guidance. Volume 6 - Mass timber structures; Building Regulation compliance B3(1)*: Structural Timber Association.

148. Stern-Gottfried, J. and Rein, G. (2012) 'Travelling fires for structural design-Part II: Design methodology', *Fire Safety Journal*, 54, pp. 96-112. DOI: https://doi.org/10.1016/j.firesaf.2012.06.011.

149. Swedish Wood (2022) *The CLT Handbook UK Edition: CLT Structures – Design and Detailing*. 1st edn. Stockholm, Sweden: Swedish Forest Industries Federation.

150. The Building Regulations 2010 *SI 2010 No. 2214*.

151. Thi, V. D., Khelifa, M., Oudjene, M., Ganaoui, M. E. and Rogaume, Y. (2017) 'Finite element analysis of heat transfer through timber elements exposed to fire', *Engineering Structures,* 143, pp. 11-21. DOI: https://doi.org/10.1016/j.engstruct.2017.04.014.

152. Thiel, A. 'ULS and SLS Design of CLT and its Implementation in the CLTdesigner.'. *European Conference on Cross Laminated Timber (CLT)*, Graz University of Technology, Austria.

153. Thomas, P. H. and Heselden, A. J. M. (1972) *Fully-developed fires in single compartments: A co-operative research programme of the Conseil International du Bâtiment.* Borehamwood: Fire Research Station.

154. Timoshenko, S. P. and Gere, J. M. (1961) *Theory of elastic stability.* 2nd edition edn.: McGraw-Hill Book Company, Inc.

155. Tondini, N., Morbioli, A., Vassart, O., Lechêne, S. and Franssen, J.-M. (2016) 'An integrated modelling strategy between a CFD and an FE software: Methodology and application to compartment fires', *Journal of Structural Fire Engineering,* 7(3), pp. 217-233. DOI: https://doi.org/10.1108/JSFE-09-2016-015.

156. Torero, J. L., Law, A. and Maluk, C. (2017) 'Defining the thermal boundary condition for protective structures in fire', *Engineering Structures,* 149, pp. 104-112. DOI: https://doi.org/10.1016/j.engstruct.2016.11.015.

157. Torero, J. L., Majdalani, A. H., Abecassis-Empis, C. and Cowlard, A. 'Revisiting the compartment fire'. *IAFSS 2014: 11th International Symposium on Fire Safety Science*: IAFSS, 28-45. DOI: https://doi.org/10.3801/IAFSS.FSS.11-28.

158. Trahair, N. S. (1993) *Flexural-Torsional Buckling of Structures.* Boca Raton: CRC Press.

159. UK Green Building Council (2021) *Net Zero Whole Life Carbon Roadmap: A Pathway to Net Zero for the UK Built Environment*. Available at: https://ukgbc.org/our-work/topics/whole-life-carbon-roadmap/.

160. UNEP (2025) *Global Status Report for Buildings and Construction 2024/2025.* United Nations Environment Programme.

161. Usmani, A. S., Rotter, J. M., Lamont, S., Sanad, A. M. and Gillie, M. (2001) 'Fundamental principles of structural behaviour under thermal effects', *Fire Safety Journal,* 36(8), pp. 721-744. DOI: https://doi.org/10.1016/S0379-7112(01)00037-6.

162. Vila Real, P. M. M., Cazeli, R., Simões da Silva, L., Santiago, A. and Piloto, P. (2004) 'The effect of residual stresses in the lateral-torsional buckling of steel I-beams at elevated temperature', *Journal of Constructional Steel Research,* 60(3), pp. 783-793. DOI: https://doi.org/10.1016/S0143-974X(03)00143-3.

163. Wang, Y., Burgess, I., Wald, F. and Gillie, M. (2012) *Performance-Based Fire Engineering of Structures.* London: CRC Press.

164. Wang, Y., Zhang, J., Mei, F., Liao, J. and Li, W. (2020) 'Experimental and numerical analysis on fire behaviour of loaded cross-laminated timber panels', *Advances in Structural Engineering,* 23(1), pp. 22-36. DOI: 10.1177/1369433219864459.

165. Wang, Y. C. (2002) *Steel and Composite Structures: Behaviour and Design for Fire Safety.* London: CRC Press.

166. Wang, Y. C. and Yin, Y. Z. (2006) 'A simplified analysis of catenary action in steel beams in fire and implications on fire resistant design', *Steel and Composite Structures,* 6, pp. 367-386. DOI: https://doi.org/10.12989/scs.2006.6.5.367.

167. Watson, N. (2020) 'Lean design: 10 things to do now', 98. DOI: https://doi.org/10.56330/CDJA1258.

168. Węgrzyński, W., Turkowski, P. and Roszkowski, P. (2019) 'The discrepancies in energy balance in furnace testing, a bug or a feature?', *Fire and Materials,* 2019, pp. 1-12. DOI: https://doi.org/10.1002/fam.2735.

169. Welch, S., Miles, S. D., Kumar, S., Lemaire, T. and Chan, A. 'FIRESTRUC - Integrating advanced three-dimensional modelling methodologies for predicting thermo-mechanical behaviour of steel and composite structures subjected to natural fires'. *IAFSS 2014: 11th International Symposium on Fire Safety Science*: IAFSS, 1315-1326. DOI: https://doi.org/10.3801/IAFSS.FSS.9-1315.

170. White, R. H. and Dietenberger, M. A. (2001) 'Wood Products: Thermal Degradation and Fire', in Buschow, K.H.J., Cahn, R.W., Flemings, M.C., Ilschner, B., Kramer, E.J., Mahajan, S. and Veyssière, P. (eds.) *Encyclopedia of Materials: Science and Technology*. Oxford: Elsevier, pp. 9712-9716.

171. Wiesner, F., Xu, H., Lange, D., Gupta, V., Pope, I., Torero, J. L. and Hidalgo, J. P. (2025) 'Large-scale compartment fires to develop a self-extinction design framework for mass timber-Part 2: Results, analysis and design implications', *Fire Safety Journal,* 152, pp. 104346. DOI: https://doi.org/10.1016/j.firesaf.2025.104346.

172. World Green Building Council (2019) *Bringing embodied carbon upfront: Coordinated action for the building and construction sector to tackle embodied carbon*. Available at: https://worldgbc.org/climate-action/embodied-carbon/.

173. Xu, H., Pope, I., Gupta, V., Cadena, J., Carrascal, J., Lange, D., McLaggan, M. S., Mendez, J., Osorio, A., Solarte, A., Soriguer, D., Torero, J. L., Wiesner, F., Zaben, A. and Hidalgo, J. P. (2022) 'Large-scale compartment fires to develop a self-extinction design framework for mass timber—Part 1: Literature review and methodology', *Fire Safety Journal,* 128, pp. 103523. DOI: https://doi.org/10.1016/j.firesaf.2022.103523.

174. Xu, Q., Hofmeyer, H. and Maljaars, J. (2024) 'A two-scale method to include essential behaviour of bolted connections in structures including elevated temperatures', *Theoretical and Applied Mechanics Letters,* 14(6), pp. 100526. DOI: https://doi.org/10.1016/j.taml.2024.100526.

175. Yang, R., Li, H., Lorenzo, R., Ashraf, M., Sun, Y.-f. and Yuan, Q. (2020) 'Mechanical behaviour of steel timber composite shear connections', *Construction and Building Materials*. DOI: https://doi.org/10.1016/j.conbuildmat.2020.119605.

176. Yin, Y. Z. and Wang, Y. C. (2003) 'Numerical simulations of the effects of non-uniform temperature distributions on lateral torsional buckling resistance of steel I-beams', *Journal of Constructional Steel Research,* 59(8), pp. 1009-1033. DOI: https://doi.org/10.1016/S0143-974X(03)00003-8.

177. Yin, Y. Z. and Wang, Y. C. (2004) 'A numerical study of large deflection behaviour of restrained steel beams at elevated temperatures', *Journal of Constructional Steel Research,* 60(7), pp. 1029-1047. DOI: https://doi.org/10.1016/j.jcsr.2003.09.005.

178. Younis, A. and Dodoo, A. (2022) 'Cross-laminated timber for building construction: A life-cycle-assessment overview', *Journal of Building Engineering,* 52, pp. 104482. DOI: https://doi.org/10.1016/j.jobe.2022.104482.

179. Zhang, C., Li, G.-Q. and Usmani, A. (2013) 'Simulating the behavior of restrained steel beams to flame impingement from localized-fires', *Journal of Constructional Steel Research,* 83, pp. 156-165. DOI: https://doi.org/10.1016/j.jcsr.2013.02.001.

180. Zhang, J. C., Zhang, D. S., Dong, Y. L. and Wang, W. H. (2019) 'Experimental study on internal force variation of steel-concrete composite beam under fire', *Engineering Mechanics*, 36(6), pp. 183-192,210. DOI: https://doi.org/10.6052/j.issn.1000-4750.2018.05.0281.

181. Zhao, Y., Yuan, Y., Wang, C.-L., Zheng, J. and Zhou, Y. (2022) 'Experimental study on shear performance of steel-timber screw connectors with grout pockets', *Engineering Structures,* 266, pp. 114535. DOI: https://doi.org/10.1016/j.engstruct.2022.114535.